SOLUTION OF UNBOUNDED FIELD PROBLEMS BY BOUNDARY RELAXATION

Ivan A. Cermak, B.Eng., M.Eng.

SOLUTION OF UNBOUNDED FIELD PROBLEMS BY BOUNDARY RELAXATION

Electrical Ivan A. Cermak, B.Eng., M.Eng. Ph.D.

ABSTRACT

A new accurate and efficient numerical method, belonging to the recently discovered class of boundary relaxation techniques, is presented for the solution of infinitely extending problems of elliptic type, with particular application to unbounded problems of Laplace's or Poisson's equation. The boundary conditions at infinity are transformed to an arbitrary, finite, closed contour in terms of a potential shift operator. The solution within the arbitrary contour is obtained as the solution of an interior Dirichlet problem simultaneously with the shift relationship, and corresponds exactly with that of the infinitely extending problem. The problem is formulated in finite differences and standard iterative theory applied to the resulting linear system of equations. Optimization of the iterative schemes is considered and an error analysis is developed. Application of the method is illustrated for two-dimensional, three-dimensional axially symmetric and coaxial line problems. All pertinent computational algorithms are presented in detail.

SOLUTION OF UNBOUNDED FIELD PROBLEMS BY BOUNDARY RELAXATION

by

Ivan A. Cermak, B.Eng., M.Eng.

A thesis submitted to the Faculty of Graduate Studies and Research in partial fulfillment of the requirements for the degree of Doctor of Philosophy

Department of Electrical Engineering,
McGill University,
Montreal, Quebec,

March, 1969.

ABSTRACT

A new accurate and efficient numerical method, belonging to the recently discovered class of boundary relaxation techniques, is presented for the solution of infinitely extending problems of elliptic type, with particular application to unbounded problems of Laplace's or Poisson's equation. The boundary conditions at infinity are transformed to an arbitrary, finite, closed contour in terms of a potential shift operator. The solution within the arbitrary contour is obtained as the solution of an interior Dirichlet problem simultaneously with the shift relationship, and corresponds exactly with that of the infinitely extending problem. The problem is formulated in finite differences and standard iterative theory applied to the resulting linear system of equations. Optimization of the iterative schemes is considered and an error analysis is developed. Application of the method is illustrated for two-dimensional, three-dimensional axially symmetric and coaxial line problems. All pertinent computational algorithms are presented in detail.

ACKNOWLEDGEMENTS

The success of any endeavour is in no small measure dependent upon the help and cooperation of many. The author is above all indebted to Dr. P. Silvester whose guidance and encouragement throughout the course of this research were invaluable. It is hoped that this work demonstrates that some of his enthusiasm, motivating spirit and thirst for knowledge have rubbed off to at least a small degree.

To Dr. T.J.F. Pavlasek, the author is sincerely grateful for his cheerful guidance and encouragement during Dr. Silvester's absence.

Special thanks are due to Mr. M.F. Yan for his discussions concerning Hankel transforms and linear spaces. Thanks are also due to the entire Electrical Engineering staff for their cooperation and willing assistance.

Grateful acknowledgement is made to McGill University for financial support in the form of a McConnell Memorial Fellowship, and to the National Research Council under whose grant this research was conducted.

Last, but not least, the author is forever grateful to his dear wife, Joan, who not only expertly typed the manuscript, but showed patience and provided encouragement and motivation far beyond the call of duty.

TABLE OF CONTENTS

CHAPTER 1

INTRODUCTION

A great variety of physical problems that arise in engineering or physics may be represented by differential equations of the form

$$A(x,y)\frac{\partial^2\phi}{\partial x^2} + 2B(x,y)\frac{\partial^2\phi}{\partial x\partial y} + C(x,y)\frac{\partial^2\phi}{\partial y^2} = F(\phi,\phi_x,\phi_y,x,y)$$

which have the property that the sign of the quantity

$$(B^2 - AC)$$

is unaffected by a change of variable [1],[2]. The equations are classified as elliptic, parabolic, or hyperbolic according to whether the above expression is less than, equal to, or greater than zero respectively. Only special cases of the elliptic equation will be considered in this thesis, namely the degenerate elliptic class corresponding to the Laplace or Poisson equation, although some of the theory possibly holds for more general cases.

Solutions of elliptic problems fall, in general, into one of three categories:analytic, analogue and numerical. Analytic solutions in general are limited to problems which can

be posed in a coordinate system in which the variables are separable, not only for the elliptic operator but for the given boundary conditions as well. There exist, of course, many special problems that may be solved by special techniques such as conformal transformation, by the method of images, or some other special analytic method, but, in general, analytic solution is usually practical only for simple problems that have limited application.

Analogue methods do not suffer from the same limitations as analytic methods, in that problems that are fairly complicated are solved almost as easily as ones with simple configurations of sources and boundaries. Of all the various available analogue methods, the ones used most widely in engineering applications have been the electrolytic tank and the resistive mesh analogue. In the electrolytic tank, a conductive liquid sheet represents the plane in which the problem is formulated [3],[4]. Accuracy is limited, however, and special models have to be constructed for each problem to be solved. The resistive mesh analogue [5] is versatile enough to eliminate need for construction of special jigs for each problem, and, indeed, may be constructed so that infinitely extending problems may be solved [6]; however, accuracy is again limited and special measuring equipment may be required for meaningful solutions to be obtained. Higgins [7] gives an extensive bibliography of various electro-analogic methods, and the reader is referred to his papers for further details.

Numerical methods have come into prominence in recent years, since the widespread availability of large digital computers has made solution of complicated problems possible without the need for special equipment. Numerical methods have also extended the practical range of problems that are analytically solvable, since the evaluation of complicated functions and the evaluation of series of many terms, to name just two, is now not only practical, but simple and convenient as well. Of all numerical methods available for solution of elliptic problems, none has come into as widespread use as finite differences; an extensive literature exists on the subject. Finite differences have proved popular for two main reasons that are not entirely separate: they are relatively simple to program or code for digital computer solution and a large variety of complicated problems can be handled fairly easily. Theoretical consideration of finite differences is not trivial; however, their wide acceptance by academe and industry has prompted an extensive theoretical literature and the subject is far from exhausted.

Flexibility and wide use of finite differences notwithstanding, there exists a large category of elliptic problems that have up to now resisted rigorous treatment. This is the class of infinitely extending problems, i.e., those problems that have boundary conditions at infinity. It is these problems that are considered in this thesis, specifically those problems that may be posed in terms of the Laplace or Poisson equation. First, however, finite differences in general will be considered briefly.

1.1 Finite Difference Formulation of Fields

As the name suggests, finite difference methods are based on the replacing of a partial differential equation by a number of difference approximations and then solving the large number of resulting algebraic equations. The solutions to the approximate system represent solution values at discrete points in the region of interest. The continuous differential operator is replaced, or approximated by, a matrix operator. Necessary and sufficient conditions for uniform approximation of a continuous operator by a matrix may be found in any text on linear spaces [8], and will not be detailed here. The elliptic operators under consideration here conform to these conditions and hence may be approximated by matrices. To illustrate the method of approximation, one finite difference equivalent of the Laplacian will be derived.

Suppose a regular rectangular mesh is superimposed on the continuous plane. Let the function values V at the nodes of the mesh be representative of the continuous function ϕ at that point in the continuous plane. Define a five-point star in the mesh by the compass notation shown in Figure 1.1.

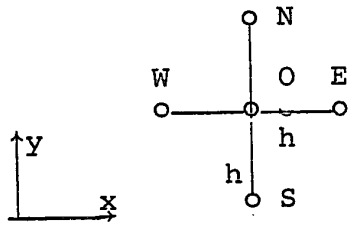

FIGURE 1.1: REGULAR FIVE-POINT STAR

The first partial derivatives about the point O in the star may be approximated in terms of the forward and back differences as,

$$\left.\frac{\partial\phi}{\partial x}\right|_f \simeq \frac{1}{h}(V_E - V_O), \quad \left.\frac{\partial\phi}{\partial x}\right|_b \simeq \frac{1}{h}(V_O - V_W), \quad \left.\frac{\partial\phi}{\partial y}\right|_f \simeq \frac{1}{h}(V_N - V_O), \quad \left.\frac{\partial\phi}{\partial y}\right|_b \simeq \frac{1}{h}(V_O - V_S)$$

The second partial derivatives may be taken as the second divided differences, [9],

$$\left.\frac{\partial^2\phi}{\partial x^2}\right|_o \simeq \frac{1}{h}\left(\left.\frac{\partial\phi}{\partial x}\right|_f - \left.\frac{\partial\phi}{\partial x}\right|_b\right), \quad \left.\frac{\partial^2\phi}{\partial y^2}\right|_o \simeq \frac{1}{h}\left(\left.\frac{\partial\phi}{\partial y}\right|_f - \left.\frac{\partial\phi}{\partial y}\right|_b\right)$$

so that the approximation to the Laplacian becomes,

$$\left.\frac{\partial^2\phi}{\partial x^2} + \frac{\partial^2\phi}{\partial y^2}\right|_o \simeq \frac{1}{h^2}(V_N + V_E + V_S + V_W - 4V_O)$$

This derivation serves to illustrate the finite difference approximation but does not, however, give rise to any convenient estimate of the error incurred, though it is seen by inspection that the error involved is of the order of h^2. Moreover, the mesh lengths have been assumed equal. A more precise expression may be obtained by taking a Taylor expansion about the point 0 and ignoring high order terms [10],[11]. The resulting system of equations, however, may not always be symmetric. A symmetric system is guaranteed by derivation of the finite difference formulas by a variational method [12],

which is based on minimizing an integral of the form

$$I(\phi) = \iint [-(\phi_x^2 + \phi_y^2) + F\phi] \, d_x d_y$$

Whatever the method used, the resulting formula at each point is the so-called five-point finite difference Laplacian, with an error of $O(h^2)$. The approximating error may be reduced by including more points in the formula. For example, inclusion of four more mesh points in the star, as shown in Figure 1.2, yields a much more accurate nine-point equation [10] which, however, is often not as easily incorporated in computer programmes, particularly if complicated material interfaces are encountered. The reader is again referred to the literature for details of the various approximating techniques [10], [11], [12], [13].

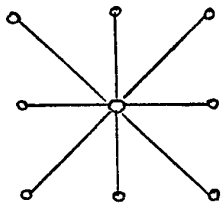

FIGURE 1.2: NINE-POINT STAR

When a finite difference formula is written for each node in the mesh, there results a large number of algebraic equations which must be solved simultaneously. Written in matrix form, the resulting system is of high order and very

sparse, i.e., the coefficient matrix contains a large number of zero elements. Direct methods, such as inversion of the large matrix, are, as a rule, inconvenient, although they have been used [14]. Iterative solutions of such systems are more common since the coefficient matrix need not be stored, but is generated as needed and the iterative processes are, as a rule, free from round-off error propagation.

Finite differences can be traced back to Gauss [15] and one of the oldest iterative methods, the classical Gauss-Seidel, dates back to 1873 [16]. The word "relaxation" is due to Southwell [17] who described a method of solving a stressed, jointed framework by the systematic relaxation of strains. Some of the more common as well as historical iterative methods are discussed in the next section.

1.2 Iterative Solution of the Resulting System of Equations

1.2.1 SOUTHWELL RELAXATION: Southwell relaxation [17] is intended for hand solution of elliptic problems. The method consists of rewriting the difference equations at each node in the mesh in the form

$$C_N V_N + C_E V_E + C_S V_S + C_W V_W - C_O V_O - t = R_O$$

where the c_i are positive constants, the constant t represents the forcing function (if any), and the quantity R_O is termed the "residual". If V is the solution, then the

residual R_O is zero. At first, arbitrary values are assigned to the vector V at each point O. The residual is then evaluated at each point, and the mesh is scanned for the residual with the largest magnitude. At that point, the residual is brought to zero by solving for V_O as

$$V_O^* = \frac{c_N V_N + c_E V_E + c_S V_S + c_W V_W - t}{c_O}$$

Changing V_O at any point changes the value of the residual for each of its neighbours. The neighbouring residuals are then up-dated and the field is scanned again for the residual with the largest magnitude and the process repeated.

This process can be speeded up by overrelaxing as follows

$$V_O^{(new)} = V_O^{(old)} + \omega[V_O^* - V_O^{(old)}]$$

where if $\omega = 1$, the process is called normal relaxation, if $\omega > 1$, overrelaxation and $\omega < 1$, underrelaxation. This process is not well suited for use on digital computing machines since the search for the largest residual is a relatively inefficient process.

1.2.2 RICHARDSON'S METHOD: This method [18], also known as the method of simultaneous displacements, was first considered in 1845 by Jacobi [19]. In this method, the residuals are systematically evaluated at each point in the field and the

potential at each point is then subsequently corrected. If the superscript (k) refers to the number of complete iterations, the correction scheme may be stated as

$$V_0^{(k+1)} = V_0^{(k)} + \omega\left[\frac{c_N V_N^{(k)} + c_E V_E^{(k)} + c_S V_S^{(k)} + c_W V_W^{(k)} - t}{c_0} - V_0^{(k)}\right]$$

Convergence of the method is poor and, in general, the best value of ω is different for each iteration. The method also suffers from the disadvantage that two full sets of function values must be stored. It is rarely used in practice.

1.2.3 LIEBMANN'S METHOD OR GAUSS-SEIDEL: The classical Gauss-Seidel method [16], which when applied to the Dirichlet problem is termed the Liebmann method [20], [21], and also called the method of successive displacements [22], is a simple modification of Richardson's method. In this scheme, the most recently computed values of the function V are used at each stage. If the superscript (k) again refers to the number of completed iterations, one possible correction formula is

$$V_0^{(k+1)} = \frac{c_N V_N^{(k+1)} + c_W V_W^{(k+1)} + c_E V_E^{(k)} + c_S V_S^{(k)} - t}{c_0}$$

This method requires storage of only one complete set of values of V and it can be shown [12] that the rate of convergence is twice that of Richardson's method. A complete discussion of the method is contained in a paper by Frankel [23].

1.2.4 YOUNG-FRANKEL SUCCESSIVE OVERRELAXATION: This method developed independently by Young [24] and Frankel [23] is also known as the extrapolated Liebmann method, since it is derived from the ordinary Liebmann method by the introduction of an overrelaxation factor. Using the above notation,

$$V_O^{(k+1)} = V_O^{(k)} + \omega\left[\frac{c_N V_N^{(k+1)} + c_W V_W^{(k+1)} + c_E V_E^{(k)} + c_S V_S^{(k)} - t}{c_O} - V_O^{(k)}\right]$$

When $\omega = 1$ this reduces to the above Liebmann method. It can be shown that the method converges for $0 < \omega < 2$, [12].

Consider the set of linear equations that has to be solved

$$AV = B$$

Split the coefficient matrix A into three matrices

$$A = L + D + U$$

where L is the lower triangular matrix of A with zeros on the diagonal, D is a diagonal matrix whose elements are the diagonal elements of A, U is an upper triangular matrix containing the elements of A above the diagonal. The extrapolated Liebmann method then reduces to

$$\left[\frac{1}{\omega} D+L\right] V^{(k+1)} + \left[\left(1-\frac{1}{\omega}\right) D+U\right] V^{(k)} = B \qquad (1.1)$$

Define an error vector $e^{(k)}$ whose components are

$$e_i^{(k)} = V_i^{(k)} - V_i$$

where V_i is the solution. Substitute into (1.1) to yield

$$e^{(k+1)} = -(D+\omega L)^{-1} [(\omega-1)D+\omega U] e^{(k)} \qquad (1.2)$$

which is the fundamental error equation for successive over-relaxation.

Equation 1.2 may be written as

$$e^{(k+1)} = M e^{(k)}$$

and in order that $\lim_{k\to\infty} e^{(k)} = 0$ it is necessary for all eigenvalues of M lie within the unit circle. It can be shown that [24]

$$\lambda = \frac{\omega\mu \pm \sqrt{\omega^2\mu^2 - 4(\omega-1)}}{2} \qquad (1.3)$$

where λ is an eigenvalue of M and μ is an eigenvalue of $(I - D^{-1}A)$, which is the Jacobi matrix corresponding to the Jacobi iteration in § 1.2.2. This may be done by invoking Young's property "A" on the matrix A [24]. Moreover, it can be shown that the optimum value of ω lies between 1 and 2.

The problem of choosing ω_{opt} has received considerable attention in the literature [11], [25], [26] and will not

be discussed here. In general, the methods depend on the acquisition of a good estimate of μ in equation 1.3, thus allowing a better estimate of λ and hence ω_{opt}.

1.2.5 PEACEMAN-RACHFORD ALTERNATING DIRECTION LINE RELAXATION: In this method, lines of nodes are considered simultaneously [27],[11]. This method, although extremely fast for rectangular regions in comparison with the above methods, is difficult to optimize and involves tedious programming for problems with complicated boundaries.

1.2.6 OTHER METHODS: Many variations of the standard iterative methods have been presented in the literature. These methods fall roughly into two classes: In the first class Chebyshev polynomials are used for acceleration of the usual iterative schemes [28] and are reported to be useful even in the case of problems for which the relaxation matrix has complex eigenvalues [29]. The second class involves conversion of the standard schemes into a quasi-doubly-iterative scheme, again in order to hasten convergence, or in fact to obtain convergence at all [30],[31],[11]. The reader is again referred to some of the extensive literature on all the above subjects for details [11],[12],[22],[31],[32].

1.3 Main Limitation of Present-Day Finite Difference Schemes

It has been shown, though perhaps sketchily, that formulation of an elliptic problem in finite differences produces a finite, though large, system of equations and unknowns. However, it has been implicitly assumed in the above discussion that the problem is defined over a finite portion of space and hence may be modeled by a mesh of finite size. A large number of elliptic problems are unbounded, i.e., they extend to infinity in space, with at least one boundary condition at infinity. Straightforward application of finite differences to this type of problem would result in an infinite number of equations and unknowns. Various attempts have been made to reduce the problem to one of finite size, usually by means of some approximation. The infinitely extending problem is discussed in the next chapter.

CHAPTER 2

THE EXTERIOR ELLIPTIC PROBLEM

2.1 STATEMENT OF PROBLEM

Assume some prescribed distribution of sources and boundaries exists within a finite region R of the (x,y) or (r,z) plane. The region R may contain any combination of material inhomogeneities, time-varying fields and material non-linearities. Outside the region occupied by these distributions assume Laplace's equation is valid everywhere (see Figure 2.1)*. Three-dimensional axially symmetric problems, i.e., problems in the (r,z) plane, will be treated here, although the discussion is valid for two-dimensional problems in the (x,y) plane except for a few differences which will be pointed out.

---

* It is not necessary that the z-axis form a part of R, and certainly in the (x-y) plane R may be located anywhere. The development, in any case, is the same.

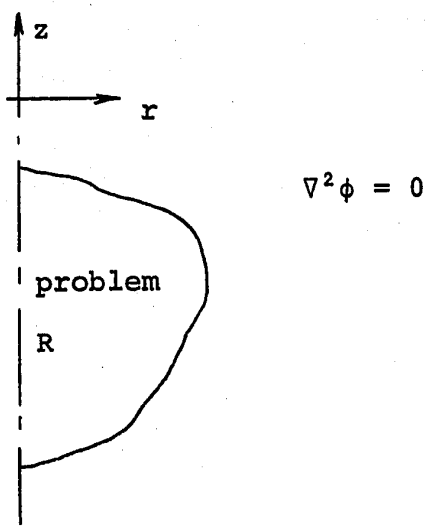

FIGURE 2.1: PROBLEM DEFINITION

The problem to be solved is as follows:

$$\nabla^2\phi = f, \quad (r,z) \in R \tag{2.1}$$

$$\nabla^2\phi = o, \quad (r,z) \notin R \tag{2.2}$$

with the boundary conditions

$$Bl(\phi) = b_1(r,z)\phi + b_2(r,z)\frac{\partial\phi}{\partial r} + b_3(r,z)\frac{\partial\phi}{\partial z} + b_4(r,z) = 0,$$

$$(r,z) \in R \tag{2.3}$$

$$\frac{\partial\phi}{\partial r}, \frac{\partial\phi}{\partial z} \to 0, \quad r,z \to \infty \tag{2.4}$$

where $\phi = \phi(r,z)$ is the potential, and $Bl(\phi)$ represents the prescribed sources and boundaries in the region R. As was stated above, formal formulation of this problem in finite

differences requires the superposition of an infinitely extending mesh on the problem, resulting in an infinite number of equations and unknowns. Various past methods designed to cope with the infinity boundary condition are discussed in the next section. Some theoretical background literature on the subject is considered by Greenspan [32], who considers the problem largely unsolved.

2.2 Past Methods Designed to Cope with the Infinity Boundary Condition

Since the solution to the problem is rarely desired over the entire infinite plane, all approximations to the infinitely extending problem involve solution of the problem in a finite "region of interest", within which the solution is desired. The methods fall roughly into four classes:

2.2.1 IMPOSITION OF AN ARTIFICIAL BOUNDARY: By far the most widespread method of conversion of the infinitely extending problem to one of finite size has been the imposition of an artificial boundary which encloses the region of interest. The problem is, in this way, converted into an interior boundary value problem and the artificial boundary is intuitively chosen in such a way that the resulting interior problem is thought to possess properties that are similar to the infinitely extending problem. For example, Binns and Lawrenson [11] solve the problem of a rectangular permeable

conductor in space by calculating values of potential along a boundary some distance away, the values on the boundary being obtained by imagining all the current in the conductor to be concentrated at the center. In this example, the accuracy of the solution depends on the distance of the artificial boundary from the conductor and the method suffers from two major disadvantages: many more nodes than are actually required are used in the solution and the errors incurred by the use of the artificial boundary are not easily estimated. The most common procedure in this class of approximations is merely to impose a flux-line or equipotential boundary some distance away from the region of interest and then proceed to solve the resulting interior problem [14],[33],[34],[35]. Again, the accuracy of the solution cannot easily be estimated and a very large mesh is required, along with an unnecessarily large increase of computing time and core storage requirement.

2.2.2 CONFORMAL MAPPING TECHNIQUES: An inversion transformation may be used to convert the infinite region outside the region of interest into a second finite region. It is then possible to perform a finite difference solution over both regions [36], where the transformed region becomes a "terminating region" much as in the case of the infinitely extending resistive mesh analogue [6]. The disadvantages in this method are again largely twofold: many more nodes are used than are actually required, and special equations must be written for the irregular configurations at the dividing

line between the region of interest and the terminating region.

A technique similar in principle has been used by Greenspan [37], who describes a numerical inversion mapping technique for the solution of the exterior Dirichlet problem. Greenspan's solution is valid only for simple Dirichlet problems, namely those problems in which the desired region of solution is the exterior of a simply-connected Dirichlet boundary and its applications are therefore limited.

2.2.3 FOURIER EXPANSION OF THE INFINITE REGION SOLUTION:

For problems in which the region exterior to the region of interest has a special geometric configuration (such as the exterior to a circle, or an infinitely extending strip), the solution in this exterior source-free region may be expanded in a Fourier series, which, though containing an infinite number of terms, may be truncated without too much error after a finite number of terms. One such solution concerned the scattering of plane waves from conducting cylinders [38]. The scattering body was modeled in a polar mesh just large enough to enclose it; the scattered field exterior to the resulting circular "region of interest" was expanded in terms of the Hankel functions, the expansion being terminated after a finite number of terms. The coefficients in the expansion were kept variable and the problem solved by a doubly-iterative scheme in which the coefficients in the expansion were corrected after each finite difference solu-

tion of the interior region of interest.

Another such solution concerned the eddy currents in a conductive strip infinite in length [39],[40]. The technique used was similar to the above. The disadvantages of these methods are as follows: First, the geometrical configuration of the region of interest must be such that a Fourier expansion can be found for the exterior region. This may involve use of an awkward mesh (such as the polar mesh in the first above example) or a difficult expansion. Second, there is no a priori knowledge as to where the series expansion may be terminated and hence errors incurred in this method of approximation are not easily (if at all) estimable. Third, an efficient correction scheme for the coefficients of the Fourier expansion is difficult to determine. These methods are then, in general, practical only for special classes of problems.

2.2.4 BOUNDARY RELAXATION TECHNIQUES: Similar to the above class, boundary relaxation, as the name implies, consists of the imposition of an arbitrary contour, or boundary, around the region of interest. A mathematical expression is then derived that relates the potential values on the boundary (and therefore the infinite region solution) to the values of potential (or the potential gradient) in the interior region of interest. The potential values on the arbitrary contour are then corrected iteratively until the solution in the interior region of interest corresponds to the infinitely

extending solution. Some experimental work, limited to 2-dimensional regions of interest with balanced sources has been done [41]. The work was subsequently extended to include unbalanced sources and externally applied fields [42]. In both the above references, the boundary relaxation process was based on a relationship between the potentials and their gradients on the arbitrary artificial boundary. Investigation of convergence and acceleration of the iterative process was empirical, and no error analysis could be given.

Boundary relaxation as developed in this thesis, differs from the above reported methods in four major respects:

1. A potential shift operator is used on the artificial boundary thus eliminating the need to evaluate gradients.
2. The process is formulated in such a way that the standard iterative theory may be applied for its solution.
3. An efficient acceleration algorithm is used to hasten convergence of the iterative process.
4. The need for special boundary operators for different source balances in the region of interest is eliminated.

The above as well as the following are claimed to be original work:

- Rigorous solution of the infinitely extending problem without physical alteration, applied to (x,y), (r,z), coaxial and strip configurations including proof of existence, uniqueness and convergence;
- Formulation of the problem such that standard iterative theory may be applied for its solution;
- A consistent finite difference formulation that links interior and exterior problems and shows that ordinary interior problems are a special case of the general problem;
- Formulation of the problem in a familiar form so that errors may be easily estimated; errors are rigorously examined and an upper bound is derived;
- Development of an accurate, efficient solution algorithm including two acceleration techniques for the iterative process, and
- Derivation of an iterative scheme for the determination of boundary operators for coaxial lines and strips.

2.3 Solution of the Infinitely Extending Problem as the Simultaneous Solution of Two Simple Problems

Let S1 be an arbitrary closed contour enclosing the region R of the problem defined in Section 2.1, as shown in Figure 2.2.

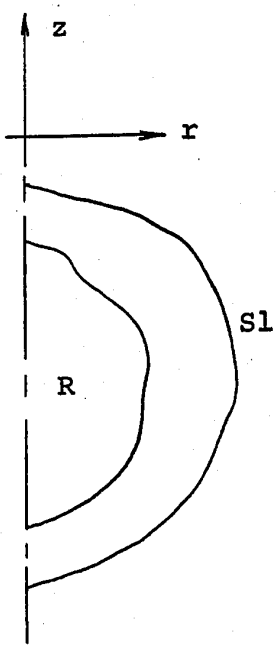

FIGURE 2.2: DIVISION OF THE INFINITE PLANE BY AN ARBITRARY CONTOUR S1

The potential in the region exterior to S1 may be considered to be caused by a source distribution $\sigma(r,z)$ on S1, uniquely defined by [1],

$$\phi(r,z) = \iint_{S1} K(r,z;\rho,\zeta)\ \sigma_{S1}(\rho,\zeta)\,d\rho d\zeta \qquad (2.5)$$

where K is the elementary solution of Laplace's equation in free space *. The source density may be expressed in terms of the outward normal derivative of potential on S1,

$$\sigma = -\varepsilon \frac{\partial \phi}{\partial n_e} \tag{2.6}$$

where n_e denotes the outward normal to S1. Equation 2.5 may now be written as

$$\phi(r,z) = \iint_{S1} K(r,z;\rho,\zeta) \frac{\partial \phi(\rho,\zeta)}{\partial n_e} d\rho d\zeta \tag{2.7}$$

Given the potential values ϕ_{S1} on S1, the normal derivatives everywhere on S1 can be found by solving the integral equation 2.7. The potential everywhere may then be determined by evaluating (2.7) for any desired (r,z). Solving the system (2.1) and (2.2) within S1 simultaneously with (2.7) and imposing continuity of potential and derivatives on S1 yields the solution to the problem.

---

* In the r-z plane the kernel K is given as the solution to a ring charge [43],

$$K(r,z;\rho,\zeta) = \frac{1}{2\pi}\left(\frac{\rho}{r}\right)^{\frac{1}{2}} \frac{2(r\rho)^{\frac{1}{2}}}{\{(z-\zeta)^2+(r+\rho)^2\}^{\frac{1}{2}}} M\left(\frac{2(r\rho)^{\frac{1}{2}}}{\{(z-\zeta)^2+(r+\rho)^2\}^{\frac{1}{2}}}\right)$$

where M is the complete elliptic integral of the first kind. In the (x,y) plane, K is the familiar solution to a line charge,

$$K(x,y;\xi,\eta) = \frac{1}{2\pi} \log_e \sqrt{(x-\xi)^2+(y-\eta)^2}$$

Although (2.7) can be formulated in finite differences [41],[42] the presence of the derivative makes it inconvenient to handle. The derivative may be eliminated from the problem as follows: let S2 be another arbitrary closed contour outside S1, within which it is desired to inspect the solution as shown in Figure 2.3. Equation 2.5 holds for the entire region exterior to S1, including S1. Hence, the potentials ϕ_{S1} and ϕ_{S2} may be expressed as

$$\phi_{S1}(r,z) = \iint_{S1} K(r,z;\rho,\zeta)\ \sigma_{S1}(\rho,\zeta)\ d\rho d\zeta, \quad (r,z) \in S1 \qquad (2.8)$$

$$\phi_{S2}(r,z) = \iint_{S1} K(r,z;\rho,\zeta)\ \sigma_{S1}(\rho,\zeta)\ d\rho d\zeta, \quad (r,z) \in S2 \qquad (2.9)$$

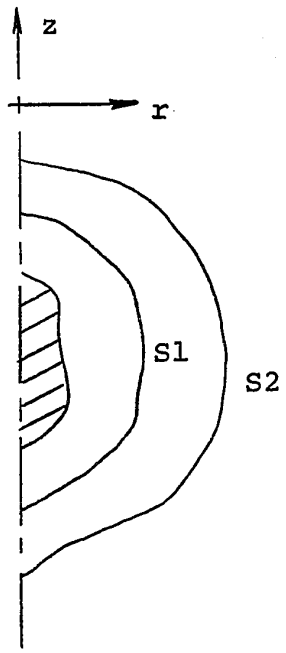

FIGURE 2.3: DEFINITION OF THE CONTOUR S2

Equations 2.8 and 2.9 may be expressed in the symbolic form,

$$\phi_{S1} = L_1 \sigma_{S1} \tag{2.10}$$

$$\phi_{S2} = L_2 \sigma_{S1} \tag{2.11}$$

which may be combined to eliminate the source distribution as

$$\phi_{S2} = L_2 L_1^{-1} \phi_{S1} \tag{2.12}$$

Equation 2.12 represents the solution along S2 of the exterior Dirichlet problem of S1. It, in fact, describes a potential shift from S1 to S2. This shift is unique [44] since ϕ is harmonic outside S1. Since the solution to the original infinitely extending problem is unique [1], simultaneous solution of (2.12) with the interior problem defined by the system (2.1) and (2.2) within S2 provides the required solution to the problem.

A relationship of the form (2.12) is not easy to determine in explicit analytic terms but as will be shown below, is entirely practicable when done by finite difference techniques.

2.4 Linear Space Formulation and Derivation of Boundary Relaxation

The original problem may be stated as follows (see Figure 2.4):

FIGURE 2.4

$$D\phi = f, \quad (r,z) \in R$$
$$D\phi = 0, \quad (r,z) \notin R \tag{2.13}$$

with boundary conditions

$$B1(\phi) = 0, \quad (r,z) \in R$$
$$\lim_{r \to \infty} \phi = \text{const} \tag{2.14}$$

where D is the Laplacian and the boundary conditions in R defined by B1 have been defined in the preceding section. It has also been shown in the preceding section that if the plane is divided as shown in Figure 2.5, where $R \in R1$, the problem may be reduced to solving

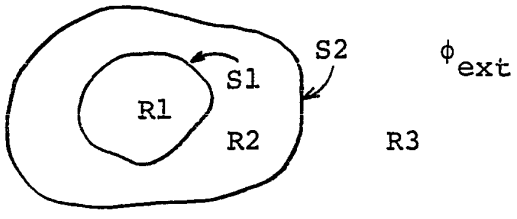

FIGURE 2.5

$$D\ \phi_{int} = f,\ (r,z) \in R1 \cup S1 \cup R2 \cup S2 \tag{2.15}$$

with conditions

$$B1(\phi_{int}) = 0,\ (r,z) \in R$$

$$\phi(S2) = \phi_{S2},\ (r,z) \in S2$$

simultaneously with

$$\phi_{S2} = Q\ \phi_{int} \tag{2.16}$$

where Q contains the second boundary condition (2.14) and is an integro-differential operator. Equations 2.15 and 2.16 may be represented in the symbolic form

$$\phi_{int} = g(\phi_{S2}) \tag{2.17}$$

$$\phi_{S2} = q(\phi_{int}) \tag{2.18}$$

It has been shown in the preceding section that simultaneous solution of (2.17) and (2.18) gives the required unique solution. Equation 2.17 defines a mapping of ϕ_{S2} into ϕ_{int} and equation 2.18 defines a mapping of ϕ_{int} into ϕ_{S2}.

LEMMA 2.1: The mapping defined by

$$\phi_{int} = g(\phi_{S2}) \tag{2.17}$$

exists.

Proof: Given the potential ϕ_{S2}, ϕ_{int} is defined as the solution of the resulting interior Dirichlet problem. For any properly posed problem in the class considered here, this solution exists [1],[44]. Furthermore, this solution is unique [1],[44].

This is stated as

LEMMA 2.2: The mapping defined by (2.17) is unique.

LEMMA 2.3: The mapping defined by

$$\phi_{S2} = q(\phi_{int}) \tag{2.18}$$

exists.

Proof: As has been shown in section 2.3, the operator q acts only on that part of ϕ_{int} on S1, i.e., on ϕ_{S1} ϕ_{int}. The mapping (2.18) defines an exterior Dirichlet problem with given potentials on S1. The solution again exists [1],[37],[44]. Furthermore, the solution is again unique [1],[37],[44]. Hence,

LEMMA 2.4: The mapping defined by (2.18) is unique.

Let F_1 be the space of all functions ϕ_1 satisfying (2.17) with ϕ_{S2} as independent variable. Let F_2 be the space of all functions ϕ_2 satisfying (2.18) with ϕ_{int} as independent variable. The required solution is then given by

$$\phi = F_1 \cap F_2 \tag{2.19}$$

THEOREM 2.1: The required solution to the original problem exists and is uniquely defined by (2.19).

Proof: Existence and uniqueness of the solution to the (well-posed) original problem have been shown elsewhere [1],

[44]. The proof of the second statement of the theorem may be developed as follows: Suppose the solution ϕ to the original problem is known. Considering Lemmas 2.1 to 2.4 and the uniqueness of ϕ, it need merely be shown that the solution ϕ satisfies both (2.17) and (2.18). Given the solution ϕ on S2, suppose that $\phi \in R2 \cup S1 \cup R1$ does not satisfy (2.17). This implies that there exists another solution ϕ^* to (2.17) with $\phi^*_{S2} = \phi_{S2}$, and hence at least two solutions to the original problem, an obvious contradiction. Hence ϕ satisfies (2.17). Now since $R2 \cup S2 \cup R3$ is a source-free region (by definition) and since $\phi = \phi_{ext}$ is harmonic [44] in $R2 \cup S2 \cup R3$, then given ϕ along and exterior to an arbitrary contour S1, the principle of virtual sources [45] guarantees that $\phi_{ext} \in \phi$ and the theorem is proved.

For numerical solution of (2.17) and (2.18), the continuous spaces F_1 and F_2 are inconvenient. Let Ω be a space defined by a point set $\{P_j\}$, j=1,...,n, and let V, an n-vector be the projection of $\phi \in R1 \cup S1 \cup R2 \cup S2$ on the point set $\{P_j\}$, where each element V_j is a representative value of ϕ at that point. Further, define the mapping of ϕ into Ω such that $V \to \phi$ as $n \to \infty$. Let Ω_1 be the projection of F_1 onto Ω and Ω_2 be the projection of F_2 onto Ω. Then the solution in V is given as

$$V = \Omega_1 \cap \Omega_2 \tag{2.20}$$

THEOREM 2.2: The finite difference formulation of ϕ in V is convergent.

Proof: The convergent nature of finite differences is shown elsewhere [10],[11],[12]. Hence the formulation is convergent for consistent finite difference mappings (2.17) and (2.18). Equation 2.17 is the standard interior Dirichlet problem. Moreover, it is shown in the next chapter that a consistent finite difference formulation can be found for (2.18).

Often the construction of the operator q in (2.18) is not convenient in finite differences. As shown in section 2.3, $q \equiv L_2 L_1^{-1}$ where L_1 and L_2 are integral operators of the type

$$L_j\sigma = \iint_S K(r,z;\rho,\zeta)\sigma_{S1}\, dS$$

where K is the elementary solution of D and is well-known. Let L_1 and L_2 be approximated by

$$L_j\sigma \simeq h \left[\sum_{i=1}^{n-1}{}' \left(\int_S K\delta(i)\, dS \right) \sigma + D(K)\sigma\big|_o \right] \equiv L_j'\sigma \qquad (2.21)$$

where the prime on the summation sign means that the singularity point is omitted, h is the mesh length and the contribution due to the singularity is given by the additional additive term, defined by the finite difference operator D. This approximation is convergent (and indeed very useful), i.e., $L_1'\phi \to L_1\phi$, $n \to \infty$. The additive term is justified

since K is a weakly-singular kernel [46]. The approximation belongs to the class of moment methods [47] with impulse functions as the space of testing functions. This result will be exploited in Chapter 3, section 3.2 and Appendices 1 and 2.

Direct simultaneous solution of (2.17) and (2.18) may not always be practical, or indeed possible. An iterative process is suggested by these two equations, as follows:

0) Pick a starting vector (or function) $\phi_{S2}^{(k)}$ in the domain of g.

1) Form a trial solution $\phi_1^{(k)}$ F_1 from (2.17)

2) Form $\phi_2^{(k)}$ F_2 from (2.18)

3) Form an error vector (function) as $e^{(k)} = \phi_2^{(k)} - \phi_1^{(k)}$

4) is $||e^{(k)}||_m \leq \Delta?$, m = 1, or 2, etc.

<u>if not,</u> $\phi_{S2}^{(k+1)} = \phi_{S2}^{(k)} + \beta e^{(k)}$

return to 1)

<u>if yes,</u> solution complete.

The above process can be illustrated as shown in Figure 2.6.

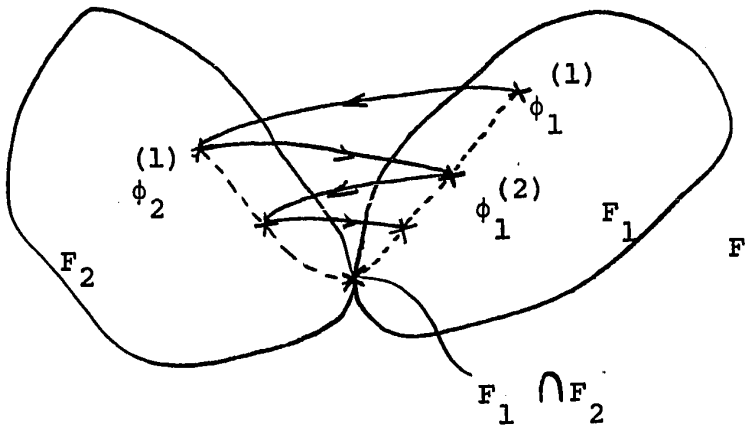

FIGURE 2.6: ITERATIVE SOLUTION OF THE DUAL PROBLEM

It is not yet certain that the above iterations converge. However, the known uniqueness and existence of the solution indicate that if the iterations converge at all, they converge to the solution. In the following chapters it will be shown that the finite difference equivalent iterative schemes converge for ~~all~~ $n \to \infty$. The iterative process is thus convergent, since $\lim_{n \to \infty} V = \phi$. Finite difference formulation of the problem is considered in the next chapter.

CHAPTER 3

FINITE DIFFERENCE FORMULATION

3.1 THE INTERIOR PROBLEM

The method chosen for solution of the interior region was point successive overrelaxation (hereafter abbreviated S.O.R.) using a five-point finite difference formula in a regular square mesh [11],[12]. Although a more sophisticated solution method for the interior region could have been used, it was felt that this method would be the most useful in the study of boundary relaxation for the following two main reasons: First, the method is easily programmed, allowing solution of problems with complicated boundaries and/or material interfaces without extremely complicated or sophisticated housekeeping routines, and secondly, the solution is easily terminated when some desired accuracy is reached, the solution accuracy being easily estimated at any stage. The second reason may seem, at first, trivial; however, as will be seen later, it is by no means necessary (nor desirable) to carry the interior region solution to a high degree of accuracy in the initial stages of boundary relaxation, thus making the boundary relaxation process com-

putationally more efficient. The validity of the first reason may easily be seen on inspection of some of the illustrative examples in Chapter 6.

The five-point formula used for problems in Cartesian coordinates (or x-y) plane) was one allowing material interfaces centered between meshlines. The most general configuration of the five-point star is illustrated in Figure 3.1, which also shows the compass notation used.

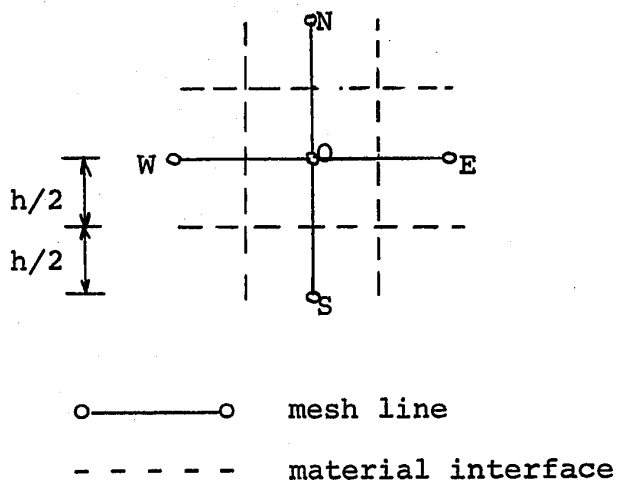

FIGURE 3.1: FIVE-POINT STAR IN X-Y PLANE SHOWING POSSIBLE MATERIAL INTERFACES HALFWAY BETWEEN MESH LINES

With reference to the figure, if the constant K_{ij} is defined as

$$K_{ij} = \frac{\varepsilon_j(\text{region } j)}{\varepsilon_i(\text{region } i)} = \frac{\mu_i(\text{region } i)}{\mu_j(\text{region } j)} \tag{3.1}$$

where ε_i is the permittivity of region i and μ_i is the permeability of region i, the five-point formula is given as [41]

$$\frac{2K_{ON}}{1+K_{ON}} V_N + \frac{(1-K_{ON})}{(1+K_{ON})} V_O + \frac{2K_{OE}}{1+K_{OE}} V_E + \frac{(1-K_{OE})}{(1+K_{OE})} V_O + \frac{2K_{OS}}{1+K_{OS}} V_S \ldots$$

$$+\frac{(1-K_{OS})}{(1+K_{OS})} V_O + \frac{2K_{OW}}{1+K_{OW}} V_W + \frac{(1-K_{OW})}{(1+K_{OW})} V_O - 4V_O + t = 0 \qquad (3.2)$$

The term t in (3.2) represents the source (if any) at the point O*. For the case where the region is homogeneous, i.e., all $K_{ij}=1$, equation 3.2 reduces to the familiar

$$V_N + V_E + V_S + V_W - 4V_O + t = 0 \qquad (3.3)$$

The five-point formula used for 3-dimensional axially symmetric problems (or r-z plane) was one allowing material interfaces along mesh lines as well as along diagonals in the mesh. Figure 3.2 shows the most general configuration of the five-point star, where the permittivity of the medium is assumed to be different in each octant about the point O. Following the convention in Figure 3.2, the finite difference formula at the point O is given as [33]

---

* For electrostatic problems, t is the discretized Poissonian term $t = h^2 \frac{q}{\varepsilon}$ where q is the charge at O and ε is the permittivity. In magnetostatics, $t = h^2 \mu J$, where μ is the permeability of the region O and J is the current density.

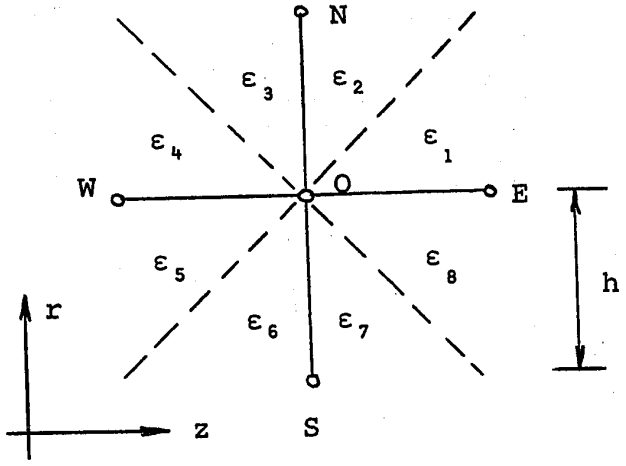

FIGURE 3.2: FIVE-POINT STAR IN R-Z PLANE SHOWING ALL POSSIBLE ALLOWED MATERIAL INTERFACES

$$\frac{1}{2}(K_N V_N + K_S V_S + K_E V_E + K_W V_W - K_O V_O) = 0 \qquad (3.4)$$

where $K_E = (1 + h/4R)\varepsilon_1 + (1 - h/4R)\varepsilon_8$

$K_N = (1 + h/2R)(\varepsilon_2 + \varepsilon_3)$

$K_W = (1 + h/4R)\varepsilon_4 + (1 - h/4R)\varepsilon_5$

$K_S = (1 - h/2R)(\varepsilon_6 + \varepsilon_7)$

$K_O = K_E + K_N + K_W + K_S$

and R is the distance of the point O from the axis of symmetry (the z-axis). For $\varepsilon_1 = \varepsilon_2 = \ldots = \varepsilon_8$, equation 3.4 again reduces to the familiar

$$V_W + V_E + (1 - h/2R)V_S + (1 + h/2R)V_N - 4V_O = 0 \qquad (3.5)$$

Let the problem be posed in a square mesh. Let the vector V represent the potential values at all the nodes within and on S2. Let V be partitioned so that the sub-vector V_{int} represents all the potentials at the nodes interior to S2, and the sub-vector V_{S2} contains all the potentials on the contour S2, viz.,

$$V^T = [V_{int}^T, V_{S2}^T] \tag{3.6}$$

It is readily seen that the five-point formula (3.2) or (3.4) may be written for all interior potentials V_{int}, but not for V_{S2}, since the mesh is not defined exterior to S2.

The interior problem may now be written as a matrix equation,

$$[A' - C] \begin{pmatrix} V_{int} \\ V_{S2} \end{pmatrix} = [B'] \tag{3.7}$$

where A' is a square coefficient submatrix relating the interior potentials V_{int}; C is a rectangular connection matrix with zero or positive elements relating the interior potentials to those on S2, and the column vector B' depends on the prescribed sources and fixed potentials in the interior region. C has been written with a minus sign for reasons of convenience which will be apparent later. The system (3.7), as it stands, has no solution since the overall coefficient matrix is not square, i.e., there are more unknowns than there are equations.

If, however, the potentials V_{S2} are known (or given), then there is obtained, by direct substitution, the familiar solvable system for the interior Dirichlet problem,

$$AV = B \tag{3.8}$$

However, since the potentials on S2 are not known a priori for the exterior problem, more equations are required. This is considered in the next section.

3.2 Approximation of the Boundary Operator

It was shown in Chapter 2 that the solution of the infinitely extending problem may be obtained as the solution to the interior problem within the contour S2, simultaneously with

$$\phi_{S1}(r,z) = \iint_{S1} K(r,z;\rho,\zeta)\sigma_{S1}(\rho,\zeta)\, d\rho d\zeta, \quad (r,z) \in S1 \tag{2.8}$$

and

$$\phi_{S2}(r,z) = \iint_{S1} K(r,z;\rho,\zeta)\sigma_{S1}(\rho,\zeta)\, d\rho d\zeta, \quad (r,z) \in S2 \tag{2.9}$$

which were combined as

$$\phi_{S2} = L_2 L_1^{-1} \phi_{S1} \tag{2.12}$$

The problem, as was stated in the previous section,

is posed in a regular square mesh*. Let the contours S1 and S2 be contours of adjacent nodes in the mesh as shown in Figure 3.3. S1 is represented by x's and S2 by o's. The potentials on S1 and S2 are represented by the vectors V_{S1}, an n-vector, and by V_{S2}, an m-vector, respectively. Suppose the potential distribution due to a source at one point in the infinite mesh is known to be,

$$V(r,z) = I_o(r_o,z_o)\ \psi(r,z;r_o,z_o) \tag{3.9}$$

where (r_o,z_o) are the coordinates of the source, V is the potential at the point (r,z) and I_o is the source strength. For problems in Cartesian coordinates, (r,z) should be replaced by (x,y). Equations 2.8 and 2.9 may now be approximated by

$$\phi_{S1} \simeq V(r,z)\big|_{S1} = \sum_{(r_o,z_o)\in S1} I_o(r_o,z_o)\psi(r,z;r_o,z_o),\ (r,z)\in S1 \tag{3.10}$$

$$\phi_{S2} \simeq V(r,z)\big|_{S2} = \sum_{(r_o,z_o)\in S1} I_o(r_o,z_o)\psi(r,z;r_o,z_o),\ (r,z)\in S2 \tag{3.11}$$

---

* The mesh does not necessarily have to be square, nor even regular. Use of a square mesh simplifies computation considerably, but does not detract from the generality of the analysis.

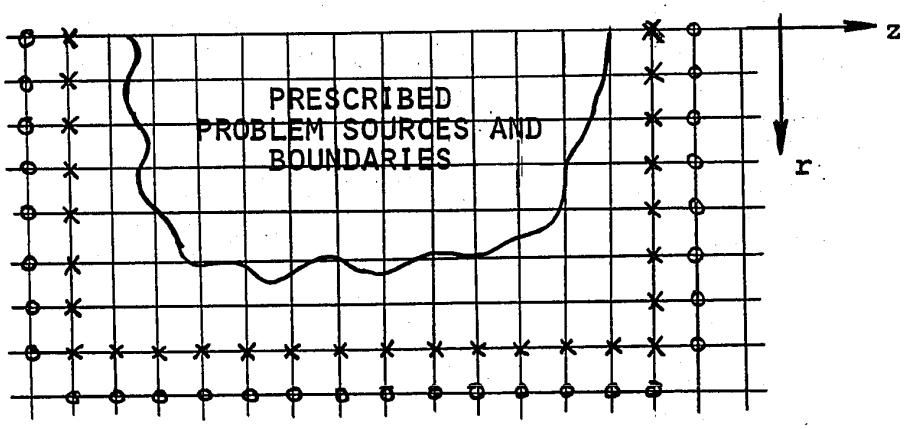

FIGURE 3.3: DEFINITION OF S1 AND S2 FOR A RECTANGULAR INTERIOR REGION IN THE R-Z PLANE

which may be written in matrix notation as

$$V_{S1} = SI_o \tag{3.12}$$

and

$$V_{S2} = PI_o \tag{3.13}$$

where S is an n by n square matrix, P is an m by n rectangular matrix, and each element of P and S is an appropriate value of ψ.

Equations 3.12 and 3.13 yield an expression for V_{S2} in terms of V_{S1}, viz.,

$$V_{S2} = PS^{-1}V_{S1} \tag{3.14}$$

or,

$$V_{S2} = QV_{S1} \tag{3.15}$$

where Q is an m by n rectangular matrix. Equation 3.15 is the finite difference equivalent of (2.12).

In order to maintain a consistent finite difference formulation, the function ψ (values of which form the matrices P and S) must be chosen to be the exact elementary solution of the finite difference Laplacian. Such a solution can be found for both the x-y and r-z planes. The discretized Green's function for the x-y plane has been found by Amstutz [48] who gives the solution as a convergent integral of the form

$$\psi(m,n) = \frac{1}{8\pi^2} \int_{\Gamma} \frac{1 - \cos(ma+nb)}{2 - \cos a - \cos b} \, da \, db \tag{3.16}$$

where Γ is the square $(-\pi \leq a \leq \pi, -\pi \leq b \leq \pi)$. This integral is conveniently evaluated for the case m=n and by symmetry and application of the five-point operator may be evaluated for other values of m and n. This is discussed in detail in Appendix 1, as well as the methods of computing Q matrices for rectangular regions in the x-y plane.

The Green's function for the discretized Laplacian in the r-z plane has been discussed by Sander [49], who formulates ψ as a convergent integral involving trigonometric and hypergeometric functions. His solution is computationally prohibitive; however, point values of the Green's function in the continuous plane (the complete elliptic integral of the

first kind) have been found to give good results. Sander's solution as well as the method used to general Q matrices for the r-z plane are discussed in Appendix 2.

The matrix Q in equation 3.15 is referred to as a "shift" matrix, since it represents the potential shift from the contour S1 to the contour S2. As will be shown, the shift matrix provides the necessary remaining equations (for equation 3.7) to make solution of the problem possible.

The shift matrix relates potentials on S1 to those on S2. As is readily seen, the potentials V_{S1} on S1 are a subset of the potentials V_{int} of the interior region. Equation 3.15 may therefore be rewritten as

$$[-Q' \; I] \begin{pmatrix} V_{int} \\ V_{S2} \end{pmatrix} = 0 \qquad (3.17)$$

where the rectangular submatrix Q' contains columns of Q and columns of zeros, and I is the identity matrix. The system (3.17) along with the system (3.7) allows solution of the problem. Before the actual solution is discussed, however, some of the properties of the shift matrix Q will be examined briefly.

3.3 Some Shift Matrix Properties

A variation of the maximum principle [12],[32] will be stated first:

Let the mesh exterior to the contour S1 be denoted by R_h. Further, let the nodes on the contour S1 be denoted by S_h. Assume that the region R_h is connected and that in R_h the function V satisfies

$$D_h(V_O) \equiv c_N V_N + c_E V_E + c_S V_S + C_W V_W - c_O V_O = 0 \qquad (3.18)$$

where $c_{N,E,S,W} > 0$ and $c_O = \sum_{NESW} c_i$. Then the maximum principle may be stated as

THEOREM 3.1: A function V which satisfies (3.18) at each grid point in R_h, takes on its maximum value in S_h.

Proof: Assume the contrary, namely that at some point P in R_h the function takes on its maximum value, say M. Then, from equation 3.18,

$$c_N V_N + c_E V_E + c_S V_S + c_W V_W - (c_N+c_E+c_S+c_W)V_P = 0$$

or

$$c_N(V_N-V_P) + c_E(V_E-V_P) + c_S(V_S-V_P) + c_W(V_W-V_P) = 0$$

which implies that

$$V_N = V_E = V_S = V_W = V_P = M$$

In other words, V must assume the value M at the four adjacent points. Since R_h was assumed to be connected, the process may be continued for all points in R_h, including those adjacent to S_h. Hence all points in R_h and S_h take on the value

M. This, however, contradicts the original assumption that V takes on its maximum value at P, Q.E.D.

The maximum principle may be used to show uniqueness of (3.15), i.e., that the shift operation (or the shift matrix) is unique for given contours S1 and S2. This may be done as follows: All points in S2 are in the region R_h where (3.18) holds. Assume that, for given potentials in S_h, the solution V in R_h is not unique. Then there must exist at least two solutions V_1 and V_2, both of which satisfy the given boundary conditions, namely,

$$D_h(V_1) = 0 \text{ in } R_h, \quad V_1 = f(S) \text{ in } S_h$$

and

$$D_h(V_2) = 0 \text{ in } R_h, \quad V_2 = f(S) \text{ in } S_h$$

Since D_h is a linear operator,

$$D_h(V_1-V_2) = D_hV_1 - D_hV_2 = 0$$

and if $V_d = V_1-V_2$, the problem in V_d becomes

$$D_h(V_d) = 0 \text{ in } R_h, \quad V_d = 0 \text{ in } S_h$$

From the maximum principle, the solution satisfies

$$V_d \leq 0 \text{ in } R_h$$

However,

$$D_h(-V_d) = 0 \text{ in } R_h, \quad -V_d = 0 \text{ in } S_h,$$

hence

$$-V_d \leq 0 \text{ in } R_h.$$

Therefore, $V_d = 0$, $V_1 = V_2$, and the solution is unique. The potential values on S2 are a subset of the solution V, hence, given potentials on S1, the potentials on S2 are uniquely determined. A similar proof holds for equations 3.12 and 3.13, though slight modifications are required. (All sources but one are sequentially set to zero and a source term is introduced in the difference operator D_h; the maximum principle is used to show uniqueness of each solution, and all solutions are then added to obtain the total solution). Existence of (3.12) and (3.13) has been shown [48],[49]. Since the matrix in (3.12) is square, and the solution is unique, the matrix S in (3.12) possesses an inverse, and Q can be found. All the above results are stated in

THEOREM 3.2: Given the contours S1 and S2, the potential shift from S1 to S2 is uniquely determined by equation 3.14 or 3.15.

The shift matrix Q also possesses two positivity properties * that are useful in the derivation of further

---

* It is implicitly assumed that the potential reference is zero potential, located outside S2 in the case of the x-y plane, and at infinity in the r-z plane.

results. These properties are stated in two lemmas:

LEMMA 3.1: All elements q_{ij} of the matrix Q in (3.15) satisfy

$$\sum_{j=1}^{n} q_{ij} < 1, \quad i=1,2,\ldots,m$$

LEMMA 3.2: All elements q_{ij} of the matrix Q in (3.15) satisfy

$$0 < q_{ij} < 1$$

Proof: Since S2 is in a Laplacian region, the proof of the first lemma follows easily from the maximum principle on setting all potentials on S1 to unity. This applies to any simply-connected contour S2. The proof of the second lemma follows on setting all potentials on S1 to zero and then setting each, in turn, to unity.

3.4 The Combined Problem

Equations 3.7 and 3.17 may be conjoined into a single matrix equation, written in the partitioned form,

$$\begin{bmatrix} A' & -C \\ -Q & I \end{bmatrix} \begin{bmatrix} V_{int} \\ V_{S2} \end{bmatrix} = \begin{bmatrix} B' \\ 0 \end{bmatrix} \tag{3.19}$$

where the square submatrix A' is the same as would be obtained for an interior problem with a Dirichlet boundary at S2, I is

the identity matrix, C is the connection matrix defined in section 3.1 above, and Q' is as defined in section 3.2 above. The submatrix A' has positive diagonal elements and negative or zero off-diagonal elements. All elements of C and Q are either positive or zero.

In the formulation of the problem as in (3.19), the set of equations may be thought of as follows: All interior potentials V_{int} satisfy a five-point difference formula of the form

$$\sum_{NESW} c_j V_j - c_O V_O = 0$$

At all nodes on S2, the potentials V_{S2} satisfy an n-point formula of the form

$$\sum_{j=1}^{n} (q_{ij} V_{S1_j}) - V_{S2_i} = 0, \quad i=1,2,\ldots,m$$

where the potentials V_{S1} are a subset of the interior potentials V_{int}. Equation 3.19 may thus be written in the form

$$A V = B \tag{3.20}$$

in the manner of an interior problem. It remains to prove

THEOREM 3.3: $A^{-1} > 0$

Proof: The usual coefficient matrix for the interior problem satisfies the theorem (i.e., the submatrix A' in

equation 3.19). It is therefore only necessary to show that the introduction of the n-point formula for the potentials on S2 does not change the conditions for which this result is known to hold true. Specifically, A is a real, square matrix with $a_{ii} > 0$ and $a_{ij} \leq 0$, $i \neq j$ (by Lemma 3.2). Also, $a_{ii} \geq \sum_{j} |a_{ij}|$, by Lemma 3.1 with strict inequality for some i, i.e., A is diagonally dominant. The matrix A is also irreducible (this can be shown though very tedious, as in ref. 31, pp. 19-20). Therefore [31], $\det(A) \neq 0$ and $A^{-1} > 0$, Q.E.D.

A solution to the problem may thus be obtained as

$$V = A^{-1} B \tag{3.21}$$

Since the matrix A is usually of very high order, direct inversion is rarely convenient. The next chapter shows how standard iterative theory may be applied to the system (3.19) or (3.20). First, however, the relationship of the exterior problem, as formulated here, to the interior problem will be discussed.

3.5 Relationship between Interior and Exterior Problems

Consider a slightly generalized version of equation 3.19, viz.,

$$\begin{bmatrix} A' & -C \\ -Q' & I \end{bmatrix} \begin{bmatrix} V_{int} \\ V_{S2} \end{bmatrix} = \begin{bmatrix} B' \\ D \end{bmatrix} \tag{3.22}$$

where the zero subvector in the right-hand side of (3.19) has been replaced by the more general subvector D. It will be shown that the interior Dirichlet, interior Neumann as well as the exterior problem can be formulated as in (3.22).

INTERIOR DIRICHLET PROBLEM: In this problem, the potential on S2 is prescribed, i.e., D is non-zero in general. The problem may be put into the form (3.22) by setting the shift operator to zero, viz.,

$$\begin{bmatrix} A' & -C \\ 0 & I \end{bmatrix} \begin{bmatrix} V_{int} \\ V_{S2} \end{bmatrix} = \begin{bmatrix} B' \\ D \end{bmatrix}$$

and by substitution, may be reduced to

$$A'' \, V_{int} = B'' \tag{3.23}$$

which is the familiar form.

INTERIOR PROBLEM WITH A CLOSED NEUMANN BOUNDARY HALFWAY BETWEEN MESH LINES: For this problem, the contours S1 and S2 are chosen to lie one-half mesh unit inside and outside the given Neumann boundary respectively. The problem may now be written as

$$\begin{bmatrix} A' & -C \\ -I' & I \end{bmatrix} \begin{bmatrix} V_{int} \\ V_{S2} \end{bmatrix} \quad \begin{bmatrix} B' \\ D \end{bmatrix}$$

where the submatrix I' contains columns of zeros interspersed with columns that contain one unity element with the rest zero. In the case that the boundary is a flux line, i.e., a homogeneous Neumann boundary, the subvector D is zero. By substitution, the problem may again be reduced to the form (3.23).

CLOSED NEUMANN BOUNDARY ALONG MESH LINES: This problem is similar to the above, with S1 and S2 chosen to lie one mesh unit inside and outside the given boundary respectively. Again, for a homogeneous Neumann boundary, D is zero and the problem may be formulated as above. The matrix operator I' may be thought of as being a "unity shift" operator, since it reflects potentials from S1 to S2.

Thus it is seen that interior and exterior problems of the type considered here differ only in the definition of the boundary operator, a fact that may be useful in further research in this area.

CHAPTER 4

ITERATIVE SOLUTION

As was mentioned in Chapter 3, the matrix problem, because of its size, is probably most conveniently solved by some iterative method. Direct inversion of the coefficient matrix has been considered [14] to overcome convergence difficulties due to inhomogeneous regions with widely-differing material constants. Iterative convergence difficulties of such problems have been overcome, however [30], so that this reason is assuming less importance. Iterative methods offer, in the main, two distinct advantages over the so-called direct methods. First, the coefficient matrix is such that individual elements are easily generated as needed and do not need to be stored. These matrices are, as a rule, very sparse; that is, they contain a large number of zero elements. Direct inversion destroys, in general, the sparsity of these matrices. As more and more fast access memory becomes available to the programmer, however, this advantage is becoming less important. Second, many iterative methods do not suffer from round-off error propagation as, for the most part, they tend to be self-correcting in this respect. It is shown in this Chapter that the standard iterative theory may be applied to the linear system (3.19) or (3.20).

4.1 Preliminary Background Theory

In order to demonstrate how an iterative method may be arrived at, consider a system of equations such as the following

$$Ax = b \tag{4.1}$$

Write the coefficient matrix A as the sum of two matrices

$$A = M - N \tag{4.2}$$

Substitute (4.2) into (4.1) to yield

$$Mx = Nx + b$$

or

$$x = M^{-1}Nx + M^{-1}b \tag{4.3}$$

Equation 4.3 suggests an iterative method as,

$$x^{(k+1)} = M^{-1}Nx^{(k)} + M^{-1}b, \quad k \geq 0 \tag{4.4}$$

where the superscript (k) again refers to the number of completed iterations. Define an error vector as

$$e^{(k)} = x^{(k)} - x,$$

where x is the solution. Then, substitution into (4.4) and use of (4.3) yields

$$e^{(k+1)} = M^{-1}Ne^{(k)} \tag{4.5}$$

In order for convergence to be obtained, that is, for the condition

$$\lim_{k \to \infty} e^{(k)} = 0$$

to hold for any arbitrary $e^{(0)}$, it is necessary that all eigenvalues of the matrix $M^{-1}N$ lie within the unit circle; or stated another way, the spectral radius, $\mu(M^{-1}N)$ must be less than unity.

A definition and a theorem from matrix theory [31] will now be stated:

DEFINITION 4.1: For nxn real matrices A, M and N, $A = M-N$ is a regular splitting of the matrix A if M is non-singular with $M^{-1} \geq 0$ and $N \geq 0$.

THEOREM 4.1: If $A = M-N$ is a regular splitting of the matrix A and $A^{-1} \geq 0$ then

$$\mu(M^{-1}N) = \frac{\mu(A^{-1}N)}{1 + \mu(A^{-1}N)} < 1$$

i.e., the spectral radius of $M^{-1}N$ is less than one.

The iterative method associated with this splitting converges for any initial vector. That is, the sequence of $v^{(k)}$ obtained from

$$Mv^{(k+1)} = Nv^{(k)} + B, \quad k \geq 0 \tag{4.6}$$

which can be written as

$$v^{(k+1)} = M^{-1}Nv^{(k)} + M^{-1}B, \quad k \geq 0 \tag{4.7}$$

converges for any $v^{(0)}$. The proof may be found in ref. 31, p.89.

4.2 Convergence of Some Standard Iterative Schemes

The regular-splitting theorem 4.1 may be used to prove convergence of the classical Jacobi [19] and Gauss-Seidel [16] methods when applied to the system of equations (3.19) or (3.20). Application to the system (3.20) yields what are conventionally termed "point methods", while application to the system as posed in (3.19) suggests the iterative "block methods", which correspond to the iterative method suggested in Chapter 2, § 2.4. The point methods will be discussed first.

In the system of equations

$$AV = B \tag{3.20}$$

the coefficient matrix A may be written as the matrix sum

$$A = D - L - U \tag{4.7}$$

where D= diag. $\{a_{11}, a_{22}, \ldots, a_{nn}\}$ and L and U are respectively strictly lower and upper triangular nxn matrices, i.e., possess zero diagonal elements. Note that D has all positive, non-zero diagonal elements, the elements of L and U are all positive or zero and no special ordering of A has been assumed.

To obtain the point-Jacobi method, the matrices M and N in equation 4.6 or 4.7 are chosen as

$$M = D, \qquad N = L + U \tag{4.8}$$

Equation 4.7 then becomes

$$v^{(k+1)} = D^{-1}(L+U)\ v^{(k)} + D^{-1}B \tag{4.9}$$

Since all diagonal elements of D are positive, clearly $D^{-1} \geq 0$. Also by inspection, $(L+U) \geq 0$. The splitting is therefore regular and by Theorem 4.1 the point-Jacobi method converges. This is stated as

COROLLARY 4.1: The point Jacobi method for solution of (3.20) converges.

To obtain the point Liebmann method, or point Gauss-Seidel, the matrices M and N are chosen as

$$M = D - L, \qquad N = U \tag{4.10}$$

By Theorem 3.3, $(D-L)^{-1} \geq 0$. Also, by inspection, $U \geq 0$. The splitting is again regular, and by Theorem 4.1, the point Liebmann method converges. This is stated as

COROLLARY 4.2: The point Liebmann method for solution of (3.20) converges.

The extrapolated Liebmann method, or point successive overrelaxation (S.O.R.) is obtained by choosing M and N as

$$M = \frac{1}{\omega}(D - \omega L), \qquad N = \frac{1}{\omega}\left[\omega U + (1-\omega)D\right], \ \omega \neq 0 \tag{4.11}$$

where ω is a real constant, termed the overrelaxation or acceleration factor. The splitting is regular for $0 < \omega \leq 1$. The iterative method associated with this splitting therefore converges for that interval of ω, and, by continuity, point S.O.R.

converges for some interval of ω containing one. This result is stated as

COROLLARY 4.3: The point S.O.R. method for solution of (3.20) converges for some interval of ω containing one, and convergence is assured for $0 < \omega \leq 1$.

The lack of an upper bound of ω for which convergence is assured is discussed further in section 4.4 below. The fact that such a bound does not yet exist does not, however, detract from the usefulness of the method.

The block methods are derived from the formulation of the problem as in

$$\begin{bmatrix} A' & -C \\ -Q' & I \end{bmatrix} \begin{bmatrix} V_{int} \\ V_{S2} \end{bmatrix} = \begin{bmatrix} B' \\ 0 \end{bmatrix} \tag{3.19}$$

The block Jacobi method is obtained by choosing M and N as

$$M = \begin{bmatrix} A' & 0 \\ 0 & I \end{bmatrix}, \quad N = \begin{bmatrix} 0 & C \\ Q' & 0 \end{bmatrix} \tag{4.12}$$

This splitting is regular. Hence the block Jacobi method

$$\begin{bmatrix} V_{int} \\ V_{S2} \end{bmatrix}^{(k+1)} = \begin{bmatrix} 0 & (A')^{-1}C \\ Q' & 0 \end{bmatrix} \begin{bmatrix} V_{int} \\ V_{S2} \end{bmatrix}^{(k)} + \begin{bmatrix} (A')^{-1} & 0 \\ 0 & I \end{bmatrix} \begin{bmatrix} B' \\ 0 \end{bmatrix} \tag{4.13}$$

converges. This is stated as

COROLLARY 4.4: The block Jacobi method for solution of (3.19) converges.

A more useful method is the block successive relaxation, or block Gauss-Seidel method, obtained by choosing M and N as

$$M = \begin{bmatrix} A' & 0 \\ -Q' & I \end{bmatrix}, \qquad N = \begin{bmatrix} 0 & C \\ 0 & 0 \end{bmatrix} \tag{4.14}$$

The splitting is clearly regular. Hence, the iterative method

$$\begin{bmatrix} V_{int} \\ V_{S2} \end{bmatrix}^{(k+1)} = \begin{bmatrix} A' & 0 \\ -Q' & I \end{bmatrix}^{-1} \begin{bmatrix} 0 & C \\ 0 & 0 \end{bmatrix} \begin{bmatrix} V_{int} \\ V_{S2} \end{bmatrix}^{(k)} + \begin{bmatrix} A' & 0 \\ -Q' & I \end{bmatrix}^{-1} \begin{bmatrix} B' \\ 0 \end{bmatrix} \tag{4.15}$$

converges according to Theorem 4.1. Note that

$$\begin{bmatrix} A' & 0 \\ -Q' & I \end{bmatrix}^{-1} = \begin{bmatrix} (A')^{-1} & 0 \\ Q'(A')^{-1} & I \end{bmatrix}$$

so that (4.15) may be written as

$$\begin{bmatrix} V_{int} \\ V_{S2} \end{bmatrix}^{(k+1)} = \begin{bmatrix} 0 & (A')^{-1}C \\ 0 & Q'(A')^{-1}C \end{bmatrix} \begin{bmatrix} V_{int} \\ V_{S2} \end{bmatrix}^{(k)} + \begin{bmatrix} (A')^{-1} & 0 \\ Q'(A')^{-1} & I \end{bmatrix} \begin{bmatrix} B' \\ 0 \end{bmatrix} \tag{4.16}$$

and decomposed into its two constituent equations

$$V_{int}^{(k+1)} = (A')^{-1}CV_{S2}^{(k)} + (A')^{-1}B' \tag{4.17}$$

and

$$V_{S2}^{(k+1)} = Q'V_{int}^{(k+1)} \tag{4.18}$$

In equation 4.18, the vector V_{int} may be replaced by the subvector V_{S1} if Q' is replaced by Q (see equation 3.15). Hence (4.18) becomes

$$V_{S2}^{(k+1)} = QV_{S1}^{(k+1)} \tag{4.19}$$

Equations 4.17 and 4.19 describe an iterative scheme as follows: an estimate is made of $V_{S2}^{(0)}$. The resulting interior Dirichlet problem is then solved to find $V_{int}^{(1)}$, and hence $V_{S1}^{(1)}$. $V_{S2}^{(1)}$ is then found from (4.19) and the process is repeated until convergence is obtained. This result is stated as

COROLLARY 4.5: The block successive relaxation method described by equations 4.17 and 4.19 converges.

This result will be useful in the derivation of further results, as shown below. The next section deals with error estimates.

4.3 Error Estimates

It has been shown that a consistent finite difference formulation can be found for the infinitely extending

problem, in the manner of an interior problem. Solutions of problems in finite differences are, as a rule, subject to two sources of error. The first main source of error arises from the fact that even an exact solution to the matrix problem is just that, a solution to the matrix problem, which, it will be recalled, is merely an approximation to the original differential or integral equation. The approximation or discretization error may be reduced to an arbitrarily small value by decreasing the mesh size. This subject has received (and indeed is still receiving) attention in the literature [10],[11],[12],[50] and will not be expounded upon here.

The other source of error arises from the fact that the set of linear equations is not solved exactly. This is true, in general, whether an iterative method is used or not. In direct solution of the equations (such as by Gaussian elimination or direct inversion of the matrix), finite-precision arithmetic limits the accuracy of solution (round-off error). This can sometimes be compensated by one or more iterative passes subsequent to the direct solution; however, this is not always practical or possible. The iterative methods discussed here are self-correcting as regards round-off error [12]. However, the iterative process is usually terminated before solution accuracy comparable to machine precision is reached. It is therefore desirable that the error, or at least a bound, at any stage in the iterative process be determinable.

Since the finite difference formulation of the problem is consistent, the iteration errors for the point methods are consistent with errors in interior problems, and may be determined in the same manner [10],[11],[12],[25], [32]. Error estimates have to be derived for the block methods, however. Again, in the block methods, point methods are used for the solution of the interior region. Hence, all that is required is an estimate of the error on the contour S2 at any stage of the process. An analysis similar to that of Schiske and Ühlig [51] yields the following:

Equation 4.18 may be written as

$$V_{S2}^{(k+1)} = Q'(A')^{-1}C\, V_{S2}^{(k)} + Q'(A')^{-1}B' \qquad (4.20)$$

An upper bound $\gamma < 1$ on the row-sums of the matrix $Q'(A')^{-1}C$ is required. This may be obtained as follows:

a) Set all V_{S2} to unity and all other sources to zero (making B' identically zero). Solve the interior problem for V_{int}. Let

$$\alpha_1 = \max \{V_{int_j}\}$$

α_1 is then the highest row-sum of the matrix $(A')^{-1}C$.

b) Let $\alpha_2 = \max \{ \sum_{j=1}^{n} q_{ij} \}$, $i = 1,2,\ldots,m$

$\gamma = \alpha_1\alpha_2$ is then an upper bound on the row-sums of $Q'(A')^{-1}C$. When, after the k^{th} step of the iteration procedure, it is found that, for all j,

$$|V_{S2_j}^{(k)} - V_{S2_j}^{(k-1)}| \leq \varepsilon$$

then after the $(k+1)^{th}$ step, for all j,

$$|V_{S2_j}^{(k+1)} - V_{S2_j}^{(k)}| \leq \varepsilon\cdot\gamma$$

after k+n steps,

$$|V_{S2_j}^{(k+n)} - V_{S2_j}^{(k)}| \leq \sum_{i=1}^{n} \varepsilon\cdot\gamma^i$$

Now, since $\lim_{k\to\infty} V_{S2_j}^{(k+n)} = V_{S2_j}$, where V_{S2_j} is the solution, then

$$|V_{S2_j} - V_{S2_j}^{(k)}| \leq \varepsilon\cdot\frac{\gamma}{1-\gamma} \qquad (4.21)$$

which gives the required error estimate.

4.4 Acceleration of the Iterative Methods

As in the iterative solution of the interior problem, the iterative methods discussed here may be accelerated by overcorrecting the potential values at each stage of the process. The standard methods of acceleration can be applied to boundary relaxation, though many of the theoretical results

valid for interior problems do not necessarily apply. As before, the point methods are discussed first.

Extension of point successive overrelaxation to boundary relaxation has been introduced in section 4.2 above, where point successive underrelaxation was shown to be convergent (Corollary 4.3), and, by continuity, has been shown to be convergent for some interval of overrelaxation factor ω, containing unity. An upper bound of ω for which convergence is assured has not been derived. Numerical studies have shown that acceleration is obtained for $\omega > 1$, though the increase in the rate of convergence is not so dramatic as for the corresponding interior problem. The reason for this is that the coefficient matrix in (3.20) is not symmetric, and the corresponding Jacobi matrix $D^{-1}(L+U)$ of equation 4.9 has eigenvalues that have significant imaginary parts. Wrigley [29] discusses acceleration of problems of this type and concludes that very significant acceleration cannot be achieved. In any event, the point S.O.R. method has not been found computationally efficient because of the large number of arithmetic operations in application of the n-point formula on the contour S2. Moreover, the coefficient matrix of equation 3.20 does not possess Young's property "A" [24], so that the standard theoretical results for point S.O.R. do not necessarily apply. Further research is indicated in this area.

The block methods, specifically the block Gauss-Seidel, have been found to be more practical. Acceleration of the above block Gauss-Seidel method may be accomplished as follows. In

equation 4.6 or 4.7 the matrices M and N are chosen as

$$M = \frac{1}{\omega}\begin{bmatrix} A' & 0 \\ -\omega Q' & I \end{bmatrix}, \quad N = \frac{1}{\omega}\begin{bmatrix} (1-\omega)A' & \omega C \\ 0 & (1-\omega)I \end{bmatrix}, \omega \neq 0$$

Substituting into (4.7) and noting that

$$M^{-1} = \omega \begin{bmatrix} (A')^{-1} & 0 \\ \omega Q'(A')^{-1} & I \end{bmatrix}$$

there is obtained

$$\begin{bmatrix} V_{int} \\ V_{S2} \end{bmatrix}^{(k+1)} = \begin{bmatrix} (1-\omega)I & \omega(A')^{-1}C \\ \omega(1-\omega)Q' & \omega^2 Q'(A')^{-1}C+(1-\omega)I \end{bmatrix} \begin{bmatrix} V_{int} \\ V_{S2} \end{bmatrix}^{(k)}$$

$$+ \omega \begin{bmatrix} (A')^{-1} & 0 \\ \omega Q'(A')^{-1} & I \end{bmatrix} \begin{bmatrix} B' \\ 0 \end{bmatrix} \qquad (4.22)$$

Equation 4.22 may be decomposed into its two constituent equations, viz.,

$$V_{int}^{(k+1)} = (1-\omega)IV_{int}^{(k)} + \omega(A')^{-1}CV_{S2}^{(k)} + \omega(A')^{-1}B' \qquad (4.23)$$

$$V_{S2}^{(k+1)} = \omega Q'[(1-\omega)I\, V_{int}^{(k)} + \omega(A')^{-1}CV_{S2}^{(k)} + \omega(A')^{-1}B']$$

$$+ (1-\omega)I\, V_{S2}^{(k)} = \omega Q' V_{int}^{(k+1)} + (1-\omega)I\, V_{S2}^{(k)} \qquad (4.24)$$

which can be interpreted as follows:

$$V_{int}^{(k+1)} + V_{int}^{(k)} + \omega(V^*_{int} - V_{int}^{(k)}) \qquad (4.25)$$

where

$$V^*_{int} = (A')^{-1}CV_{S2}^{(k)} + (A')^{-1}B' \qquad (4.26)$$

and

$$V_{S2}^{(k+1)} = V_{S2}^{(k)} + \omega(V^*_{S2} - V_{S2}^{(k)}) \qquad (4.27)$$

where

$$V^*_{S2} = Q' V_{int}^{(k+1)} \qquad (4.28)$$

Equations 4.25 through 4.28 describe an iterative scheme as follows:

An estimate is made of $V_{S2}^{(0)}$. V^*_{int} is found from (4.26), i.e., by solving the interior problem. The interior potentials are then corrected as in (4.25). V^*_{S2} is found by application of the shift matrix, as in equation 4.28, V_{S2} is then corrected as in (4.27) and the process is repeated until convergence is obtained.

A loose upper bound on the block overrelaxation factor ω can be easily ascertained. In the partitioning of the coefficient matrix as in equation 3.19, the square submatrices A' and I are clearly nonsingular (Theorem 3.3). For this partitioning, the coefficient matrix is 2-cyclic [31]. The block Jacobi matrix corresponding to this partitioning is the iteration matrix of (4.13),

$$J \equiv \begin{pmatrix} 0 & (A')^{-1}C \\ Q' & 0 \end{pmatrix}$$

Also, the coefficient matrix is consistently ordered [31] for this partitioning. From Corollary 4.4, the block Jacobi method converges. Now let J = L+U where

$$L = \begin{pmatrix} 0 & 0 \\ Q' & 0 \end{pmatrix} \qquad U = \begin{pmatrix} 0 & (A')^{-1}C \\ 0 & 0 \end{pmatrix}$$

The block successive overrelaxation scheme may be written as

$$(I - \omega L)V^{(k+1)} = [\omega U + (1-\omega)I]\ V^{(k)} + \omega D^{-1}B \qquad (4.29)$$

where V is the vector of all potential values $V^T=[V_{int}^T, V_{S2}^T]$, $B^T = [B'^T,0]$ and

$$D \equiv \begin{pmatrix} A' & 0 \\ 0 & I \end{pmatrix}$$

The block successive overrelaxation matrix corresponding to (4.29) is

$$\mathcal{L}_\omega = (I - \omega L)^{-1} [\omega U + (1 - \omega) I] \tag{4.30}$$

Then [31]

$$\mu(\mathcal{L}_\omega) \geq |\omega - 1| \tag{4.31}$$

where $\mu(\mathcal{L}_\omega)$ is the spectral radius of $\mathcal{L}_\omega$. This means that in investigating the convergence of (4.29), only the interval $0 < \omega < 2$ need be considered. This is stated as

LEMMA 4.1: The block successive overrelaxation method does not converge outside the interval $0 < \omega < 2$.

As was the case for the point methods above, the most common methods for determination of the best value of ω cannot be used, since the matrices A and J are not symmetric. Wachspress [11] gives a method for determination of ω_{opt} for the case when J is non-symmetric. The method has not been found particularly effective in numerical trials, as the eigenvalues μ of J have significant imaginary parts. However, the optimum value of ω has not proved to be very critical for the problems attempted. Computation time can be reduced by approximately one half (as compared to the case $\omega=1$), but this decrease can be achieved by use of values of ω significantly lower than ω_{opt} (10-20%).

Block successive overrelaxation as developed above is not efficient from the standpoint of core memory requirement, as two vectors of potential values V_{int} for the interior region need to be stored. A more attractive correction scheme can be obtained by overcorrecting only the potentials V_{S2} on the contour S2 (and not the interior potentials V_{int}). In this way, storage of only one vector V_{int} is required. If overcorrection is to be applied only to either V_{S2} or V_{int}, the acceleration obtained is the same whichever vector is overcorrected. This may be shown as follows:

Let β_1 be the overcorrection factor applied to V_{int} and let β_2 be the corresponding factor applied to V_{S2}. Substitute β_1 for ω in (4.25) and β_2 for ω in (4.27). Substitute (4.25), (4.26) and (4.28) into (4.27). After some manipulation there results

$$V_{S2}^{(k+1)} = [(2-\beta_1-\beta_2)I + \beta_1\beta_2 Q'(A')^{-1}C]V_{S2}^{(k)} + (1-\beta_1)(\beta_2-1)V_{S2}^{(k-1)} + \beta_1\beta_2 Q'(A')^{-1}B' \tag{4.31}$$

Define an error vector as

$$e^{(k)} = V_{S2}^{(k)} - V_{S2} \tag{4.32}$$

where V_{S2} is the solution. Substitution into (4.31) and noting that

$$(I - Q'(A')^{-1}C)\ V_{S2} = Q'(A')^{-1}B'$$

yields

$$e^{(k+1)} = (2-\beta_1-\beta_2)I + \beta_1\beta_2 Q'(A')^{-1}C\, e^{(k)} + (1-\beta_1)(\beta_2-1)e^{(k-1)} \tag{4.33}$$

from which it is apparent that either β_1 or β_2 may be set to unity with the same results.

The modified practical block overrelaxation scheme thus becomes

$$V_{int}^{(k+1)} = (A')^{-1}C\, V_{S2}^{(k)} + (A')^{-1}B' \tag{4.34}$$

and

$$V_{S2}^{(k+1)} = V_{S2}^{(k)} + \beta(V_{S2}^{*} - V_{S2}^{(k)}) \tag{4.35}$$

where

$$V_{S2}^{*} = Q'V_{int}^{(k+1)} \tag{4.28}$$

Computational experiments have shown that the modified block method is comparable in efficiency to the more standard block overrelaxation described by equations 4.25 to 4.28. As in the standard block scheme, the value of acceleration parameter β has not been found to be very critical. This is discussed further in the next chapter. Theoretical investigation of determination of best value of ω or β has thus not been attempted, particularly in view of the fact that yet another means of accelerating convergence was available for all problems considered. This acceleration method is derived

empirically and is discussed in the next section.

4.5 Extrapolation of the Block Solution

After some initial iterations of the contour S2, the individual components $e_j^{(k)}$ of the error vector $e^{(k)}$ defined by equation 4.32 typically show monotonic convergence towards zero, in the form

$$\frac{e_j^{(k)}}{e_j^{(k+1)}} = T_j$$

where the constant T_j is a measure of the magnitude of the dominant eigenvalue of the block Jacobi matrix J. Monotonic convergence of this type has been found to occur for values of $\beta \leq 1.5$ in all problems attempted. Hence,

$$\frac{V_{S2_j} - V_{S2_j}^{(k)}}{V_{S2_j} - V_{S2_j}^{(k+1)}} = T_j, \quad \frac{V_{S2_j} - V_{S2_j}^{(k+1)}}{V_{S2_j} - V_{S2_j}^{(k+2)}} = T_j \tag{4.36}$$

Equations 4.36 may be solved to yield

$$T_j = \frac{V_{S2_j}^{(k)} - V_{S2_j}^{(k+1)}}{V_{S2_j}^{(k+1)} - V_{S2_j}^{(k+2)}} \tag{4.37}$$

and

$$V_{S2_j} = V_{S2_j}^{(k)} + \frac{T_j}{1 - T_j}(V_{S2_j}^{(k)} - V_{S2_j}^{(k+1)}) \tag{4.38}$$

or alternately,

$$V_{S2_j} = V_{S2_j}^{(k+1)} + \frac{T_j}{1 - T_j}(V_{S2_j}^{(k+1)} - V_{S2_j}^{(k+2)}) \tag{4.39}$$

Equations 4.38 and 4.39 represent extrapolated estimates of the solution value V_{S2_j} on the contour S2. The incorporation of the extrapolation process in boundary relaxation is discussed further in the next chapter.

CHAPTER 5

PRACTICAL COMPUTATIONAL ASPECTS OF BOUNDARY RELAXATION

Solution of the infinitely extending problem is, in practice, best accomplished in two stages: The generation of a suitable shift matrix Q and subsequent solution of the problem itself. It has been found most practical to generate Q by a separate program, since Q is independent of the interior problem. Once a shift matrix is generated, it may be used for solution of a great variety of problems, provided that the choice of the contours S1 and S2 and the mesh size is satisfactory. The shift matrix is punched on data cards or stored on magnetic tape and is then read in as part of the data in the boundary relaxation programs. Generation of the shift matrix has been discussed in Chapter 3, § 3.2. A detailed discussion of Q matrix generation for rectangular regions in the (x,y) and (r,z) planes is contained in Appendices 1 and 2, and shift matrix generation for coaxial line problems is discussed in the next chapter, § 6.3, and in Appendix 3.

5.1 Point Methods

The point methods, as was seen previously, make use of the shift matrix Q in regarding each row of Q as a many-point formula for the nodes on the contour S2. For this reason, computational economy dictates storage of Q entirely within the fast-access memory of the digital computer used. Because of the large number of arithmetic operations involved in the use of the many-point formula, the point methods have not been found efficient from a computational standpoint. The point S.O.R. method was programmed and several small trial problems were solved, mainly to verify the theory. The core memory requirement is the same as detailed below for the block methods with internally stored shift matrix.

In the problems attempted, convergence was found to be slow overall, though the number of iterations required was comparable to that of interior problems with a flux-line boundary along S2. The overall computation time, however, was considerably greater than for the same problems solved by block methods. The point S.O.R. method was moreover found hard to optimize, i.e., the optimum overrelaxation factor ω_{opt} was difficult to determine, though it was not found to be overly critical. A time saving of approximately fifty percent could be realized by use of a value of ω close to optimum, as compared to $\omega=1$. Figure 5.1 shows the convergence behaviour of the problem of a charged conductive sphere, of radius one mesh unit, in free space. The number of iterations

is plotted versus the arithmetic sum of the residuals in the interior region and on S2. The region size is 7 by 14 nodes and the potential on the sphere is 10 volts. Note that the average residual is approximately two orders of magnitude lower than the sum and that the solution has been taken to approximately the limit of floating point precision of the IBM 360/50 used.

5.2 Block Methods

Block boundary relaxation programs typically require two principal routines: a routine for solution of the problem in the interior region and a routine for the correction of the potentials on the contour S2. Since the interior region contains an interior Dirichlet problem, existing interior programs may be used if available. As typically of the order of twenty-five corrections are required for the potentials on S2, i.e., twenty-five block iterations, the shift matrix Q may be stored on magnetic tape or disc without sacrificing computational economy. In this case, the only extra storage requirement is a buffer to store one row of the shift matrix. Where computer hardware permits data transfers concurrently with the arithmetic, almost no time is wasted.

Since the entire mesh used is the region of interest, storage of Q in the fast-access memory is practical for a great many problems. In this case, the greatest storage requirement is due to the shift matrix. It has been found that

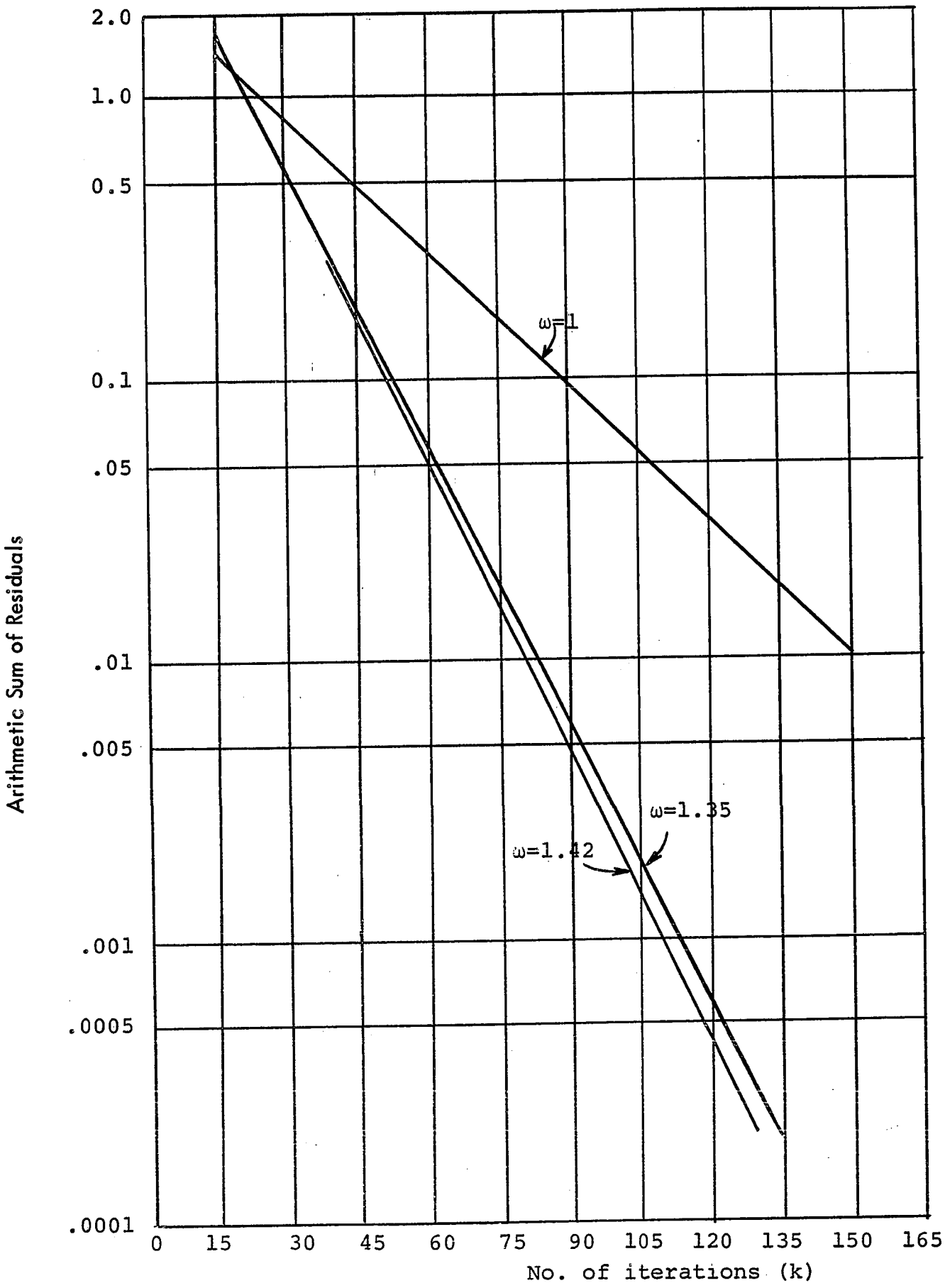

FIGURE 5.1: CONVERGENCE DATA FOR POINT S.O.R. SOLUTION OF CONDUCTING SPHERE PROBLEM IN A REGION OF 7 BY 14 NODES

a rectangular interior region is most convenient as regards programming simplicity as well as from the standpoint of Q matrix storage. Shift matrices for rectangular regions possess certain symmetries, so that the entire matrix need not be stored. Core memory requirement will be discussed for rectangular regions in the x-y and r-z planes.

In the x-y plane, let the rectangular region of interest be a square mesh of (M+2) nodes by (N+2) nodes. Let the contour S2 consist of the outermost nodes, omitting the corners, and let the contour S1 be the rectangular contour one mesh unit interior to S2. This is illustrated in Figure 5.2, where the contour S2 is indicated by o's and S1 by x's. For even M and N, the Q matrix for this region has $(2M+2N)(2M+2N-4)$ elements, of which only one quarter are independent*. (See Appendix 1 for a more detailed discussion of the structure of Q). Allowing for storage of a field description array, the overall storage requirement becomes:

independent elements of Q	:	$(M+N)(M+N-1)$
field values	:	$(M+2)(N+2)$
field description array	:	$(M+2)(N+2)$

locations, plus the program itself. For example, if M=N=56, the field values and the field description array each occupy

---

* The shift matrix actually has less independent elements, as can be seen from symmetry considerations. The word "independent" is used here to mean "easily programmable symmetry", as explained in Appendix 1.

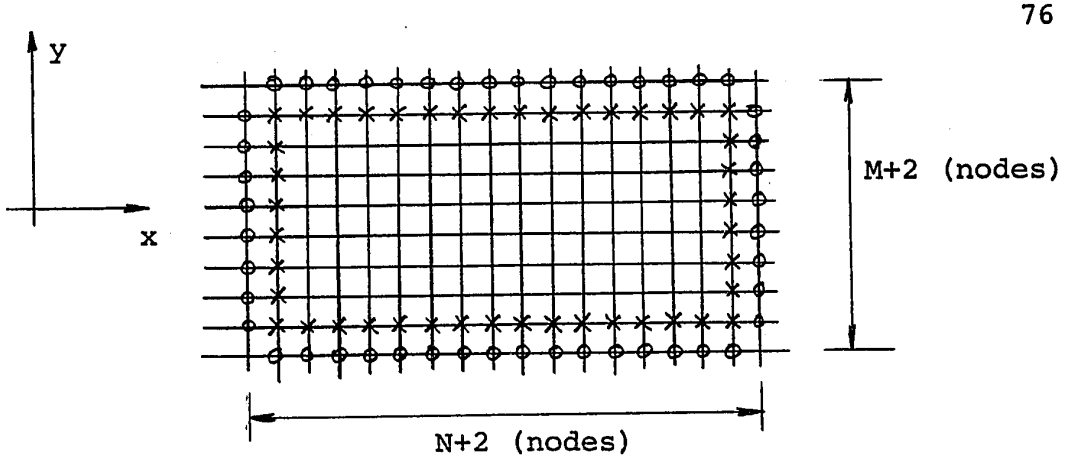

FIGURE 5.2: RECTANGULAR REGION IN X-Y PLANE

3364 locations. The shift matrix is, in this case, 224x220 and contains 12,320 independent elements. Hence, 19,048 storage locations are required in addition to the program itself. A problem of this size may be conveniently solved on an IBM 360/50 computer with 110 Kbytes of core memory and a word size of four bytes.

The size of problem that may conveniently be done in the r-z plane is approximately the same, though the figures vary somewhat. Let the region of interest be the rectangular region described by Figure 3.3. Let the number of radial nodes in the mesh be (M+1) and the axial nodes (N+2). The shift matrix in this case has (2M+N)(2M+N - 2) elements, of which, for even N, one-half are independent. The overall storage requirement thus becomes:

independent elements of Q	:	$\frac{1}{2}(2M+N)(2M+N-2)$
field values	:	$(M+1)(N+2)$
field description array	:	$(M+1)(N+2)$

locations plus the program itself. For example, if N=2M=80, i.e., the region size is 41 by 82, the field values and the field description array each occupy 3362 locations. The associated 160x158 shift matrix has 12,640 independent elements. Hence the storage requirement is 19,640 locations in addition to the program itself, which can again be accommodated by an IBM 360/50 computer. Larger machines can, of course, handle much larger problems.

Computation times are rather hard to state for boundary relaxation since they depend greatly on the complexity of the problem as well as mesh size and the various parameters of the problem. Comparison of boundary relaxation to the other methods that have been used for solution of the infinitely extending problem is not meaningful, since computation times in the earlier methods depend to a great extent on the choice of approximation. The methods reported here are significantly faster than boundary relaxation using potential gradients [41],[42], particularly when extrapolation is used, as discussed in the next section. Without extrapolation, computation times are comparable to optimized interior problems with a flux line boundary at S2. It has been found that computation time varies approximately linearly with the number of nodes in the interior region of interest and with the order of magnitude of error reduction required. Practical block relaxation dictates overcorrection of only the potentials on S2 and not in the interior region. The overcorrection factor β is not overly critical, provided it is on the low side

of optimum. This is shown in Figure 5.3, where the arithmetic sum of the corrections to the potentials on S2 is plotted against the number of block iterations (k) for the conductive sphere problem described in the preceding section. The behaviour shown here is typical, with most problems differing in the first few iterations. Practical application of the block methods is discussed in the next section.

5.3 Practical Block Method

In the initial stages of block S.O.R., it is pointless to solve the interior region to a high degree of accuracy. For this reason, point S.O.R. is convenient as an "interior" solution method, since it is easily terminated at any stage of accuracy. It has been found that a simple method of incorporating this in the block method is to simply limit the number of interior S.O.R. passes to some fixed number varying from 10 for small regions of the order of 100 nodes, to 40 or 50 for regions of 1000 nodes or more. After the first few boundary iterations, the interior S.O.R. routine typically terminates interior solution well before the maximum interior passes are executed, since a second terminating criterion is the condition that all residuals are smaller in magnitude than some prescribed constant. This constant is normally specified one-half an order of magnitude lower than the maximum allowed boundary (S2) correction, which is the terminating criterion for the boundary relaxation program.

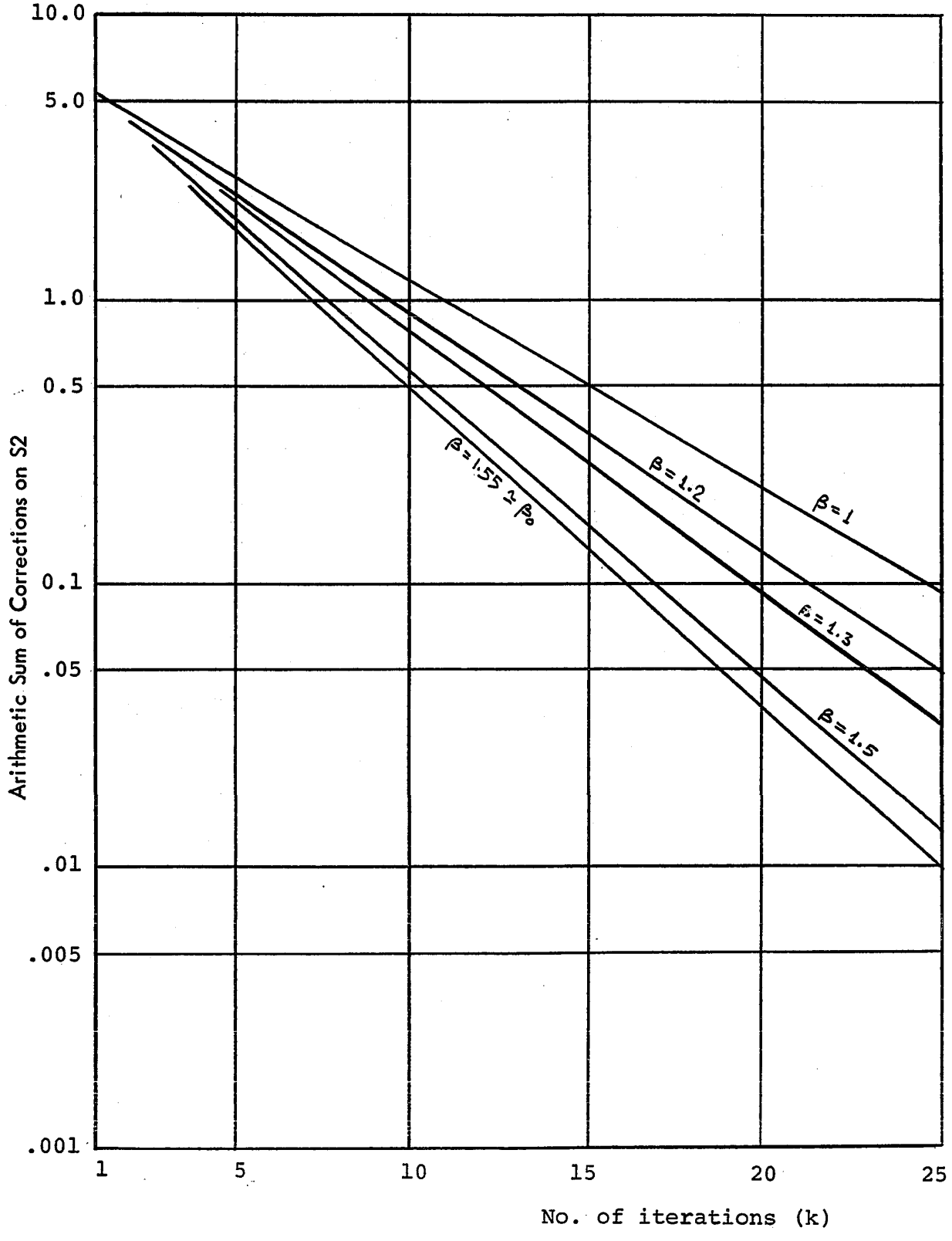

FIGURE 5.3: CONVERGENCE DATA FOR MODIFIED BLOCK S.O.R. SOLUTION OF CONDUCTING SPHERE PROBLEM IN A REGION OF 7 BY 14 NODES

No attempt was made to optimize the solution of the interior region, although for problems with many nodes determination of an optimum interior overrelaxation factor is most likely worthwhile. This factor, once determined, remains fixed for each block iteration, since the contour S2 is temporarily converted to a Dirichlet boundary.

The block relaxation factor β is not overly critical, and it has been found that a value of $\beta=1.5$ gave sufficient acceleration for most problems attempted, particularly when combined with the extrapolation method of § 4.5 above. The extrapolation, when properly used, was found to provide the equivalent of 5-30 full block iterations. It was found that the extrapolation process, if applied too early, caused block relaxation to diverge. This is shown in Figure 5.4, which shows the behaviour of the arithmetic sum of the corrections on S2 with the iteration number (k). The plot is for the pin insulator problem of Figure 6.6 in the following chapter. The region size is 20 by 40 nodes and the block overcorrection factor β is 1.5. The oscillating curve shows the behaviour for extrapolation after every eighth block iteration. The lower converging curve shows extrapolation applied after the twentieth block iteration. In this example, the number of interior relaxation passes was limited to 40 for each block iteration and the final overall solution accuracy is .001%. In a practical problem of this type, the solution is rarely required to this degree of accuracy.

It is interesting to note that, in most cases, the convergence behaviour of the problem changes somewhat after a

properly applied extrapolation. Figures 5.5 and 5.6 show the behaviour of the corrections on S2 versus iteration number for the insulator problems of Figures 6.8 and 6.9. In Figure 5.5, extrapolation is applied after the twentieth block iteration, whereas in Figure 5.6, after the fifteenth. The interior region size is approximately the same for each case. Note that in the former case, convergence (to .001%) is obtained within two iterations after the extrapolation, while in the latter, nine block iterations are required subsequent to extrapolation. In both cases, however, the total number of block iterations is approximately the same. The convergence rate in both cases is also substantially increased after extrapolation. The computation time in all the above convergent cases was substantially less than one minute of machine time on an IBM 360/75.

5.4 Programs Used

The boundary relaxation programs used in this investigation consist of two main sections: routines for solution of the interior region and boundary potential corrections routines. The shift matrix is generated by a separate program and read in as data from punch cards. As has been mentioned above, point S.O.R. is used for the solution of the interior region of interest at each block iteration.

The interior point S.O.R. routines were written so as to allow arbitrary sources and material interfaces to be

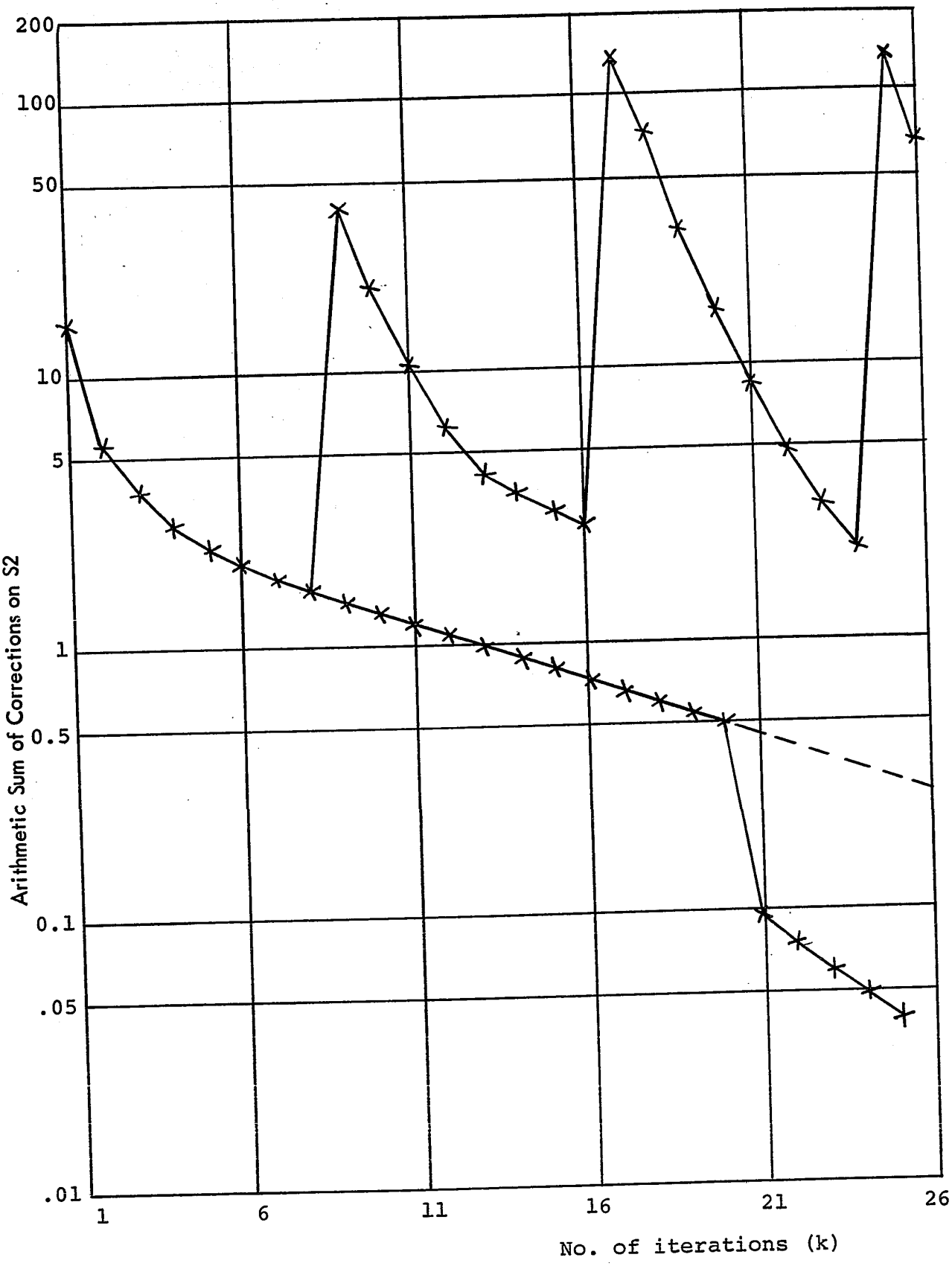

FIGURE 5.4: CONVERGENCE BEHAVIOUR OF PIN INSULATOR PROBLEM OF FIGURE 6.7 SHOWING EFFECT OF EXTRAPOLATION AFTER EVERY EIGHTH ITERATION AND AFTER THE TWENTIETH ITERATION

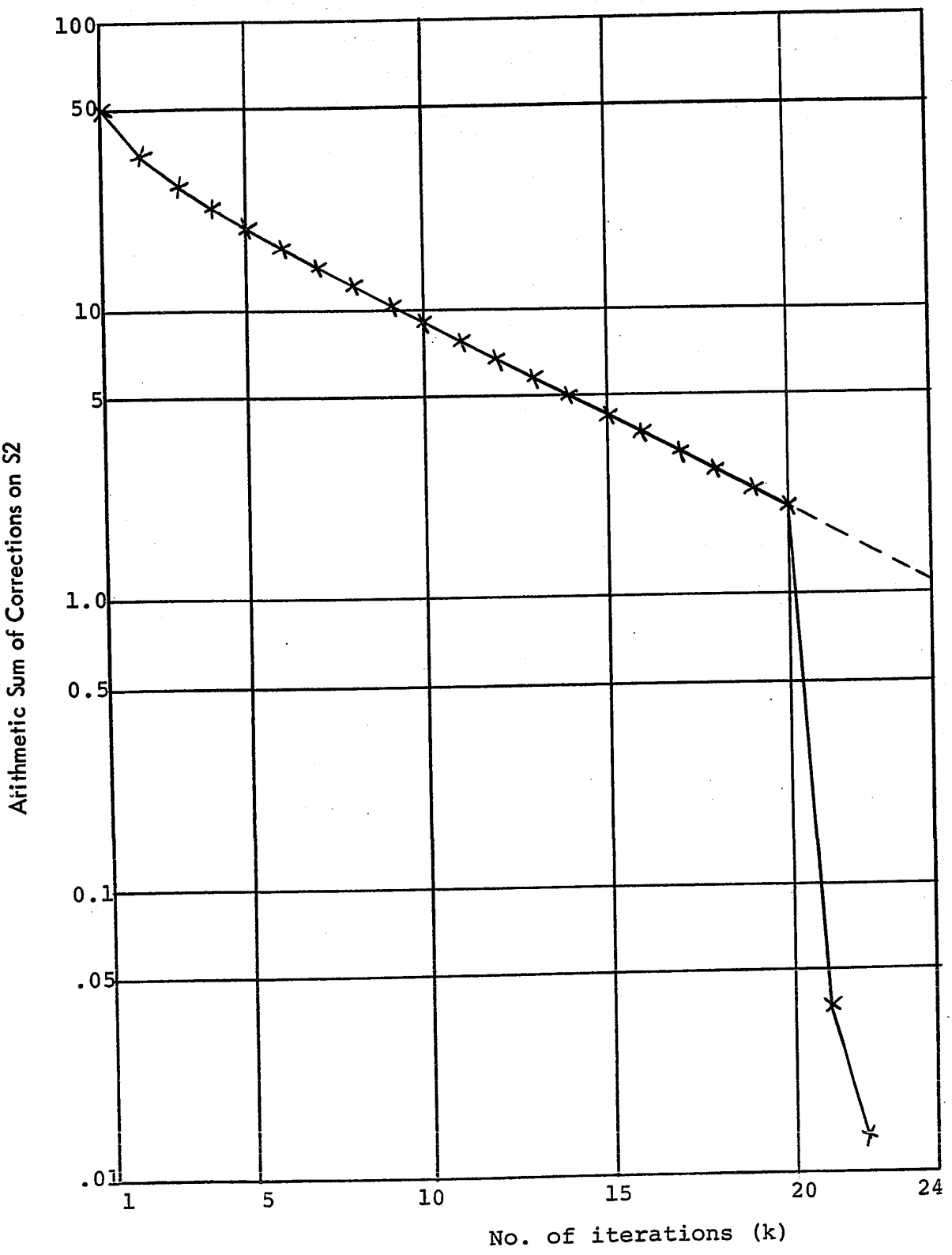

FIGURE 5.5: CONVERGENCE BEHAVIOUR OF CONTAMINATED SUSPENSION INSULATOR PROBLEM OF FIGURE 6.9 SHOWING EXTRAPOLATION AFTER TWENTY BLOCK ITERATIONS

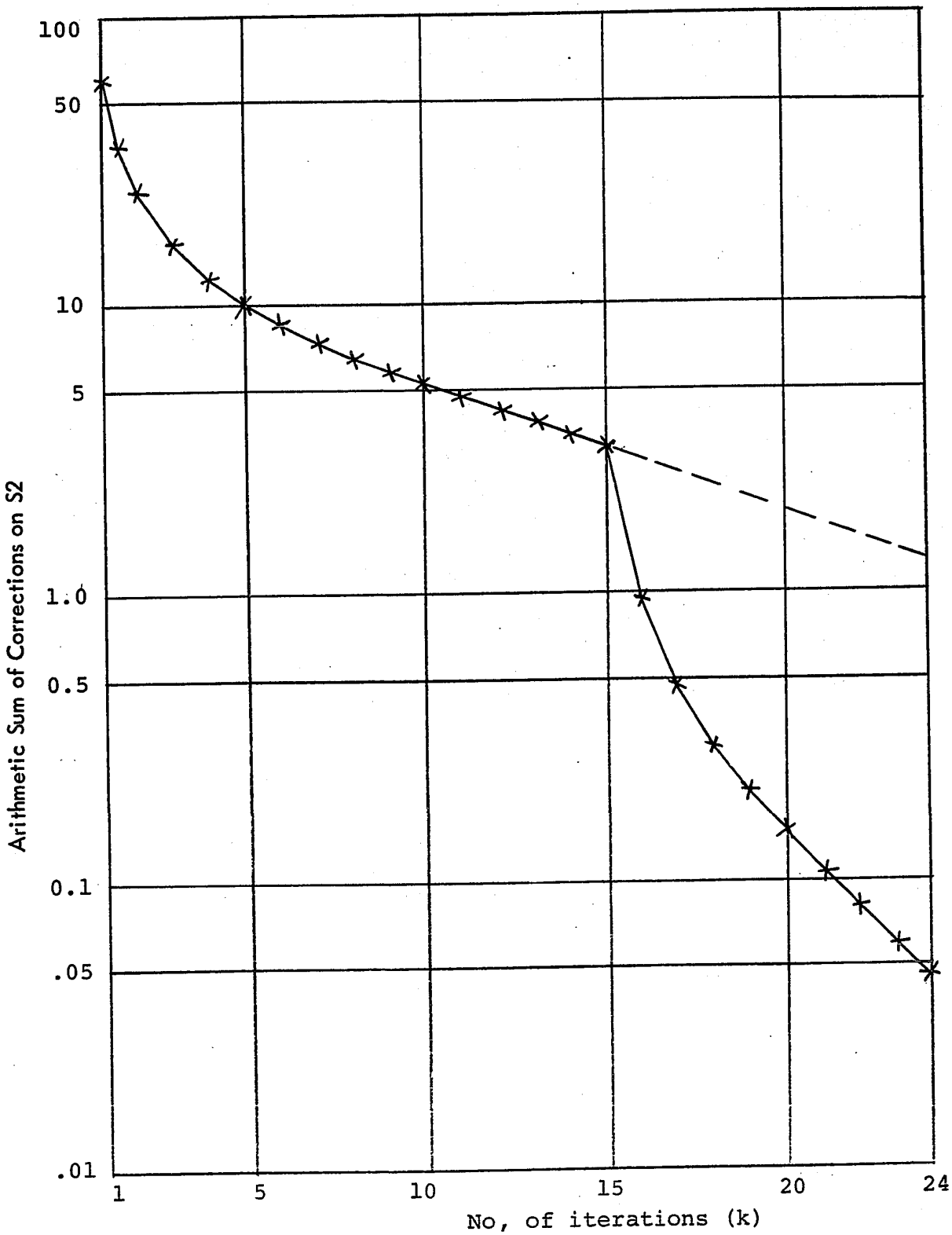

FIGURE 5.6: CONVERGENCE BEHAVIOUR OF SUSPENSION INSULATOR PROBLEM OF FIGURE 6.10 SHOWING EXTRAPOLATION AFTER FIFTEEN BLOCK ITERATIONS

specified. The problem geometry is read-in in quasi-graphical form from a data deck in which punches indicate the presence or absence of conductors or dielectrics. In the x-y plane, material interfaces halfway between mesh lines are allowed, while in the r-z plane routines, material interfaces are allowed to follow mesh lines as well as diagonals in the mesh. A field coding routine then forms a field description matrix which is stored in an array identical to the array containing the field values, i.e., one code number is stored for each field point. The code number at each node determines the formula to be used in the interior point S.O.R. routine. The details of these routines have been described before for x-y plane programs [41]. A more detailed discussion of the interior routines for the r-z plane is contained in Appendix 4.

The interior solution routines may be thought of as one package, in that any method for solution of the interior region may be used, provided that consistency of formulation is preserved at the contours S1 and S2. The boundary correction routines are quite simple, requiring care only in the indexing involved. The problem is considered to have converged whenever the maximum correction to the potential values on S2 does not exceed an arbitrarily small preassigned number. The maximum boundary correction, as well as the arithmetic sum of the corrections and the sum of the squares, is printed out at each block iteration. Once convergence is attained, output routines are then used to print the field values, plot equi-

potential maps, calculate capacitances and any other required data.

Appendices 1 and 2 describe in detail all the necessary indexing for generation (and subsequent use) of Q matrices for rectangular regions in the x-y and r-z planes. An additional feature incorporated in the x-y plane programs is the facility to impose an externally applied field on the problem. The solution of the problem is the same as for no externally applied field, with a slight modification in the correction of the potentials on S2. The externally applied potentials are subtracted from the potentials V_{S1} before multiplication by the shift matrix. The shifted potentials V_{S2} are then augmented by the external field on S2 and the process continued as for the normal problem.

Figure 5.7 shows a flow chart of the modified block boundary relaxation program.

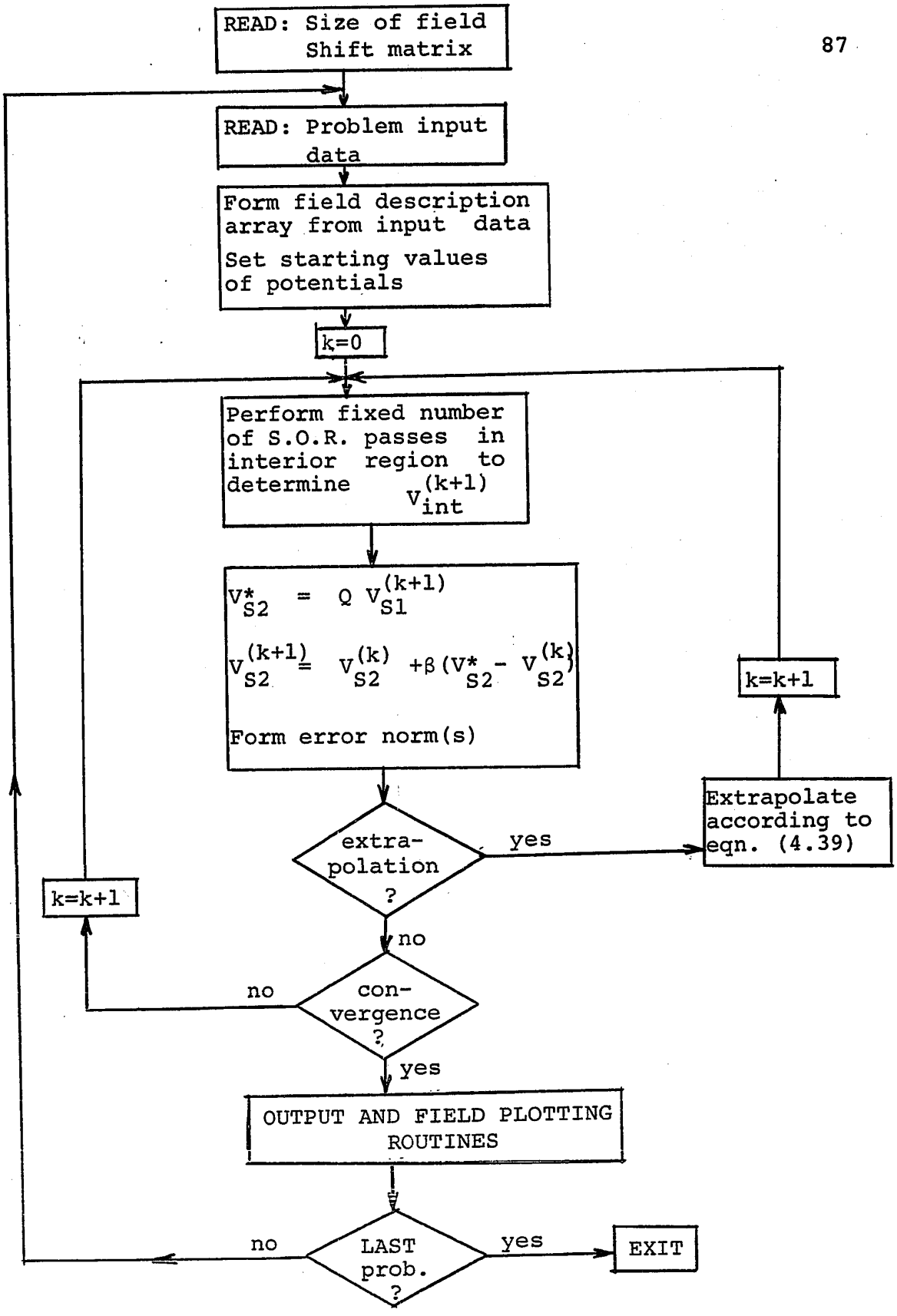

FIGURE 5.7: BLOCK BOUNDARY RELAXATION FLOW CHART

CHAPTER 6

ILLUSTRATIVE EXAMPLES

In this chapter, several sample solutions are presented in order to illustrate the application of boundary relaxation to practical problems. The selection of examples is quite arbitrary and is by no means intended to be exhaustive. Some of the solutions presented are standard "textbook" problems having known analytic solution, some are solutions to problems found in practice, and the remainder are presented for their illustrative qualities.

6.1 TWO-DIMENSIONAL PROBLEMS

The two-dimensional discretized Green's function of Laplace's equation represents, in fact, a point source in an infinite mesh. Hence, solution of a unit point source by boundary relaxation should yield values of the Green's function (see Appendix 1). Such a solution is shown in Figure 6.1, in which the computer printout for a small rectangular region is reproduced. Enlarging or reducing the region has no effect on the actual potential values. It is interesting to note that if the mesh lines are replaced by unit resistances, the po-

3.94 4.01 4.07 4.10 4.12 4.10 4.07 4.01 3.94 3.85

4.10 4.19 4.27 4.31 4.33 4.31 4.27 4.19 4.10 4.00

4.28 4.39 4.49 4.55 4.58 4.55 4.49 4.39 4.28 4.15

4.47 4.62 4.74 4.84 4.87 4.84 4.74 4.62 4.47 4.31

4.66 4.86 5.04 5.17 5.23 5.17 5.04 4.86 4.66 4.47

4.86 5.12 5.38 5.59 5.70 5.59 5.38 5.12 4.86 4.62

5.04 5.38 5.75 6.13 6.36 6.13 5.75 5.38 5.04 4.74

5.17 5.59 6.13 6.82 7.50 6.82 6.13 5.59 5.17 4.83

5.23 5.70 6.36 7.5010.00 7.50 6.36 5.70 5.23 4.87

5.17 5.59 6.13 6.82 7.50 6.82 6.13 5.59 5.17 4.83

5.04 5.38 5.75 6.13 6.36 6.13 5.75 5.38 5.04 4.74

4.86 5.12 5.38 5.59 5.70 5.59 5.38 5.12 4.86 4.62

4.66 4.86 5.04 5.17 5.23 5.17 5.04 4.86 4.66 4.47

4.47 4.62 4.74 4.84 4.87 4.84 4.74 4.62 4.47 4.31

4.28 4.39 4.49 4.55 4.58 4.55 4.49 4.39 4.28 4.15

4.10 4.19 4.27 4.31 4.33 4.31 4.27 4.19 4.10 4.00

FIGURE 6.1: POINT SOURCE IN AN INFINITE MESH

tential values represent node voltages, and the resistance between two diagonally opposing nodes in the mesh is obtained, as by Amstutz [48], to be $2/\pi$.

Figures 6.2 and 6.3 show the equipotential plots of the familiar problem of a circular dielectric cylinder in an externally applied uniform field [10]. The actual dielectric interface is shown by the dashed lines. The region of interest in each case is a square region of 18x18, or 324 nodes. The first example shows the plot for cylinder dielectric permittivity $\varepsilon_r=2$, while the second is for $\varepsilon_r=5$. Note that the equipotential lines run true right to the edge of the region of interest, i.e., right to the contour S2, quite unlike any solution obtained by assuming S2 to be a flux line or other hypothetical boundary. An interesting point to note in these two examples is the fact that even a crude modeling of a circular cylinder as shown here produces a solution that is almost identical to the classical analytic one.

The last 2-dimensional example is an artificial problem whose accurate solution is difficult by analytic means. Figure 6.4 shows the equipotential map of a charged wire in the presence of a dielectric cylinder of rectangular cross-section, easily obtained by boundary relaxation. Once more, $\varepsilon_r=5$. Of course, more complicated conductor and cylinder shapes are solved just as easily, as may any configuration of sources and boundaries, provided they can be contained in the region of interest.

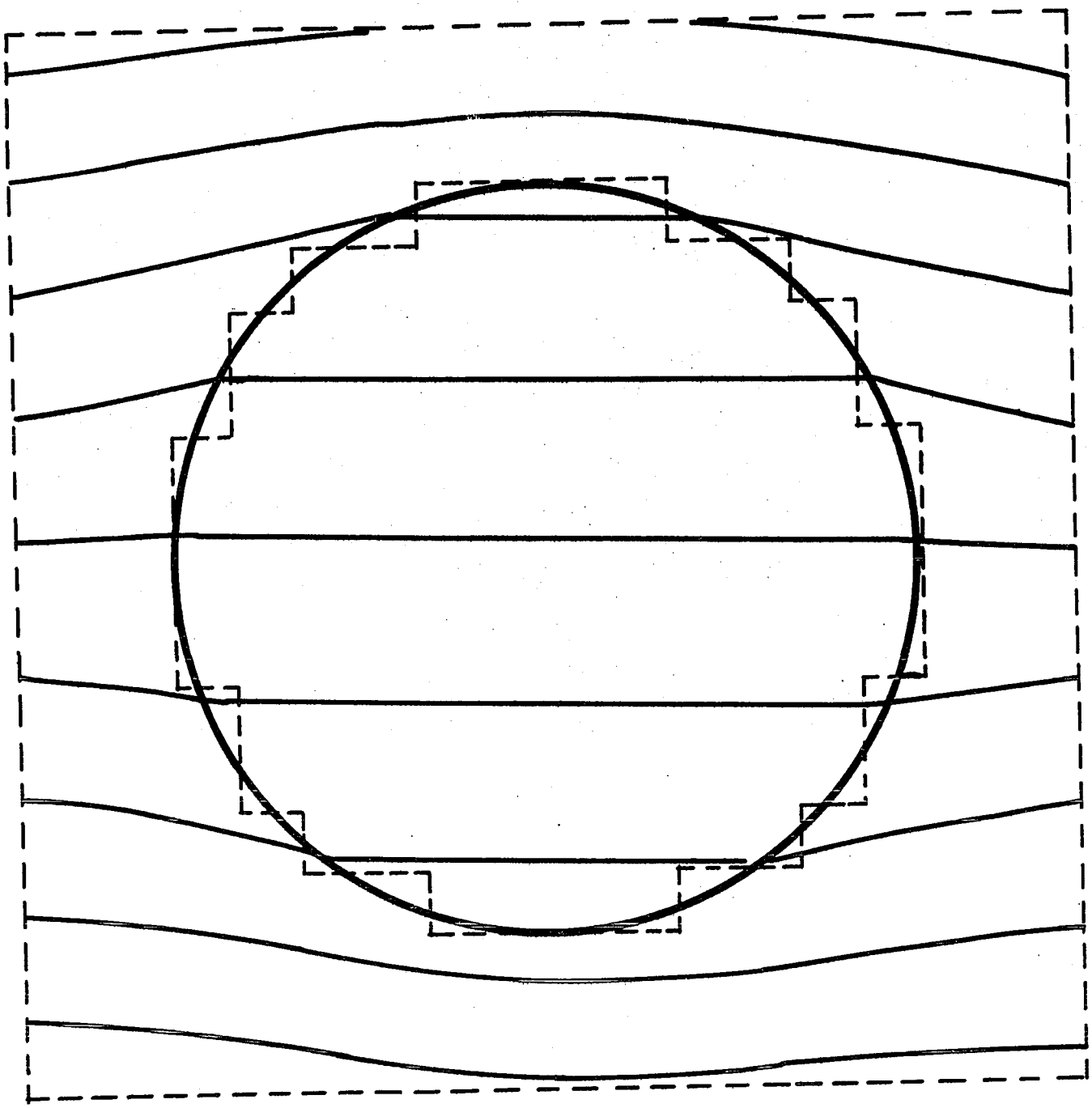

FIGURE 6.2: CIRCULAR DIELECTRIC CYLINDER IN UNIFORM APPLIED FIELD, $\epsilon_r = 2$.

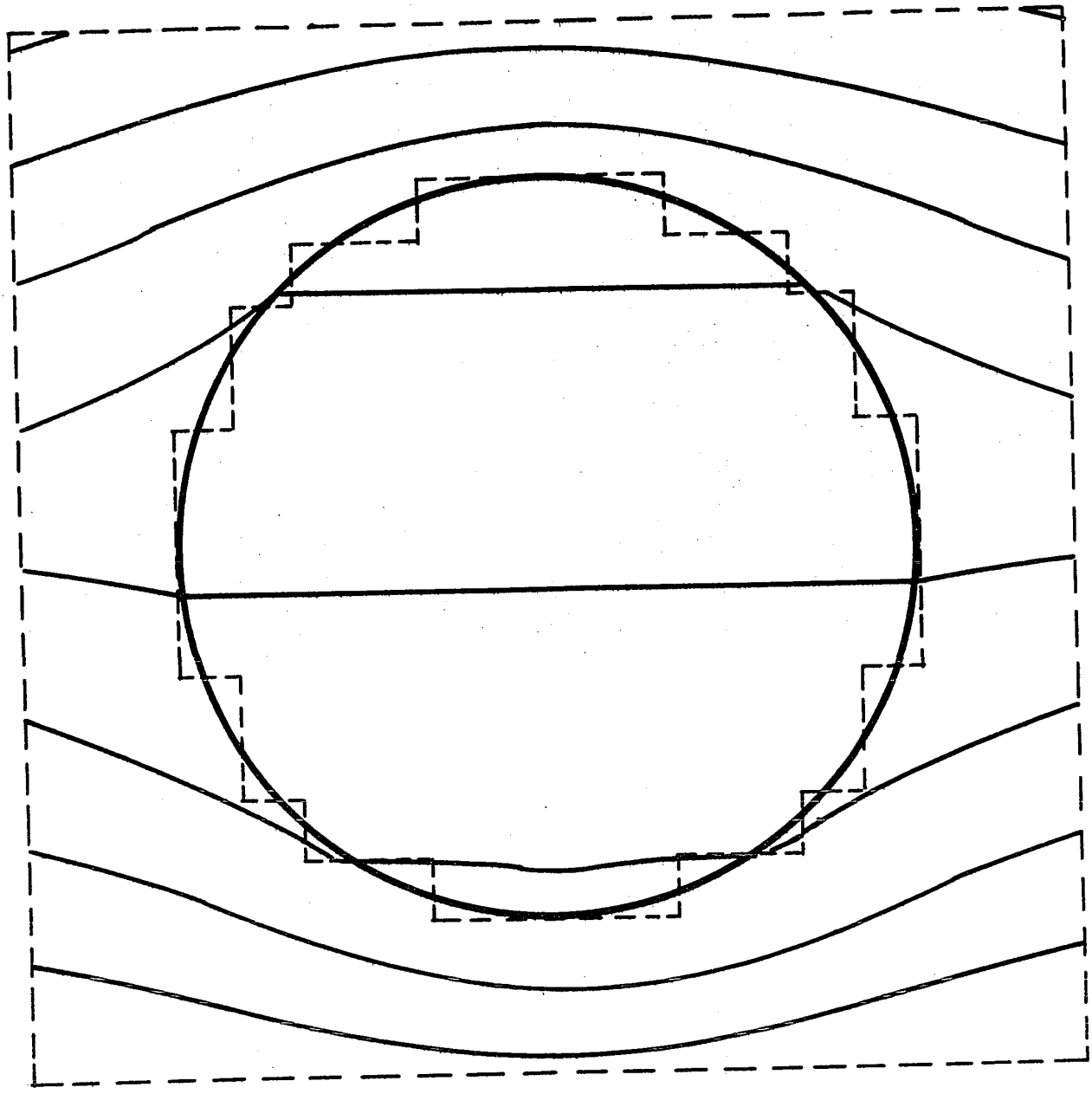

FIGURE 6.3: CIRCULAR DIELECTRIC CYLINDER IN UNIFORM APPLIED FIELD, $\varepsilon_r = 5$.

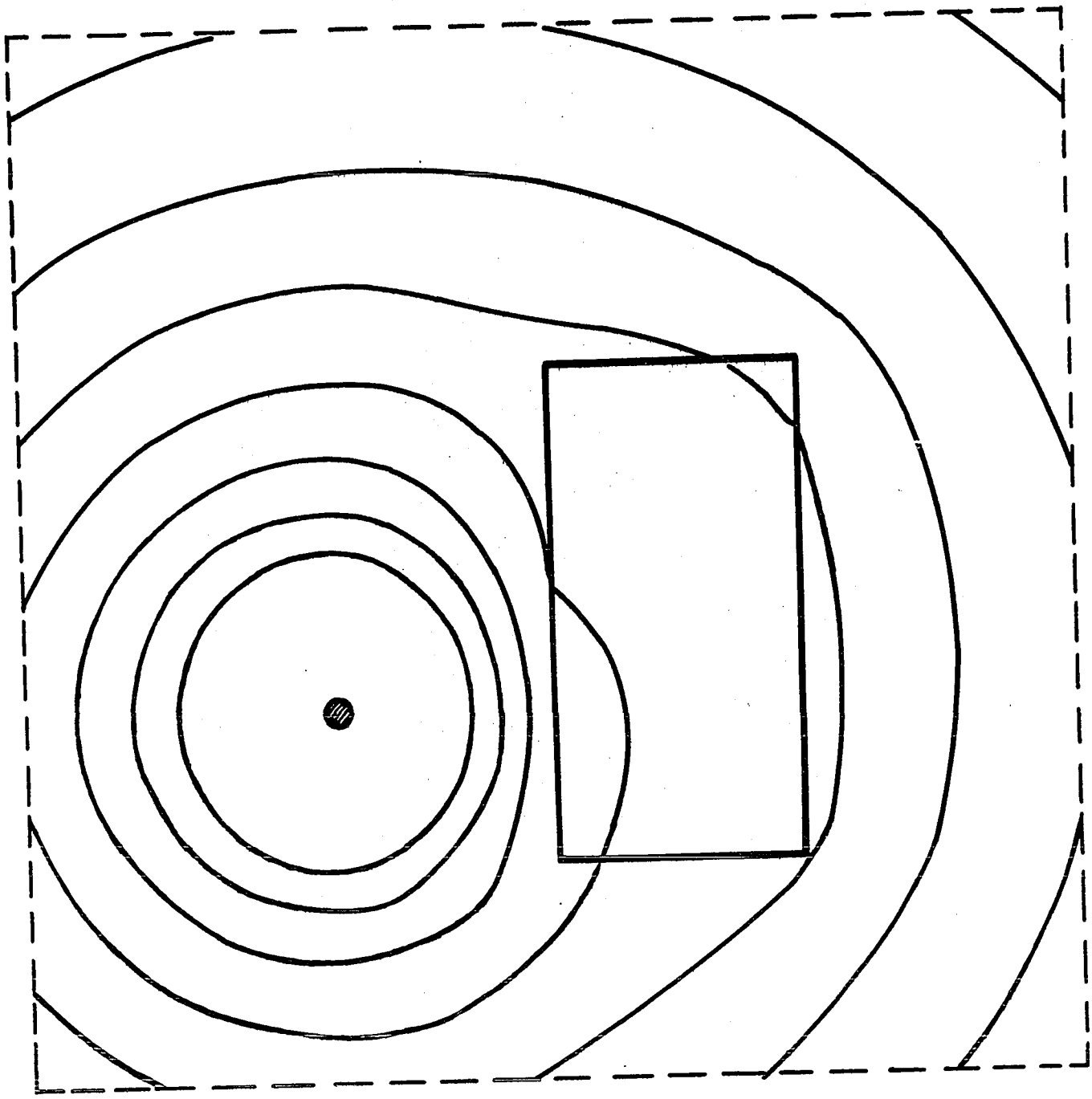

FIGURE 6.4: CHARGED WIRE NEAR RECTANGULAR DIELECTRIC CYLINDER

6.2 Axially Symmetric Three-Dimensional Problems

The first example in this section is the classical problem of the conductive sphere in free space. The square mesh used is not natural to the problem, nor is the rectangular region of interest that was chosen. As can be seen from Figure 6.5, the solution nonetheless corresponds to the one obtained analytically. The region shown in the figure is 7 radial nodes by 14 axial nodes in size. The radius of the sphere is one mesh unit and the conductive surface is thus coincident with nodes in the mesh. Once more, alternately reducing or enlarging the region of interest produces the same solution.

Figure 6.6 depicts the equipotential plot of a typical 69 Kv. pin insulator. The region size is 20 by 40 nodes and the contours shown are equispaced, with an intermediate contour shown by the dashed line. The smooth dielectric interfaces are modeled by straight line segments along mesh lines and diagonals, as shown by the fine lines in the figure. The dielectric permittivity is $\varepsilon_r=2.1$. The convergence behaviour of this problem has been discussed in the previous chapter and shown in Figure 5.4. This example, as well as the following three insulator problems are not intended as design data, but merely to illustrate the complexity of sources and material interfaces that may be handled with relative ease.

The equipotential plot of a typical suspension insulator is shown in Figure 6.7. The region size is again 20 by 40 nodes and solution is straightforward, requiring less than one

1.69 1.66 1.59 1.50 1.39 1.28 1.18

2.01 1.97 1.86 1.71 1.56 1.42 1.29

2.50 2.41 2.21 1.98 1.76 1.56 1.39

3.34 3.11 2.71 2.32 1.98 1.71 1.50

5.09 4.30 3.41 2.71 2.21 1.86 1.59

10.00 6.44 4.30 3.11 2.41 1.97 1.66

10.0010.00 5.07 3.34 2.50 2.01 1.69

10.00 6.44 4.30 3.11 2.41 1.97 1.66

5.09 4.30 3.41 2.71 2.21 1.86 1.59

3.34 3.11 2.71 2.31 1.98 1.71 1.50

2.49 2.41 2.21 1.98 1.76 1.56 1.39

2.00 1.96 1.85 1.71 1.56 1.41 1.29

1.67 1.65 1.58 1.49 1.39 1.28 1.18

1.45 1.43 1.38 1.32 1.25 1.17 1.08

FIGURE 6.5: CONDUCTIVE SPHERE IN FREE SPACE

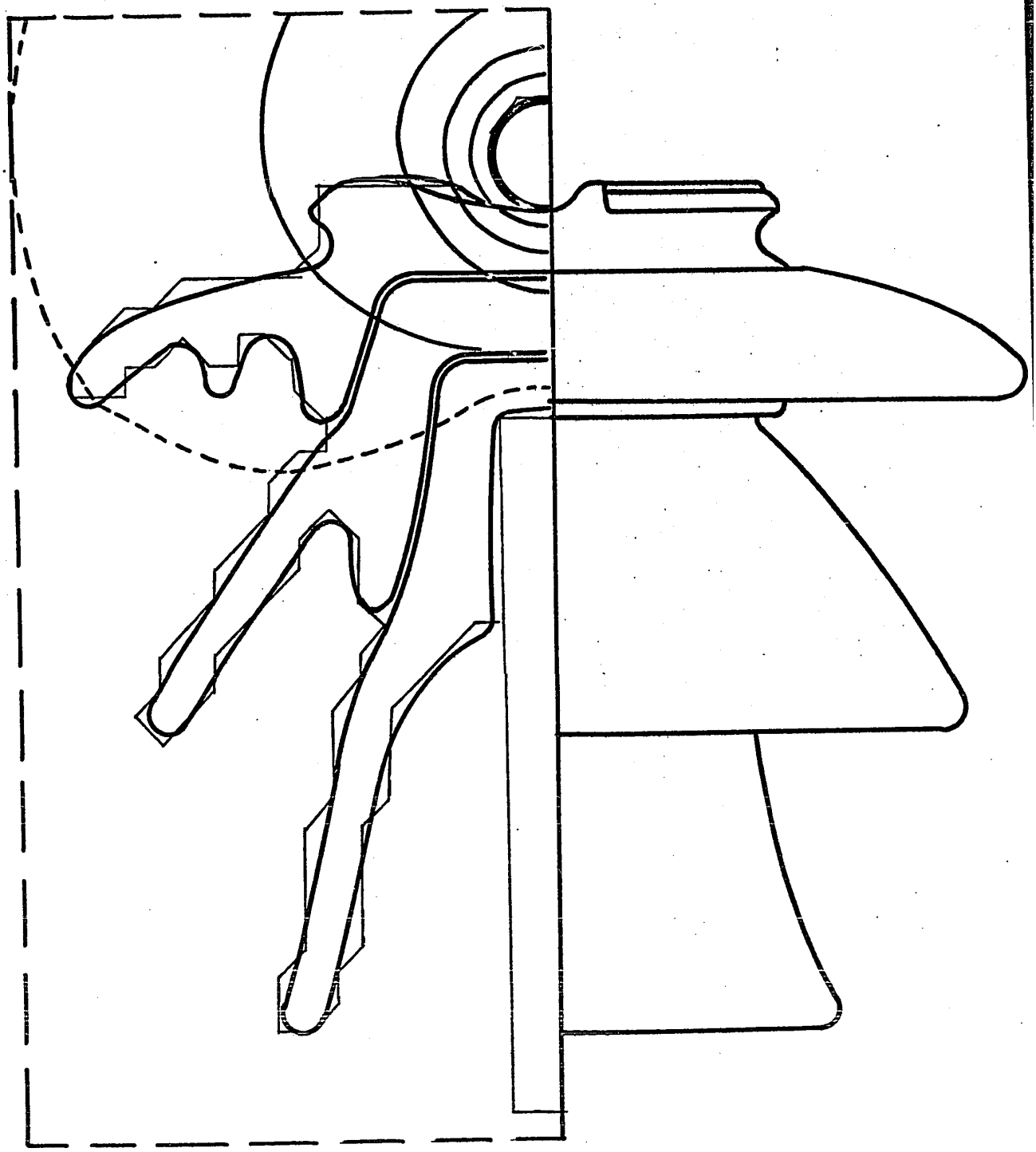

FIGURE 6.6: TYPICAL 69 Kv. PIN INSULATOR

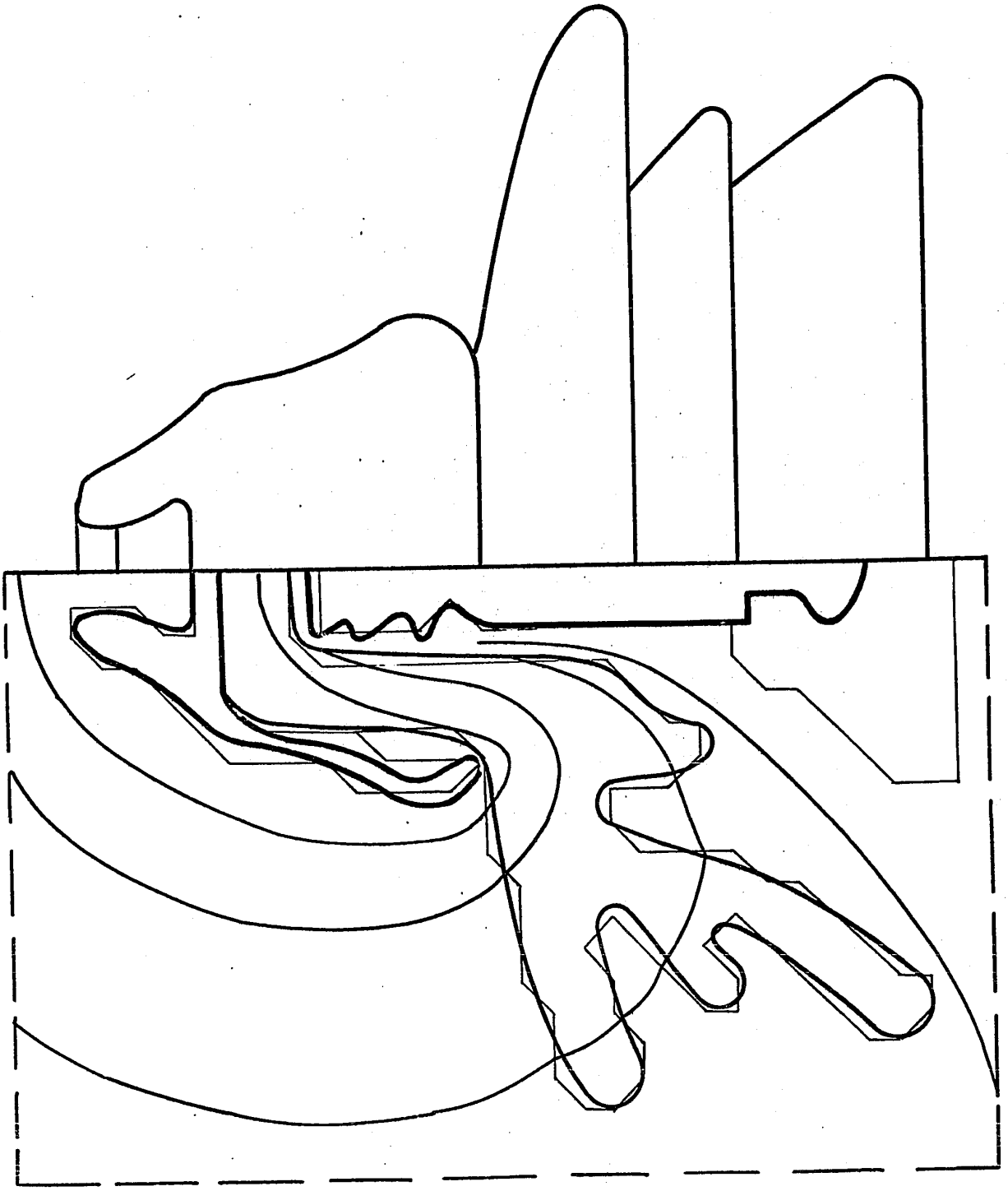

FIGURE 6.7: FIELD MAP OF TYPICAL SUSPENSION INSULATOR

minute of machine time on an IBM 360/75. Economical solution, such as allowed by boundary relaxation, permits analysis of such problems with various environmental and physical factors, such as contamination, taken into account. Figure 6.8 shows the field map of the above suspension insulator with a conductive contaminant on its upper face. This problem requires but a slight modification of the data deck for the previous one, and solution is again straightforward and economical. The convergence behaviour of this problem has been shown in Figure 5.5.

Figure 6.9 shows yet another suspension insulator unit, this time modeled in a mesh of 26 radial by 34 axial nodes. Convergence behaviour of this problem is shown in Figure 5.6 above. This example, as all the above, show clearly the fact that the problem under consideration is not physically altered in any way; the arbitrary contour S2 merely specifies the region of space in which it is desired to inspect the solution but does not alter it.

6.3 Coaxial Line Problems

The theory, methods and examples presented up to this point have been for problems that are infinitely extending in two dimensions. As will be shown in this section, boundary relaxation is applicable as well to problems that are infinite in extent in only one direction, or coordinate, as a special case of problems and will be discussed here. It will be shown

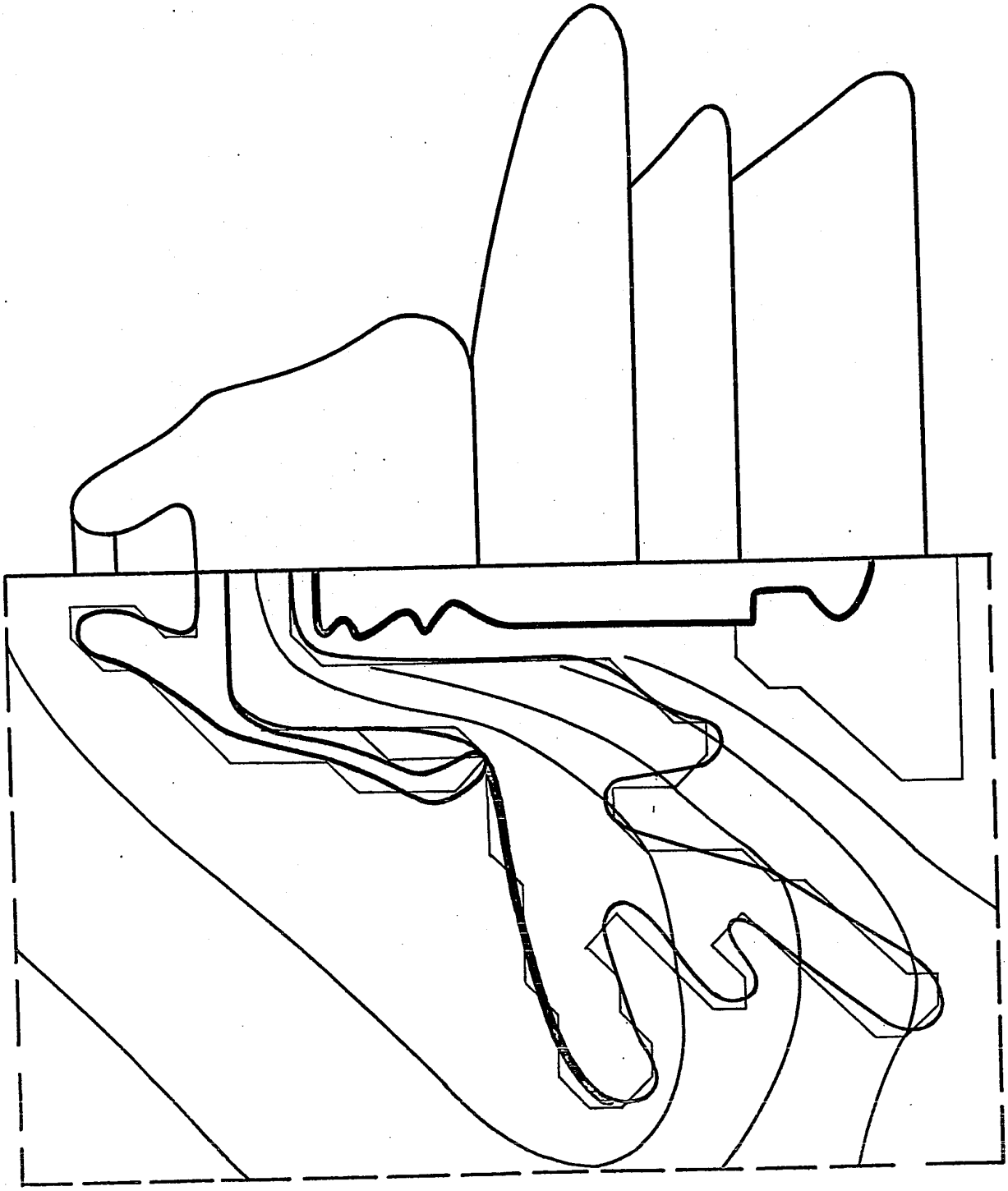

FIGURE 6.8: SUSPENSION INSULATOR UNIT OF FIGURE 6.7 WITH CONDUCTIVE CONTAMINANT ON UPPER FACE

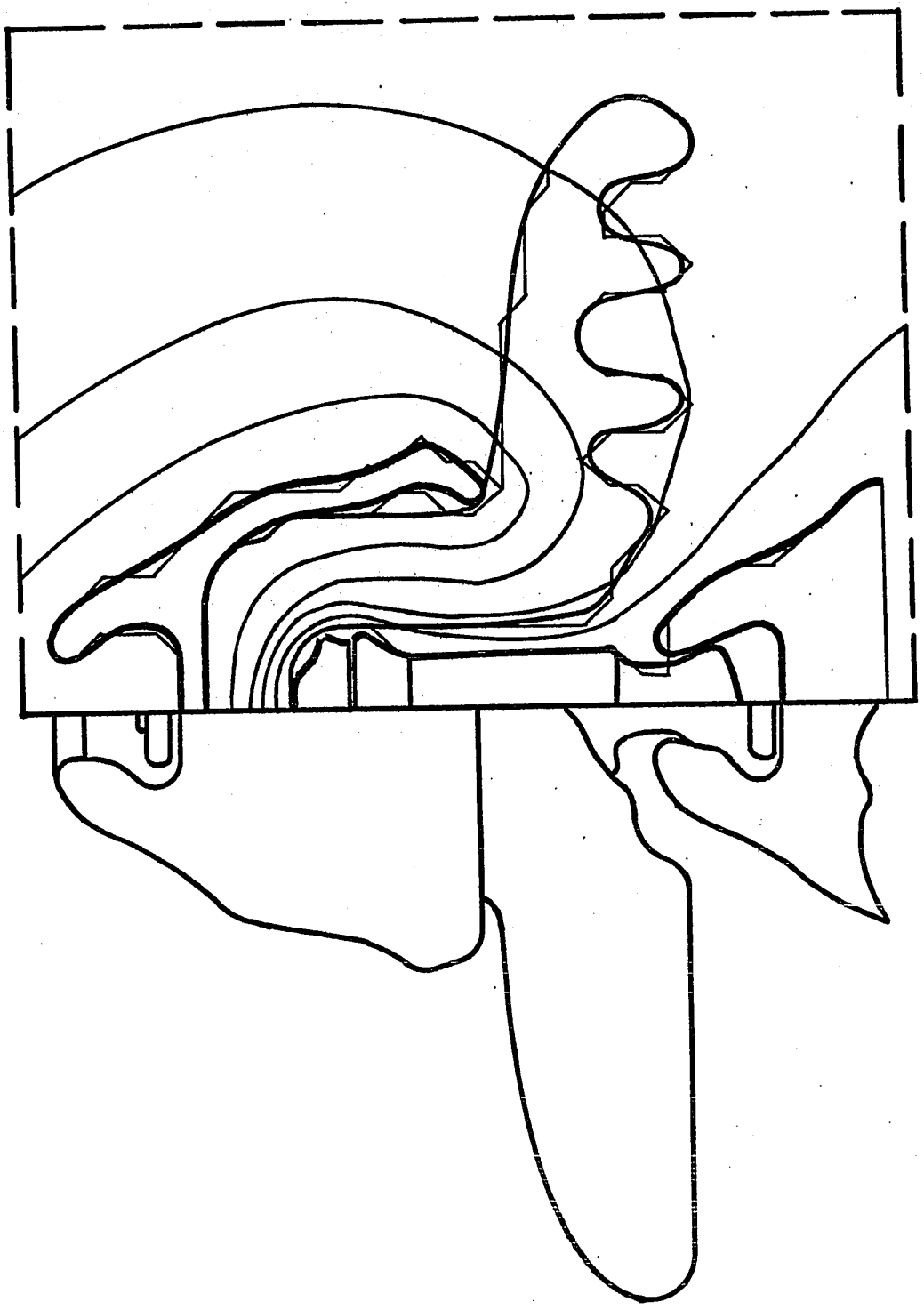

FIGURE 6.9: ANOTHER COMMON SUSPENSION INSULATOR

that, by trivial modification, the methods are also applicable to infinitely extending plane strips of finite width.

Pure TEM waves can be propagated only along uniform transmission lines. Discontinuities or nonuniformities give rise to coupling between this mode and higher order modes. For lines that have small dimensions compared to wavelength, the higher order modes are evanescent, i.e., at some distance away from the discontinuity they decay enough to be negligible. Their associated stored energy, however, cannot be neglected even at very low frequencies. Figure 6.10 shows one possible type of discontinuity created by the joining of two long uniform coaxial lines. The lines are assumed infinitely extending in either direction on each side of the discontinuity region.

The type of discontinuity most commonly treated in the literature thus far is the type which is confined to a single plane, e.g., a step discontinuity in the inner or outer conductor, or both. Whinnery and Jamieson [52] showed that this type of discontinuity can be accounted for by an equivalent shunt capacitance at the discontinuity plane. Their technique is an application of mode matching [53] and was later extended [54],[55] to produce tabulated results and curves.

One of the first finite difference treatments of coaxial line discontinuities to appear in the literature was that of Green [35], who approximated the infinitely extending lines by imposing a flux line boundary one diameter

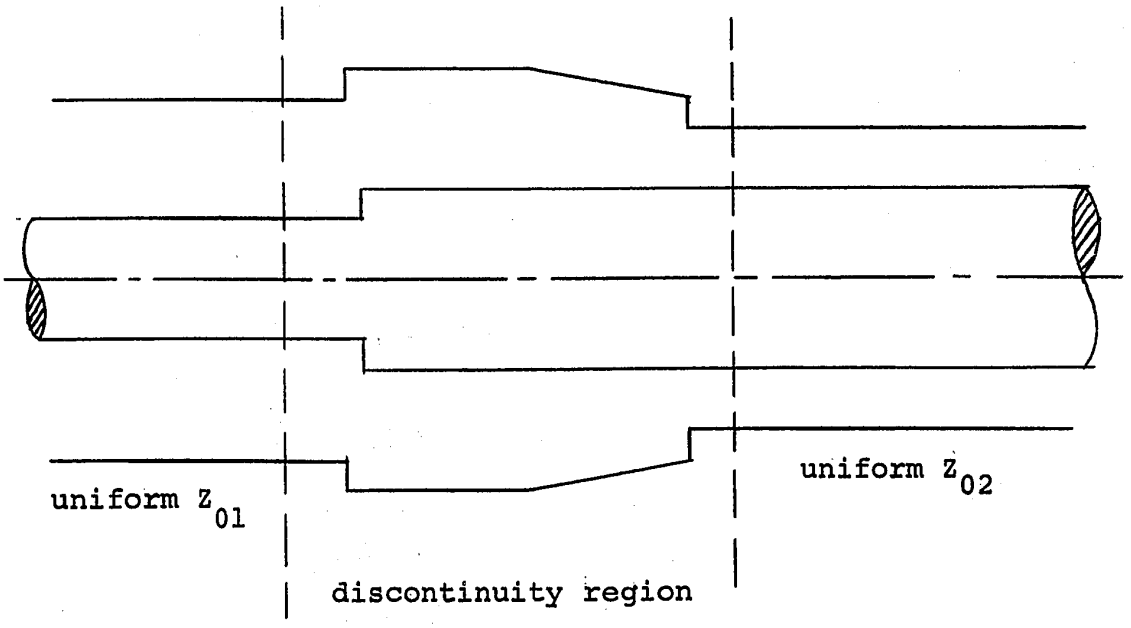

FIGURE 6.10: DISCONTINUITY REGION BETWEEN TWO UNIFORM SEMI-INFINITELY EXTENDING COAXIAL LINES

away from the discontinuity region. The equivalent shunt capacitances were then obtained from the static field map. Green's approach suffers from several defects. First, the artificial flux line boundary alters the problem physically, and though Green asserted that this boundary, if taken one diameter away from the discontinuity region, did not affect the overall solution, it has been found in this investigation that this distance is too optimistic. Secondly, many more nodes than are actually required need to be introduced into the problem, increasing computation time accordingly. Thirdly, Green's approach to calculate the equivalent shunt capacitance involves calculation of the total capacitance of the line section between the artificial flux line boundaries and then subtraction of the capacitance of an equivalent

length of uniform line(s), i.e., the subtraction of two large numbers that are almost equal, a dangerous process, at best.

Equivalent capacitance may be derived from energy considerations in a very small region containing the discontinuity [56], so that boundary relaxation provides a very economical and efficient means of treatment of this type of problem. In order to apply boundary relaxation, a shift operator for the uniform coaxial line has to be found.

The method of construction of shift operators, or matrices, thus far, has been by means of the elementary solution, or the Green's function, of the Laplacian for the appropriate region, such as the infinite plane. Such a function can be found for the uniform coaxial line by use of the finite Hankel transform [57], as shown in Appendix 3. The solution is obtained in the form of a convergent series of Bessel functions, which, unfortunately, converges too slowly to be of practical use. Because of the uniform nature of the problem, however, another simple means of construction of a shift matrix is available.

Consider an infinite uniform coaxial line, such as shown in Figure 6.11. Let some charges q be placed on the plane numbered (1) in the figure. Let the planes numbered (2) and (3) coincide with the adjacent radial mesh lines as shown. The inner and outer conductors of the line are assumed

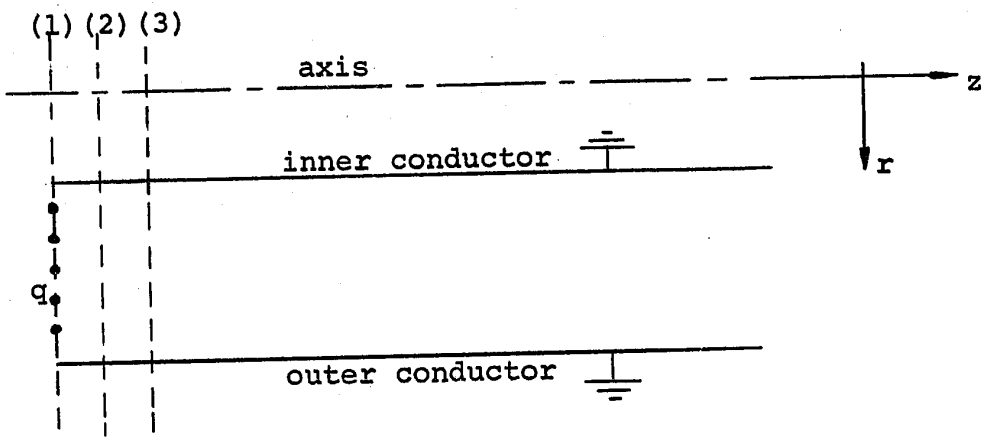

FIGURE 6.11: DEFINITION OF THREE ADJACENT PLANES IN A SEMI-INFINITE COAXIAL LINE

at zero potential*. If the vectors V_1, V_2 and V_3 represent the potential values on the planes (1), (2) and (3) respectively, then writing the finite difference equation at each node on the planes results in a system of equations

$$\begin{pmatrix} C & -2I & 0 \\ -I & C & -I \\ 0 & -Q & I \end{pmatrix} \begin{pmatrix} V_1 \\ V_2 \\ V_3 \end{pmatrix} = \begin{pmatrix} -q \\ 0 \\ 0 \end{pmatrix} \tag{6.1}$$

where C is a tri-diagonal matrix (for uniform inward or outward ordering of the potentials) containing the self and radial coefficients of the finite difference equations, I is the identity matrix, and Q is the required shift matrix. Note

* Potentials other than zero are treated in the same fashion as external fields in the x-y plane. It is merely necessary to subtract the uniform potential before application of the shift relationship and then to add it prior to solution of the interior problem.

that C is written with positive diagonal elements. The doubling of the coefficients in the first equation results from the fact that plane (1) is a plane of symmetry. Note that in this case, the shift matrix Q is a square matrix of order n where n is the number of radial nodes within the inner and outer conductors of the line.

The third row of equation (6.1) is the shift relationship from plane (2) to plane (3). However, since plane (2) is in a Laplacian region, the same shift relationship holds between planes (1) and (2). Application of the shift to the second equation (6.1) results in

$$QQ - CQ + I = 0 \tag{6.2}$$

Calculation of Q from the relationship (6.2) is not convenient. Equation 6.2 may be postmultiplied by Q^{-1} and rearranged to yield

$$Q = [C - Q]^{-1} \tag{6.3}$$

which suggests an iterative process as

$$Q^{(k+1)} = [C - Q^{(k)}]^{-1} \tag{6.4}$$

The above equation may be deduced in another fashion which gives a physical interpretation of the process involved. In equation 6.1, let the initial iterate of Q be taken as the identity matrix, zero, or any other convenient starting point. This initial iterate may be imagined to represent a certain boundary operator. Solution of the equation for unit charges q taken

one at a time yields values of potential on the planes (1) and (2). These values may be used to construct another shift matrix Q which can be used to relate the planes (2) and (3), i.e., the initially assumed boundary operator is effectively displaced one mesh unit to the right. Successive application of this procedure effectively shifts the flux line or other boundary farther and farther away, until a uniform iterate of Q is obtained. Implementation of this procedure in mathematical terms results in equation 6.4. Convergence of this process may be anticipated on purely physical grounds and has been found true in practice.

The extrapolation procedure of § 4.5 may be applied to the iterative process described in equation 6.4, so that iterative construction of Q is very efficient from a computational standpoint. It has been found practical to continue the iterations to the limit of precision available, i.e., zero computed difference on an IBM 360/50, a binary machine with 24-bit mantissa. For this accuracy, the flux line or other boundary is effectively shifted 1.5-2.0 diameters away, thus casting doubts on Green's [35] artificial boundary as regards accuracy of solution.

Once a shift matrix is obtained for each of the two semi-infinite lines in question, the calculation of the static field map in the neighbourhood of the discontinuity is but a trivial application of boundary relaxation. For plane discontinuities, e.g., steps, only three radial mesh lines need be considered, as shown in Figure 6.12. Problems of this type

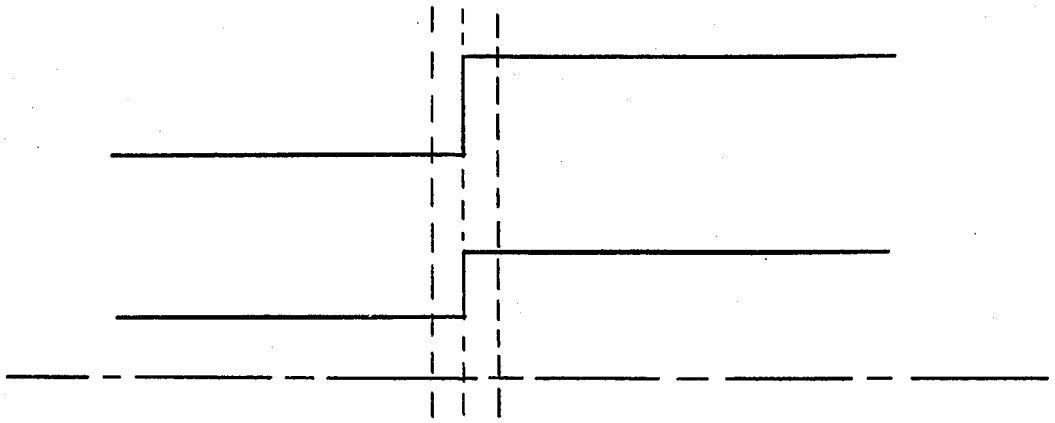

FIGURE 6.12: PLANE DISCONTINUITY IN COAXIAL LINE ILLUSTRATING RADIAL MESH LINES REQUIRED FOR SOLUTION

may be satisfactorily modeled by matrices of order 100-200, so that direct inversion may be used. For discontinuities other than plane, e.g., such as shown in Figure 6.10, point or block S.O.R. is likely to be more practical.

The field pattern obtained represents a superposition of the propagating TEM mode with other evanescent modes that exist only in and near the discontinuity region. The discontinuity capacitance is the equivalent network representation to account for the stored energy of the higher order modes. It is therefore only necessary to find this energy in the discontinuity region.

The potential at any point within the line is the superposition of a logarithmic potential (for a uniform line) which is characteristic of the TEM mode, and an added potential which can be attributed to the effect of the discontinuity. If the reference logarithmic potential is V*, the additional potential is then V-V*. Within the discontinuity region itself, this viewpoint is not justified (for the case of a non-planar discontinuity), since the potential due to the

TEM mode is not known. In this region, however, V* may well be taken equal to V (the actual solution), or some other convenient reference satisfying the Laplace equation in the discontinuity region. The energy associated with the difference potential V-V* may be expressed as

$$W_d = \frac{1}{2} \int_U (V-V^*) \frac{\nabla^2 (V^*-V) dU}{1/\varepsilon} \tag{6.5}$$

where the region of integration extends over both coaxial lines, including the discontinuity region. The integral vanishes everywhere except at the two planes bounding the discontinuity region, hence it is necessary to know the potential at these two planes only. Note that in the case of a plane discontinuity, the two bounding planes for the discontinuity region are coincident.

The actual integration is done numerically and care must be taken in obtaining the necessary second derivatives. If V* is defined to satisfy Laplace's equation everywhere except at the planes bounding the discontinuity region, the energy associated with the discontinuity may be obtained as follows: (V*-V) is formed for the uniform lines on either side of the discontinuity region (V*-V is by the above definition equal to zero within the region). The energy associated with each bounding plane is then obtained as half the energy associated with a potential distribution (V*-V) symmetric about each plane in turn. The five-point Laplacian is easily applied to this distribution, so that the energy is readily

calculated. The discontinuity capacitance is then derived from the energy as

$$C_d = 2 \frac{W_d}{V_0^2} \tag{6.6}$$

where V_o is the potential difference between the inner and outer conductors of the line.

The above methods have been implemented and several sample problems solved. Plane discontinuity capacitances were found to agree with those given by Somlo [55]. Several sample field maps are presented below.

Figure 6.13 shows the equipotential lines near a step discontinuity. The entire computed solution is shown. The mesh used was 61 by 9 nodes in extent, though a region 3 nodes wide would have been sufficient. Such a narrow region does not lend itself well to plotting, however. The figure serves to illustrate the minimal region that has to be solved for this kind of problem.

The field map of a double step discontinuity is shown in Figure 6.14. Though in this case it is only necessary to solve a mesh extending one unit beyond the step on either side, the solution is again taken slightly further beyond the steps for illustrative purposes. The mesh in this case was 31 radial by 20 axial nodes. Seven block iterations were required, with extrapolation after the sixth, for a maximum boundary correction of 0.0006 v., with 10 v. on the inner conductor and 0 v. on the outer.

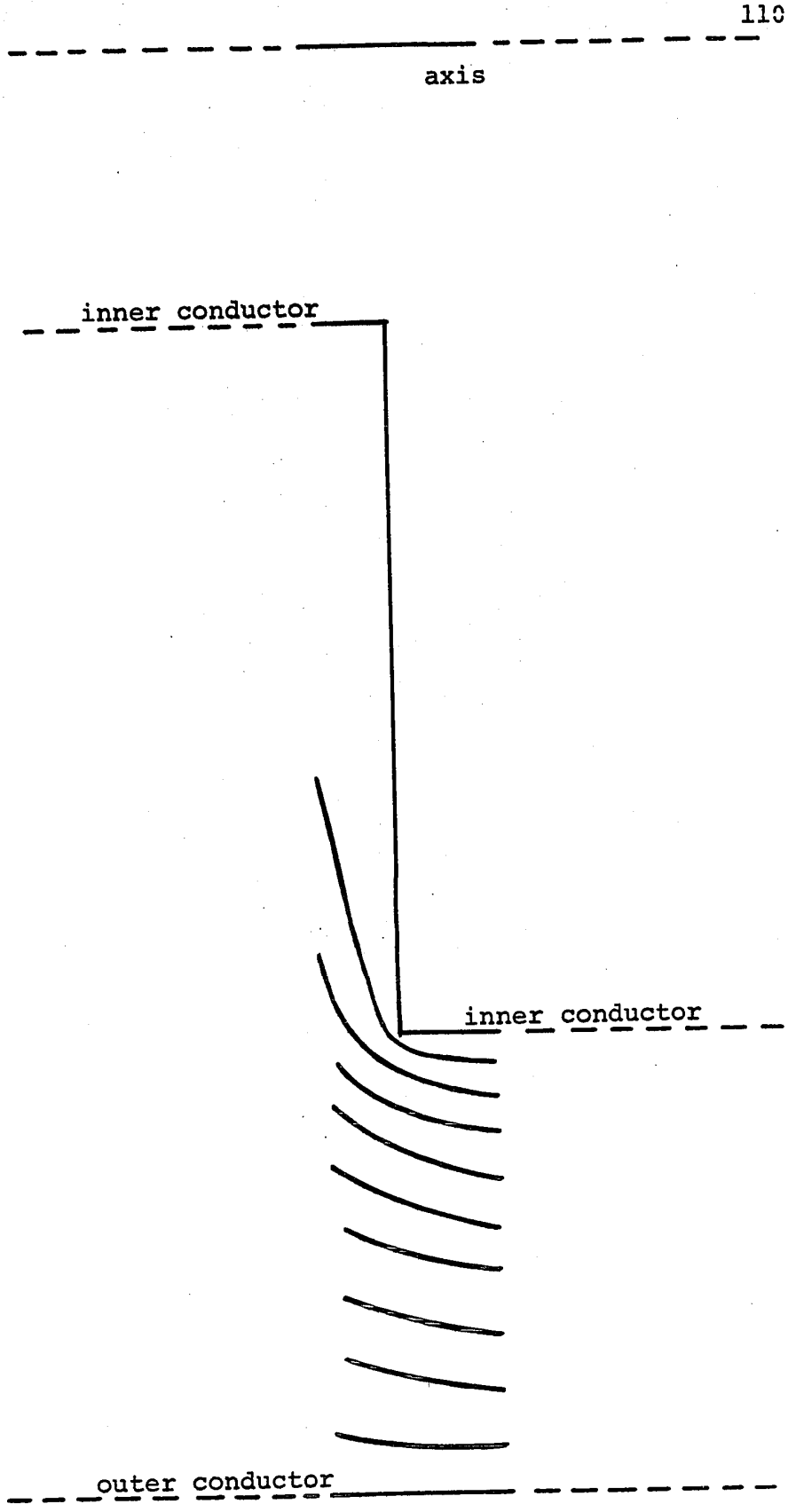

FIGURE 6.13: FIELD MAP OF COAXIAL LINE WITH STEP DISCONTINUITY IN INNER CONDUCTOR

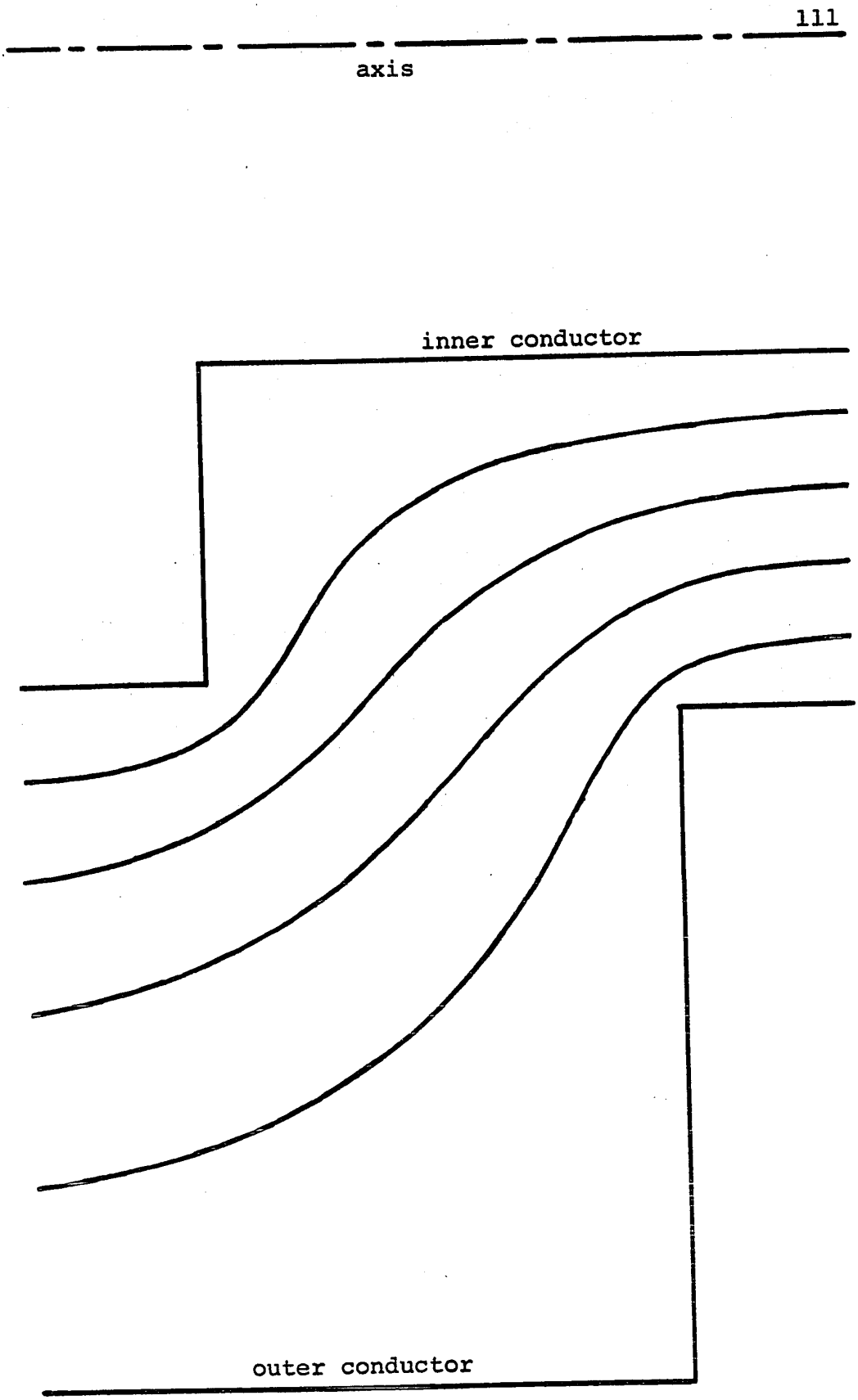

FIGURE 6.14: COAXIAL LINE WITH DOUBLE STEP DISCONTINUITY

Figure 6.15 illustrates the field map for the problem of a spherical dielectric bead support. The mesh size in this example is 16 radial by 31 axial nodes. The dielectric constant of the bead is $\varepsilon_r=2$. Five block iterations with no extrapolation reduced the maximum boundary correction to 0.0004 v., with the potential difference between the outer and inner conductors being, once more, 10 v.

Application of boundary relaxation to plane strip problems is identical to the above procedures. A slight modification is required in the matrix C of equation 6.4 since a different coordinate system is used. It is shown in Appendix 3 that the shift matrix for strips can be related to the admittance matrix obtained by Sander [58] for a similar configuration. Sander's matrix has served to verify the accuracy of the iterative method employed here. Calculation of the shift matrix for coaxial lines as well as strips is discussed further in Appendix 3.

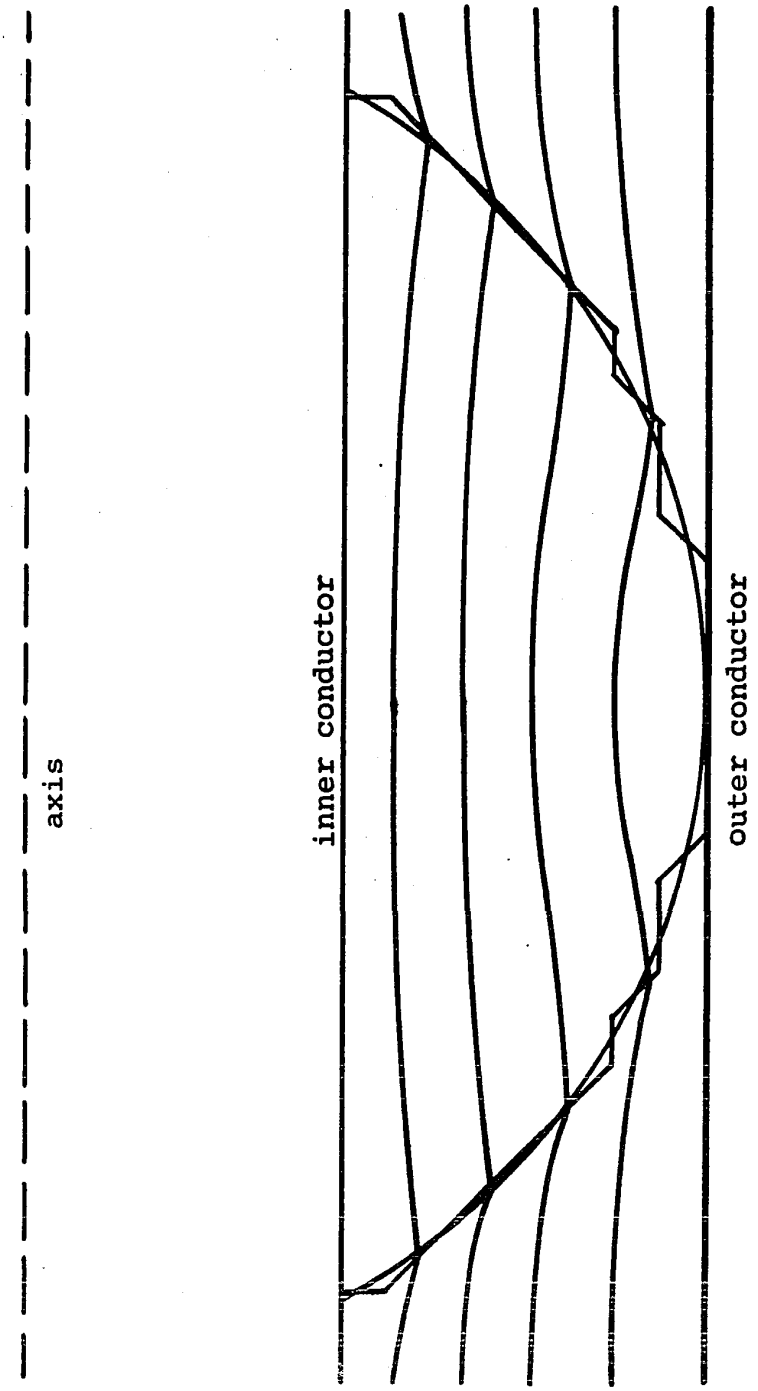

FIGURE 6.15: SPHERICAL DIELECTRIC BEAD SUPPORT
IN AIR-FILLED LINE

CHAPTER 7

CONCLUSIONS

An accurate, efficient and rigorous method has been presented for solution of infinitely extending field problems in two dimensions and three dimensions with axial symmetry. The boundary conditions at infinity are transformed to an arbitrary, finite, closed contour in terms of a potential shift operator. The solution within the arbitrary contour is obtained as the solution of an interior Dirichlet problem simultaneously with the shift relationship, and corresponds exactly with that of the infinitely extending problem. All necessary pertinent algorithms are given in detail.

The method is termed "boundary relaxation" and it is shown that the common interior Dirichlet and Neumann problems may be formulated in the same fashion as the infinitely extending problem, differing only in the definition of the shift operator.

Aside from the few special cases referred to in the text, this thesis has presented the first general numerical solution of the infinitely extending static field problem by finite differences. Existence of solution, as well as uniqueness and convergence, have been demonstrated theoretically

and by practical examples. Several convergent iterative schemes for solution of the problem are presented, and two optimizing algorithms are shown.

Boundary relaxation is shown to be an efficient solution algorithm whenever all sources and material inhomogeneities can be confined to a reasonably finite volume of space. Application has been shown to x-y, r-z and coaxial line problems by a variety of illustrative examples.

There is no objection, in principle, to application of boundary relaxation to three dimensional problems. Practical considerations of core memory and computation time have, however, prevented investigation of this topic. Practical solution of the general three dimensional problem will depend very greatly on the method of approximation used in the interior region of interest and further research is indicated in this area. Aside from a more efficient approximation of the problem in the interior region, the next obvious area of research seems to be extension of boundary relaxation to the more general elliptic operators, such as the Helmholtz operator. The applications might include scattering and diffraction problems, extension of the method used for coaxial lines to waveguide discontinuity problems and many more.

It is felt that the foundations of boundary relaxation as developed in this thesis will serve as a starting point for development of methods of solution for a great many classes of infinitely extending problems that are of interest in engineering and physics.

REFERENCES

[1] P.M. Morse and H. Feshbach, Methods of Theoretical Physics, New York: McGraw-Hill, 1953.

[2] A.G. Webster, Partial Differential Equations of Mathematical Physics, 2nd ed., New York: Dover, 1956.

[3] D. Vitkovitch (ed.), Field Analysis: Experimental and Computational Methods, London: Van Nostrand, 1966.

[4] A.R. Boothroyd, E.C. Cherry and R. Makar, "An electrolytic tank for the measurement of steady-state response, transient response, and allied properties of networks," J.IEE, Vol. 96, Part I, pp. 163-177, 1949.

[5] G. Liebmann, "Solution of partial differential equations with a resistance network analogue," BRIT. J.APPL. PHYS., Vol. 1, pp. 92-103, 1950.

[6] P. Silvester, "Network analog solution of skin and proximity effect problems", IEEE TRANS, Vol. PAS-86, No. 2, pp. 241-247, Feb., 1967.

[7] T.J. Higgins, "Electroanalogic methods," Six parts, APPL.MECH.REV., Part I : Vol. 9, pp. 1-4, Jan. 1956.
Part II : Vol. 9, pp. 5-11, Feb. 1956.

[7] continued,

Part III : Vol. 10, pp. 49-54, Feb. 1957.

Part IV : Vol. 10, pp. 331-5, Aug. 1957.

Part V : Vol. 10, pp. 443-8, Oct. 1957.

Part VI : Vol. 11, pp. 203-6, May 1958

[8] B. Friedman, Principles and Techniques of Applied Mathematics, New York: Wiley, 1960.

[9] F.B. Hildebrand, Introduction to Numerical Analysis, New York: McGraw-Hill, 1956.

[10] K.J. Binns and P.J. Lawrenson, Analysis and Computation of Electric and Magnetic Field Problems, Oxford, England: Pergamon Press, 1963.

[11] E.L. Wachspress, Iterative Solution of Elliptic Systems, Englewood Cliffs: Prentice-Hall, 1966.

[12] G.E. Forsythe and W.R. Wasow, Finite Difference Methods for Partial Differential Equations, New York: Wiley, 1960.

[13] L.M. Milne-Thomson, The Calculus of Finite Differences, London: MacMillan, 1951.

[14] R.H. Galloway, H.McL. Ryan and M.F. Scott, "Calculation of electric fields by digital computer," PROC.IEE (London), Vol. 114, No. 6, pp. 824-9, June 1967.

[15] C.F. Gauss, "Brief an Gerling," WERKE, Vol. 9, pp. 278-81, Dec. 1823. (Translated by G.E. Forsythe, MATH.TAB. WASH., Vol. 5, pp. 255-8, 1951.)

[16] L. Seidel, "Über ein Verfahren die Gleichungen, auf welche die Methode der kleinsten Quadrate führt, sowie lineäre Gleichungen überhaupt durch successive Annäherung aufzulösen," ABHANDLUNGEN DER BAYERISCHEN AKADEMIE, Vol. 11, pp. 81-108, 1873.

[17] R.V. Southwell, "Stress calculation in frameworks by the method of 'Systematic Relaxation of Constraints'," PROC.ROY.SOC., Vol. 151, A, p. 56, 1935.

[18] L.F. Richardson, "The approximate arithmetical solution by finite differences of physical problems involving differential equations with an application to the stresses in a masonry dam," PHIL.TRANS.ROY.SOC. LONDON, Vol. 210A, pp. 307-57, 1910.

[19] C.G.J. Jacobi, "Über eine neue Auflösungsart der bei der Methode der kleinsten Quadrate vordkommenden lineären Gleichungen," ASTR.NACHR., Vol. 22, No. 523, pp. 297-306, 1845.

[20] H. Liebman, "Die angenährte Ermittelung harmonischer Functionen und konformer Abbildungen," Sitzungs-berichte der Mathematisch-Naturwissenschaftlichen Klasse der Bayerischen Akademie der Wissenschaften zu Müchen, pp. 385-416, 1918.

[21] G. Shortley and R. Weller, "The numerical solution of Laplace's equation," J.APPL.PHYS., Vol. 9, pp. 334-44, 1938.

[22] H. Geiringer, "On the solution of systems of linear equations by certain iteration methods," Reissner Anniversary Volume, Ann Arbor, Mich., pp. 365-93, 1949.

[23] S. Frankel, "Convergence rates of iterative treatments of partial differential equations," Math. Tables and Other Aids to Computation, Vol. 4, pp. 65-75, 1950.

[24] D.M. Young, "Iterative methods for solving partial differential equations of elliptic type," TRANS. AMER.MATH.SOC., Vol. 76, pp. 92-111, 1954.

[25] B.A. Carré, "The determination of the optimum accelerating factor for successive over-relaxation," COMPTR.JOUR., Vol. 4, pp. 73-8, 1961.

[26] J.K. Reid, "A method for finding the optimum successive over-relaxation parameter," COMPTR.JOUR., Vol. 9, pp. 200-204, 1966.

[27] D.W. Peaceman and H.H. Rachford, "The numerical solution of parabolic and elliptic differential equations," J.SOC.INDUSTR.APPL.MATH., Vol. 3, pp. 28-41, 1955.

[28] G. Shortley, "Use of Chebyscheff-polynomial operators in the numerical solution of boundary-value problems," J.APPL.PHYS., Vol. 24, No. 4, pp. 392-6, Apr. 1953.

[29] H.E. Wrigley, "On accelerating the Jacobi method for solving simultaneous equations by Chebyshev extrapolation when the eigenvalues of the iteration matrix are complex," Report AEEW-R224, Atomic Energy Establishment Winfrith, Dorchester, Dorset, England.

[30] F. de la Vallée Poussin, "An accelerated relaxation algorithm for iterative solution of elliptic equations," SIAM J.NUMER.ANAL., Vol. 5, No. 2, pp. 340-51, June 1968.

[31] R.S. Varga, Matrix Iterative Analysis, Englewood Cliffs: Prentice-Hall, 1962.

[32] D. Greenspan, Introductory Numerical Analysis of Elliptic Boundary Value Problems, New York: Harper & Row, 1965.

[33] J.T. Storey and M.J. Billings, "General digital-computer program for the determination of 3-dimensional electrostatic axially symmetric fields," PROC.IEE, Vol. 114, pp. 824-9, Oct. 1967.

[34] D.F. Binns and T.J. Randall, "Improved spark-gap voltmeter," PROC.IEE, Vol. 113, pp. 1557-61, Sept. 1966.

[35] H.E. Green, "The numerical solution of some important transmission-line problems," IEEE TRANS., Vol. MTT-13, No. 5, pp. 676-92, Sept. 1965.

[36] H.McL. Ryan, "Application of Laplacian field analysis in the design of high voltage switchgear insulation," IEE Colloquium on APPLICATIONS OF COMPUTERS TO FIELD ANALYSIS, Colloquium Digest No. 1967/12, May 1967, p. 10.

[37] D. Greenspan and E. Silverman, "Approximate solution of the exterior Dirichlet problem and the calculation of electrostatic capacity," The University of Michigan Engineering Summer Conferences, Numerical Analysis, June 13-24, 1966.

[38] A.M. Patwari, "Analysis of some two-dimensional scattering problems," Doctoral Thesis, University of Sheffield, England, Sept. 1967.

[39] M. Poloujadoff and J.-Cl. Sabonnadière, COMPTES RENDUS C.R.ACAD.SC.PARIS, Vol. 266, pp. 230-3, Jan. 1968.

[40] _____, op.cit., pp. 272-5.

[41] I.A. Cermak, "A relaxation method for open boundary field problems," Master of Engineering Thesis, McGill University, Montreal, Canada, July 1967.

[42] I.A. Cermak and P. Silvester, "Solution of 2-dimensional field problems by boundary relaxation," PROC. IEE., Vol. 115, No. 9, pp. 1341-8, Sept. 1968.

[43] P. Silvester, Modern Electromagnetic Fields, Englewood Cliffs: Prentice-Hall, 1968.

[44] O.D. Kellogg, Foundations of Potential Theory, New York: Dover, 1953.

[45] D.S. Jones, The Theory of Electromagnetism, London: Pergamon Press, 1964.

[46] S.G. Mikhlin and K.L. Smolitskyi, Approximate Methods for Solution of Differential and Integral Equations, New York: American Elsevier, 1967.

[47] R.F. Harrington, Field Computation by Moment Methods, New York: MacMillan, 1968.

[48] P. Amstutz, "Sur la solution élémentaire d'une équation de Laplace discrétisée," ANNALES DES TELECOMMUNICATIONS, Vol. 22, No. 5, pp. 149-52, 1967.

[49] K.F. Sander, "Solution of certain finite difference equations connected with Laplace's equation," PROC. CAMB.PHIL.SOC., Vol. 58, Part I, p. 38, 1961.

[50] J.W. Duncan, "The accuracy of finite-difference solutions of Laplace's equation," IEEE TRANS., Vol. MTT-15, No. 10, pp. 575-82, Oct. 1967.

[51] P. Schiske and H.R. Uhlig, "Ein Verfahren zur effektiven Verdopplung der Maschenzahl von Widerstandsnetzen mit einer Anwendung auf die Elektronenoptik," ARCH.FUR ELECTROTECHNIK, Vol. 50, No.3, pp. 166-70, 1965.

[52] J.R. Whinnery and H.W. Jamieson, "Equivalent circuits for discontinuities in transmission lines," PROC. IRE, Vol. 32, pp. 98-114, 1944.

[53] P.J.B. Clarricoats and K.R. Slinn, "Numerical solution of waveguide-discontinuity problems," PROC. IEE, Vol. 114, pp. 878-86, 1967.

[54] J.R. Whinnery, H.W. Jamieson and T.E. Robbins, "Coaxial line discontinuities," PROC.IRE, Vol. 32, pp. 695-709, 1944.

[55] P.I. Somlo, "The computation of coaxial line step capacitances," IEEE TRANS., Vol. MTT-15, No. 1, pp. 48-53, Jan. 1967.

[56] P. Silvester and I.A. Cermak, "Analysis of coaxial line discontinuities by boundary relaxation," to be published in IEEE Trans. on Microwave Theory and Techniques, 1969.

[57] I.N. Sneddon, Fourier Transorms, New York: McGraw-Hill, 1951.

[58] K.F. Sander, "The application of network analysis to the resistance network analogue and to relaxation procedures," PROC. IEE, Vol. 109C, pp. 516-26, 1962.

APPENDIX 1

SHIFT MATRICES FOR X-Y PLANE

A1.1 DISCRETIZED GREEN'S FUNCTION.

The elementary solution of the finite difference Laplacian is derived in this section following the method of Amstutz [48], with some of the intermediate mathematical steps presented in more detail. Following the derivation, practical implementation of Amstutz's procedure is discussed.

The function sought is one defined on discrete points of the x-y plane, for example the points that have integer coordinates (m,n), and which satisfies the discretized form of Laplace's equation

$$D\psi(m,n) = 0 \tag{A1.1}$$

where D is the linear operator defined by

$$D\psi(m,n) = \psi(m+1,n) + \psi(m-1,n) + \psi(m,n+1) + \psi(m,n-1) - 4\psi(m,n) \tag{A1.2}$$

Amstutz imposes the following conditions (condition d shall be changed later) on the function ψ:

a) $D\psi = 0$ for $(m,n) \neq (0,0)$;

b) $D\psi = 1$ for $(m,n) = (0,0)$;

c) that there exist integers m_o and n_o, such that $\psi(m,n) - \psi(m-m_o,n-n_o)$ tends to zero as $r^2 = m^2 + n^2$ tends to infinity;

d) $\psi(0,0) = 0$.

A suitable function ψ is found by a heuristic reasoning as follows. From

$$D \cos(ma+nb) = -2(2 - \cos a - \cos b) \cos(ma+nb)$$

one deduces that one solution of

$$D\ F = \cos(ma+nb)$$

is

$$F = \frac{-\cos(ma+nb)}{2(2 - \cos a - \cos b)}$$

One can hence hope to find a solution of

$$D\psi = \int_{\Gamma} \cos(ma+nb)\ da\ db$$

$$= 0 \text{ for } (m,n) \neq 0$$

$$= 4\pi^2 \text{ for } (m,n) = 0,$$

on integrating F with respect to a and b over the square $\Gamma(-\pi \leq a \leq \pi, -\pi \leq b \leq \pi)$. However, F has to be adjusted by a quantity independent of m and n in order to obtain a convergent integral. One is thus led to

$$\psi(m,n) = \frac{1}{8\pi^2}\int_{\Gamma} \frac{1 - \cos(ma + nb)}{2 - \cos a - \cos b}\, da\, db \qquad (A1.3)$$

where Γ is as defined above. Amstutz shows that the function defined by (A1.3) satisfies the above conditions a) to d).

Evaluation of the integral in (A1.3) may be accomplished in a straightforward manner for the case m=n. The change of variable is introduced

$$a + b = 2s$$

$$b - a = 2t$$

which changes the region of integration from the square to the diamond-shaped area shown in Figure A1.1. The resulting function is even in s and the mapping of the function is such that the integral over area (1) in the figure equals the integral over area (2), and similarly for areas (3) and (4). The integration is done for the right half-plane only, and the integral in t may be taken as $\frac{1}{2}\int_{-\pi}^{\pi} dt$.

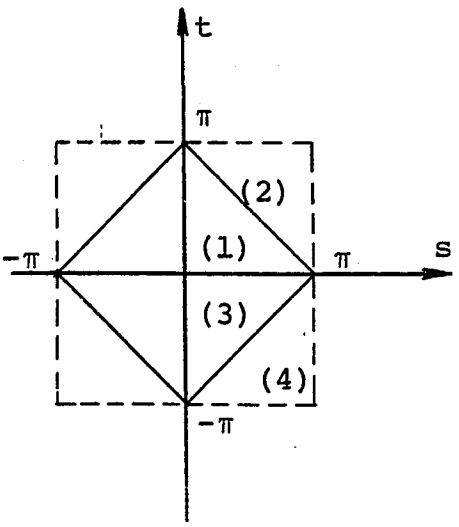

FIGURE A1.1

The integral thus becomes

$$8\pi^2\, \psi(m,m) = \int_0^{\pi}\int_{-\pi}^{\pi} \frac{1 - \cos 2ms}{1 - \cos s \cos t}\, dt\, ds$$

The integral in t may be performed by taking for a variable $z = e^{jt}$, so that

$$\int_{-\pi}^{\pi} \frac{1}{1 - \cos s \cos t}\, dt = \int_C \frac{2dz}{j(2z - z^2\cos s - \cos s)}$$

where C is the contour given by the unit circle. This integral may be evaluated by means of residues. The integrand has one pole within the contour C and the residue at this pole is readily evaluated as

$$\text{Residue} = -\frac{1}{2\sqrt{1/\cos^2 s - 1}}$$

so that the integral in t becomes $4\pi/2\sin s$. Hence the remaining integration is

$$2\pi\ \psi(m,m) = \int_0^{\pi} \frac{1 - \cos 2ms}{2\sin s}\, ds$$

The last integral is the real part of

$$-\int_0^{\pi} \frac{1 - e^{2mjs}}{1 - e^{2js}}\, de^{js}$$

$$= -\int_0^{\pi} [\ 1 + e^{2js} + \ldots + e^{2(m-1)js}\ ]\, de^{js}$$

$$= 2(\ 1 + 1/3 + \ldots + \frac{1}{2m-1}\ )$$

from which

$$\pi\,\psi(m,m) = \sum_{p=1}^{m} \frac{1}{2p-1}$$

However, there follows immediately, from (A1.3)

$$\psi(1,0) = \psi(0,1) = \tfrac{1}{4}$$

and

$$\psi(m,n) = \psi(n,m) = \psi(m,-n)$$

Hence ψ may be evaluated at all points in the plane from symmetry considerations and by application of the five-point operator of (A1.2).

For large values of m and n, the function ψ approaches the limiting function

$$\psi(m,n) \to \frac{1}{4\pi}\left(\log_e(m^2 + n^2) + 2\gamma + \log_e 8\right), \quad r \to \infty,$$

where γ is Euler's constant. Convergence to the limit is quite rapid. At the point (5,5), for example, the difference between ψ and the limiting function is 0.00026.

Actual evaluation of ψ as suggested by the above procedure leads to a few complications. The function $\psi(m,m)$ is easily evaluated but repeated application of the five-point operator (with symmetry considerations) leads to significant round-off error propagation. Hence a practical Green's function subroutine may be written so as to contain stored values of ψ in a small region surrounding the singularity and for values outside this region to use the limiting formula above.

The actual values of ψ as calculated here are not practical, especially the zero potential value at the singularity itself. Furthermore, it is desirable that ψ decrease in value for increasing radius. If the potential at the singularity point is chosen to be unity, then a suitable normalized Green's function is

$$\psi_n(m,n) = 1 - \psi(m,n) \qquad \text{(A1.4)}$$

This choice is justified, since a constant reference potential may be added or subtracted without affecting the problem.

A1.2 Construction of the Shift Matrix

A rectangular interior region of interest is convenient in the x-y plane, mainly through programming considerations, since the indexing is relatively simple, and the shift matrices possess certain symmetries which reduce the storage requirement.

Consider a rectangular region of M by N nodes as shown in Figure A1.2. The discussion will be restricted to even values of M and N, purely for reasons of convenience. The contour S2 is indicated by x's and S1 by o's. If sources are placed in S1, with source strengths I_o, then

$$V_{S1} = SI_o$$

$$V_{S2} = PI_o$$

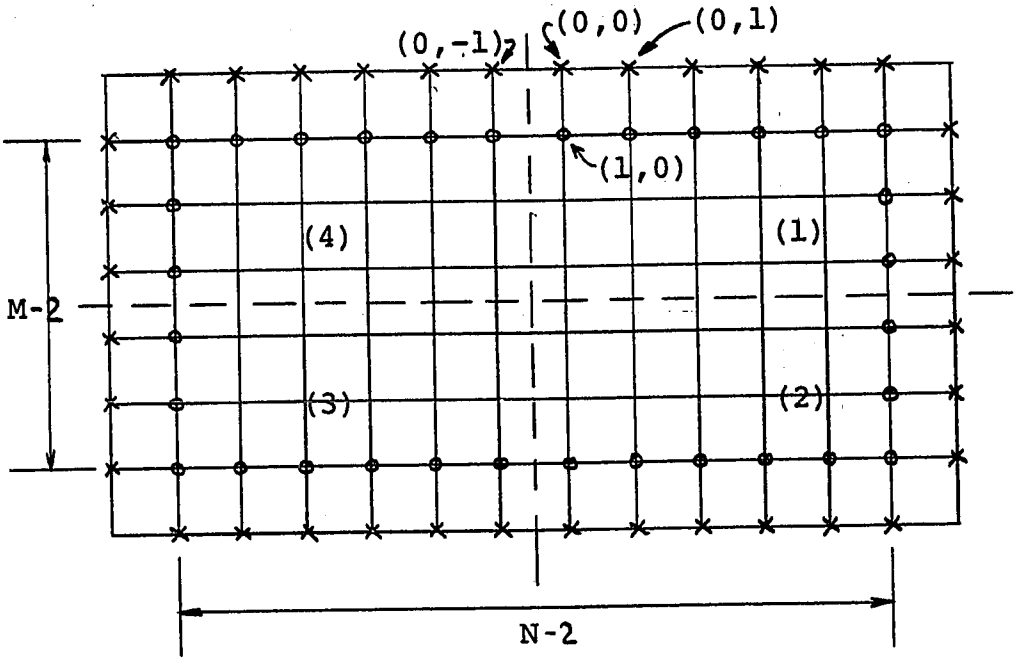

FIGURE A1.2: RECTANGULAR REGION OF INTEREST IN X-Y PLANE

where each element of the matrices P and S is an appropriate value of ψ. From the above,

$$V_{S2} = QV_{S1} = PS^{-1}V_{S1}$$

which defines the desired shift matrix.

If the origin (of the x-y coordinate system) is chosen to be the top right-hand center node of the region of interest, as shown in Figure A1.2, and if the numbering of the points on S1 and S2 is clockwise from the points (1,0) and (0,0) respectively, each of the indices (i,j) of the matrices P, S and Q may be mapped into coordinates in the mesh by a simple indexing scheme. For example, each element S_{ij} of the matrix S may be interpreted as follows: s_{ij} is the potential at the node corresponding to the index i, when the source is located at the node corresponding to the index j. Hence all that is required is a mapping of each of i and j into the coordinates

(m,n) of S1. This mapping will be termed the "S" mapping and may be carried out as follows:

Let I be the index i or j of the S matrix element to be mapped into S1. Then the "S" mapping may be constructed as

$\underline{I<N/2}$

$m = 1$

$n = I - 1$

$\underline{N/2 \leq I \leq N/2 + M - 5}$

$m = I - N/2 + 2$

$n = N/2 - 2$

$\underline{N/2 + M - 4 \leq I \leq N/2 + M + N - 7}$

$m = M - 2$

$n = N + M - 6 - I$

$\underline{N/2 + N + M - 6 \leq I \leq N/2 + N + 2M - 11}$

$m = 2M + N + N/2 - 9 - I$

$n = 1 - N/2$

$\underline{N/2 + N + 2M - 10 \leq I \leq 2(M + N) - 12}$

$m = 1$

$n = I - 2(M + N) + 11$

In mapping of the S matrix elements as above, let the index i be mapped onto the coordinates (m,n), (the "measuring" point), and the index j be mapped onto the coordinates (m_o,n_o), (the "source" point). The appropriate value of ψ then is

$$s_{ij} = \psi(m,n;m_o,n_o)$$

$$= \psi(m-m_o,\ n-n_o)$$

The mapping of the elements p_{ij} for the matrix P may be accomplished in the same fashion. The index j (corresponding to the source location) is mapped into (m_o,n_o) on S1 by the above "S" mapping. The index i, however, has to be mapped into S2. This may be done by means of the following "P" mapping:

$\underline{I < N/2}$

$m = 0$

$n = I - 1$

$\underline{N/2 \leq I \leq M + N/2 - 3}$

$m = I - N/2 + 1$

$n = N/2 - 1$

$\underline{M + N/2 - 2 \leq I \leq M + N + N/2 - 5}$

$m = M - 1$

$n = M + N - I - 4$

$\underline{M + N + N/2 - 4 \leq I \leq 2M + N + N/2 - 7}$

$m = 2M + N + N/2 - I - 6$

$n = -N/2$

$\underline{2M + N + N/2 - 6 \leq I \leq 2(M + N) - 8}$

$m = 0$

$n = I + 7 - 2(M + N)$

As in the case of the S matrix, the elements of P are obtained as

$$P_{ij} = \psi(m,n;m_o,n_o)$$
$$= \psi(m-m_o,\ n-n_o)$$

where (m,n) are obtained from i by the "P" mapping and (m_o,n_o) are obtained from j by the "S" mapping. Note that the "S" and "P" mappings may also be used in the boundary relaxation programs to construct the vectors V_{S1} and V_{S2} from the field values.

On inspection of Figure A1.2 it is readily seen that not all elements of the matrices P, S and Q are independent, since the region chosen is symmetric about two planes as shown by the dashed lines*. The corresponding matrices possess a certain structural symmetry which may be exploited. If the ordering of points on S1 and S2 is clockwise from right top center of the region, the resulting symmetries are not of the usual type. It will therefore be convenient to define a certain matrix ordering property as follows:

DEFINITION: If $A=a_{ij}$ is a matrix of size K by L, (i.e., K rows and L columns), then the reverse matrix A is defined as

$$A^r = (a_{ij})^r = (a_{K+1-i,L+1-j})$$

i.e., the reverse matrix A contains the elements of A, ordered "in reverse".

---

* This does not mean that the problem within the mesh has to possess any symmetry, since the symmetries in the shift matrix arise from the geometry of the region and not the problem.

This may easily be visualized by means of a simple example:

$$A = \begin{pmatrix} 1 & 2 \\ 3 & 4 \\ 5 & 6 \end{pmatrix}, \qquad A^r = \begin{pmatrix} 6 & 5 \\ 4 & 3 \\ 2 & 1 \end{pmatrix}$$

The shift matrix Q may thus be written in the partitioned form

$$Q = \begin{pmatrix} Q_1 & Q_2 & Q_3 & Q_4 \\ Q_2^r & Q_1^r & Q_4^r & Q_3^r \\ Q_3 & Q_4 & Q_1 & Q_2 \\ Q_4^r & Q_3^r & Q_2^r & Q_1^r \end{pmatrix}$$

where the submatrices Q_1, Q_2, Q_3 and Q_4 refer to the effect of the potentials on that part of S1 in the quadrant numbered (1) in the Figure A1.2 on those potentials on S2 in quadrants (1) to (4) respectively. The above is true of the matrices S and P as well. The elements of the submatrices Q_1 to Q_4 are easily programmable as independent elements of Q, since the entire matrix Q may be easily generated if they are known. The matrix Q has fewer independent elements than are indicated by the above partitioning, but exploitation of this fact is prohibitive as regards programming.

The matrices S^{-1}, P and Q may easily be constructed using only approximately three quarters of the memory required for storage of the entire Q matrix had the symmetries not been

exploited. The matrix S is of the form

$$S = \begin{pmatrix} X & Y \\ Y & X \end{pmatrix}$$

so that S^{-1} may be written as

$$S^{-1} = \begin{pmatrix} X & Y \\ Y & X \end{pmatrix}^{-1} = \begin{pmatrix} (X - YX^{-1}Y)^{-1} & (Y - XY^{-1}X)^{-1} \\ (Y - XY^{-1}X)^{-1} & (X - YX^{-1}Y)^{-1} \end{pmatrix}$$

where $(Y - XY^{-1}X)^{-1}$ may be written as $-(X - YX^{-1}Y)^{-1}YX^{-1}$.

The procedure for calculating Q is now as follows: Storage is reserved for the matrices X and Y. Working storage is reserved for a matrix W, which is the same size as X and Y. The elements of X and Y are then calculated. The procedure for obtaining S^{-1} (that is, the independent elements of S^{-1}) may be described in a simple fashion by using the ALGOL assignment operator:= (meaning "set equal to"), as follows:

$W := X^{-1}$

$W := YW$ ... (YX^{-1})

$Y := WY$ ... $(YX^{-1}Y)$

$X := (X - Y)^{-1}$ ... $(X - YX^{-1}Y)^{-1}$

$Y := -XW$ ... $-(X - YX^{-1}Y)^{-1}YX^{-1}$

The matrices X and Y now contain the top half of S^{-1}. The storage space allotted to W may next be used to construct the top quarter of the matrix P. A special matrix multiplication routine is used to construct the top quarter of PS^{-1}, or Q.

A1.3 FORTRAN Program Listings

This section lists the various programs necessary for implementation of the preceding computational procedures. The programs are in FORTRAN IV Language, Level G, suitable for use without modification on IBM 360 series computers. The programs are quite heavily commented, so that the preceding discussion along with the comments in the programs should be sufficient for full comprehension of the various steps in the generation of shift matrices for rectangular regions in the x-y plane. The matrix inversion routine used is a locally available Gauss-Jordan routine, called by

```
CALL INVERT(A,IJ,IK,M,N,DELTA,EPS)
```

A	is the matrix to be inverted. A is replaced by its inverse in the routine.
IJ,IK	are the dimensions of the array A in the calling program.
M,N	are the dimensions of the matrix to be inverted. Normally, M=N for direct inversion. There is provision in the routine for the solution of simultaneous equations, hence N may exceed M by the number of right hand vectors to be solved for.
DELTA	is the value of the determinant of A
EPS	is the smallest pivot used in the inversion.

MAIN

```
C  SHIFT MATRIX GENERATOR FOR RECTANGULAR REGIONS
C  IN (X,Y) PLANE.  REGION SIZE IS MM POINTS BY NN POINTS
C  WHERE BOTH MM AND NN ARE RESTRICTED TO EVEN NUMBERS.
C  NUMBERING STARTS RIGHT OF CENTER AT THE TOP OF THE
C  REGION AND PROGRESSES CLOCKWISE AROUND THE REGION.
C  ONLY THE TOP 1/4 OF THE SHIFT MATRIX IS GENERATED.
C
      DIMENSION P(35,136),A(68,68),B(68,68),C(68,68),W(136)
      EQUIVALENCE (P(1,1),C(1,1))
      II=35
      JJ=136
      IJ=68
C  INPUT ROUTINE
    1 READ(5,100) MM,NN
  100 FORMAT(16I5)
      IF(MM.EQ.0) STOP
C
C  BUILD TOP HALF OF S MATRIX AS A AND B
      CALL SMATRX(A,B,IJ,MM,NN)
C
C  ***INVERT S BY BLOCKS***
      LL2=MM+NN-6
C  STORE A IN ALTERNATE LOCATION
      DO 2 I=1,LL2
      DO 2 J=1,LL2
    2 C(I,J)=A(I,J)
C  FORM AI= A INVERSE
      CALL INVERT(C,IJ,IJ,LL2,LL2,DEL1,EPS1)
C  FORM  B*AI
      CALL PREMUL(B,C,IJ,MM,NN,W)
C  FORM  B*AI*B
      CALL PREMUL(C,B,IJ,MM,NN,W)
C  FORM (A-B*AI*B)I  AND STORE IN A
      DO 3 I=1,LL2
      DO 3 J=1,LL2
    3 A(I,J)=A(I,J)-B(I,J)
      CALL INVERT(A,IJ,IJ,LL2,LL2,DEL2,EPS2)
C  FORM   -(A-B*AI*B)I*B*AI  AND STORE IN B
      DO 4 I=1,LL2
      DO 4 J=1,LL2
      B(I,J)=0.
      DO 4 K=1,LL2
    4 B(I,J)=B(I,J)-A(I,K)*C(K,J)
C
C  ***--------***
C
C  FORM TOP 1/4 OF P MATRIX
      CALL PMATRX(P,II,JJ,MM,NN)
C  FORM TOP 1/4 OF SHIFT MATRIX
      CALL PSMULT(P,II,JJ,A,B,IJ,MM,NN,W)
C
C  OUTPUT ROUTINE
      LL=2*(MM+NN)-12
      KK=LL/4+1
```

MAIN

```
      CALL OUTPUT(P,II,JJ,KK,LL)
      WRITE(6,101) DEL1,EPS1,DEL2,EPS2
  101 FORMAT(1H0,'DEL1=',1PE9.2,'  EPS1=',E9.2,'     DEL2=',E9.2,
     &  '  EPS2=',E9.2)
      GO TO 1
      END
```

SMAP

```
      SUBROUTINE SMAP(MM,NN,I,M,N)
C  MAPS INDEX OF S MATRIX INTO POSITION IN FIELD ARRAY
C  --I--INPUT INDEX
C  --M,N--OUTPUT COORDINATES OF POINT IN ARRAY
C  -- THE POINT (0,0) IS LOCATED JUST RIGHT OF CENTER,
C     AT THE TOP OF THE FIELD ARRAY
      N2=NN/2
      IF(I.GE.N2) GO TO 1
      M=1
      N=I-1
      RETURN
    1 IF(I.GT.N2+MM-5) GO TO 2
      M=I-N2+2
      N=N2-2
      RETURN
    2 IF(I.GT.N2+MM+NN-7) GO TO 3
      M=MM-2
      N=NN+MM-6-I
      RETURN
    3 IF(I.GT.N2+NN+MM+MM-11) GO TO 4
      M=MM+MM+N2-9-I+NN
      N=-N2+1
      RETURN
    4 M=1
      N=I+11-MM-MM-NN-NN
      RETURN
      END
```

SMATRX

```
      SUBROUTINE SMATRX(A,B,II,MM,NN)
C  GENERATES TOP HALF OF S MATRIX, PARTITIONED INTO
C  MATRICES A AND B.
C  MATRICES A AND B ARE DIMENSIONED (II,II) IN THE CALLING
C  PROGRAM
C  REQUIRES MAPPING ROUTINE 'SMAP' AND GREEN'S FUNCTION
C  ROUTINE  PHI(I,J) WHERE THE SINGULARITY IS PHI(0,0).
C
      DIMENSION A(II,II),B(II,II)
C  DETERMINE SIZE OF A AND B
      LL=MM+NN-6
      LL2=LL/2
      LL1=LL2+1
C  BUILD TOP HALF OF EACH OF A AND B
      DO 1 I=1,LL2
      DO 1 J=1,LL
      CALL SMAP(MM,NN,I,M,N)
      CALL SMAP(MM,NN,J,M0,N0)
      A(I,J)=PHI(M-M0,N-N0)
      JJ=J+LL
      CALL SMAP(MM,NN,JJ,M0,N0)
      B(I,J)=PHI(M-M0,N-N0)
    1 CONTINUE
C  BUILD BOTTOM HALVES OF A AND B
      DO 2 I=LL1,LL
      I1=LL-I+1
      DO 2 J=1,LL
      J1=LL-J+1
      A(I,J)=A(I1,J1)
    2 B(I,J)=B(I1,J1)
      RETURN
      END
```

PMAP

```
      SUBROUTINE PMAP(MM,NN,I,M,N)
C  SAME AS SMAP, BUT MAPS P MATRIX
      N2=NN/2
      IF(I.GE.N2) GO TO 1
      M=0
      N=I-1
      RETURN
    1 IF(I.GT.MM+N2-3) GO TO 2
      M=I-N2+1
      N=N2-1
      RETURN
    2 IF(I.GT.MM+NN+N2-5) GO TO 3
      M=MM-1
      N=MM+NN-4-I
      RETURN
    3 IF(I.GT.MM+MM+NN+N2-7) GO TO 4
      M=MM+MM+NN+N2-6-I
      N=-N2
      RETURN
    4 M=0
      N=I+7-MM-MM-NN-NN
      RETURN
      END
```

PMATRX

```
      SUBROUTINE PMATRX(P,II,JJ,MM,NN)
C  GENERATES TOP QUARTER OF P MATRIX.
C  DIMENSIONED P(II,JJ) IN CALLING PROGRAM
      DIMENSION P(II,JJ)
C  DETERMINE SIZE OF P
      LL=2*(MM+NN)-12
      KK=LL/4+1
C  BUILD TOP QUARTER OF  P
      DO 1 I=1,KK
      DO 1 J=1,LL
      CALL PMAP(MM,NN,I,M,N)
      CALL SMAP(MM,NN,J,M0,N0)
      P(I,J)=PHI(M-M0,N-N0)
    1 CONTINUE
      RETURN
      END
```

PSMULT

```
      SUBROUTINE PSMULT(P,II,JJ,A,B,IJ,MM,NN,W)
C  POSTMULTIPLIES P BY S, TOP HALF OF S BEING STORED IN A AND B
C  ALL DIMENSIONS AS BEFORE
C  W--WORK VECTOR OF LENGTH JJ
C  OUTPUT IS P
      DIMENSION P(II,JJ),A(IJ,IJ),B(IJ,IJ),W(1)
C  DETERMINE SIZE OF MATRICES
      LL=2*(MM+NN)-12
      KK=LL/4+1
      LL2=LL/2
C  PERFORM MULTIPLICATION
      DO 1 I=1,KK
      DO 2 J=1,LL
      W(J)=0.
      IF(J.GT.LL2) GO TO 3
      DO 4 K=1,LL2
    4 W(J)=W(J)+P(I,K)*A(K,J)
      DO 5 K=1,LL2
      K1=K+LL2
    5 W(J)=W(J)+P(I,K1)*B(K,J)
      GO TO 2
    3 J1=J-LL2
      DO 6 K=1,LL2
    6 W(J)=W(J)+P(I,K)*B(K,J1)
      DO 7 K=1,LL2
      K1=K+LL2
    7 W(J)=W(J)+P(I,K1)*A(K,J1)
    2 CONTINUE
      DO 8 J=1,LL
    8 P(I,J)=W(J)
    1 CONTINUE
      RETURN
      END
```

PREMUL

```
      SUBROUTINE PREMUL(A,B,IJ,MM,NN,W)
C     FORMS PRODUCT AB AND RETURNS RESULT UNDER B.
C     IJ--DIMENSIONS OF A AND B IN CALLING PROGRAM
C     W--WORKING VECTOR OF LENFTH IJ OR MORE.
      DIMENSION A(IJ,IJ),B(IJ,IJ),W(1)
C     DETERMINE SIZE OF MATRICES
      LL=MM+NN-6
C     PERFORM MULTIPLICATION
      DO 1 J=1,LL
      DO 2 I=1,LL
      W(I)=0.
      DO 2 K=1,LL
    2 W(I)=W(I)+A(I,K)*B(K,J)
      DO 3 I=1,LL
    3 B(I,J)=W(I)
    1 CONTINUE
      RETURN
      END
```

PHI

```
      FUNCTION PHI(M,N)
C     GREEN'S FUNCTION SUBROUTINE FOR THE (X,Y) LAPLACIAN
C     PLANE, C.F.,'P.AMSTUTZ,ANN.DES TELECOMM., VOL.22,
C     1967,PP.149-152.'
C     THE FUNCTIONS UP TO INDEX (NN,NN) ARE STORED INTERNALLY
C     AND THE REMAINDER IS CALCULATED EXPLICITLY BY AMSTUTZ'S
C     FORMULA (10).  THE STORED VALUES ARE STORED ROWWISE,
C     UPPER TRIANGLE INCLUDING THE DIAGONAL.
      DIMENSION VAL(21)
      DATA VAL/1.,.75,.63662,.56972,.52301,.48710,
     1 .68169,.61338,.55962,.51760,.48375,
     2 .57559,.53779,.50404,.47470,
     3 .51192,.48606,.46181,
     4 .46645,.44685,
     5 .43108/
      DATA FPI,GAMMA/.0795775,1.154431/
      NN=5
      MA=IABS(M)
      NA=IABS(N)
      IF(MA.GT.NN) GO TO 1
      IF(NA.GT.NN) GO TO 1
      IF(NA.GE.MA) GO TO 2
      I=NA
      J=MA
      GO TO 3
    2 I=MA
      J=NA
    3 K=NN*I-(I**2-I)/2 +J+1
      PHI=VAL(K)
      RETURN
    1 PHI=1.-FPI*(ALOG(FLOAT(8*(M**2+N**2)))+GAMMA)
      RETURN
      END
```

OUTPUT

```
      SUBROUTINE OUTPUT(P,II,JJ,KK,LL)
      DIMENSION P(II,JJ),CARD(9)
      WRITE(6,104)
      LP=(LL-1)/9+1
      IND=0
      DO 11 I=1,KK
      DO 12 II=1,LP
      IND=IND+1
      JJ=9*(II-1)
      DO 13 J=1,9
   13 CARD(J)=0.
      DO 14 J=1,9
      JP=J+JJ
      IF(JP.GT.LL) GO TO 15
   14 CARD(J)=P(I,JP)
   15 CONTINUE
      WRITE(6,101)(CARD(J),J=1,9),IND
      WRITE(7,102)(CARD(J),J=1,9),IND
   12 CONTINUE
      WRITE(6,105)
   11 CONTINUE
      RETURN
  105 FORMAT(1H )
  101 FORMAT(1H ,1P9E13.5,I8)
  102 FORMAT(9Z8,I8)
  104 FORMAT(1H1)
      END
```

APPENDIX 2

SHIFT MATRICES FOR R-Z PLANE

A2.1 DISCRETIZED GREEN'S FUNCTIONS

Elementary solution of the finite difference Laplacian for the r-z plane may be accomplished by separation of variables. This has been done by Sander [49] and his method of solution is discussed briefly. As Sander's method is computationally prohibitive, a practical alternative method is presented for the evaluation of the required functions.

Following Sander's development, the finite difference Poisson's equation is written as

$$(r + \frac{h}{2})\, V(r+h,z) + (r - \frac{h}{2})\, V(r-h,z) - 2rV(r,z)$$
$$+ r\{V(r,z+h) + V(r,z-h) - 2V(r,z)\} = rh^2\sigma \qquad \text{(A2.1)}$$

For Laplace's equation, i.e., when the right hand side is zero, the substitution $V(r,z) = R(r)Z(z)$ yields two equations,

$$Z(z+h) + Z(z-h) - 2Z(z) = 2kZ(z) \qquad \text{(A2.2)}$$

$$(r + \frac{h}{2})R(r+h) + (r - \frac{h}{2})R(r-h) - 2rR(r) = -2krR(r) \qquad \text{(A2.3)}$$

Equation A2.2 may be normalized by the substitutions $z = \zeta h$, $Z(\zeta h) = F(\zeta)$. Equation A2.2 then becomes

$$F(\zeta+1) + F(\zeta-1) = 2(1+k)F(\zeta) \tag{A2.4}$$

The solution of (A2.4) are

$$F(\zeta) = e^{\mu\zeta}$$

where

$$\cosh \mu = 1 + k$$

Equation A2.3 may be normalized by the substitutions $r = \rho h$, $R(\rho h) = H(\rho)$. The equation for H is then

$$(\rho + \tfrac{1}{2})H(\rho + 1) + (\rho - \tfrac{1}{2})H(\rho - 1) - 2\rho \cosh\lambda\ H(\rho) = 0 \tag{A2.5}$$

where

$$\cosh \lambda = 1 - k = 2 - \cosh \mu$$

Equation A2.5 may be solved by standard methods. Two types of solution are required; the first representing the decaying solution of a charge distribution in an enclosed region, the second for the case of zero charge on the axis.

Solutions of equations of the form (A2.5) may be obtained as contour integrals of the type

$$H(\rho) = \int t^{\rho-1} v(t)\ dt$$

Sander shows that one solution, valid for $\rho > \frac{1}{2}$ is

$$\int_{0}^{(e^{-\lambda}+)} t^{\rho-\frac{1}{2}}(t - e^{\lambda})^{-\frac{1}{2}}(t - e^{-\lambda})^{-\frac{1}{2}}\, dt$$

A second solution, for all ρ is

$$\int_{(e^{-\lambda}+,e^{\lambda}-,e^{-\lambda}+)} t^{\rho-\frac{1}{2}}(t-e^{\lambda})^{-\frac{1}{2}}(t-e^{-\lambda})^{-\frac{1}{2}}\, dt$$

The two above solutions may be expressed in terms of the hypergeometric functions and are denoted U_1 and U_2. Once U_1 and U_2 are specified, the Wronskian L for equation A2.5 may be found. The solution (corresponding to a ring charge) is finally found as

$$n \geq n_o: \quad \psi(n,\zeta;n_o,0) = \frac{2n_o}{\pi}\int_0^{\pi} U_2(n_o,\lambda)U_1(n,\lambda)\,\frac{\cos\bar{\mu}\zeta}{L(0,\lambda)}\, d\bar{\mu}$$

$$n \geq n_o: \quad \psi(n,\zeta;n_o,0) = \frac{2n_o}{\pi}\int_0^{\pi} U_2(n,\lambda)U_1(n_o,\lambda)\,\frac{\cos\bar{\mu}\zeta}{L(0,\lambda)}\, d\bar{\mu}$$

Evaluation of ψ as in the above expressions is computationally prohibitive, both from a programming standpoint as well as required machine time. Point values of the Green's function to the continuous Laplacian may be used to approximate the required functions, as shown in Chapter 2 above.

The elementary solution to the continuous Laplacian in the r-z plane is the solution to a fine ring charge. This solution may be expressed as [43]

$$\psi(r,z;r_o,z_o) = \frac{1}{2\pi}\sqrt{\frac{r_o}{r}}\; k\, K(k) \quad , \; r_o \neq 0 \tag{A2.6}$$

where

$$k = \frac{2\sqrt{rr_o}}{\sqrt{(z-z_o)^2 + (r+r_o)^2}} \tag{A2.7}$$

and K(k) is the complete elliptic integral of the first kind, modulus k. At the singularity itself, ψ may be approximated by means of the five-point operator, viz.,

$$\begin{aligned}\psi(r_o,z_o;r_o,z_o) = \tfrac{1}{4}[&\psi(r_o,z_o+h;r_o,z_o) + \psi(r_o,z_o-h;r_o,z_o) \\ &+ \left(1 - \frac{h}{2r_o}\right)\psi(r_o-h,z_o;r_o,z_o) \\ &+ \left(1 + \frac{h}{2r_o}\right)\psi(r_o+h,z_o;r_o,z_o) + 1]\end{aligned} \tag{A2.8}$$

It is advisable from a computational standpoint to normalize ψ so that all potentials at the singularity itself are unity. This is accomplished by

$$\psi_n(r,z;r_o,z_o) = \frac{\psi(r,z;r_o,z_o)}{\psi(r_o,z_o;r_o,z_o)} \tag{A2.9}$$

The subscript n will be dropped for convenience and it will be assumed from this point that the functions ψ have been normalized.

The potential due to a point charge on the z axis, i.e., $\psi(r,z;0,z_o)$, is still required. An approximate expression may be obtained as follows: The finite difference Poisson's equation for a point charge on the axis is

$$V_N + V_S + 4V_E - 6V_0 = -\frac{q}{\varepsilon}$$

If $q/\varepsilon = 4\pi$, the potential everywhere (in the continuous case) is $1/\sqrt{r^2 + (z-z_o)^2}$. Substituting in the above equation and solving for V_0 yields

$$V_0 = 1 + 2\pi/3$$

Hence if the potential at the charge point in the mesh is taken as unity, the normalized Green's function corresponding to a point charge on the axis may be taken as

$$\psi(r,z;0,z_o) = \frac{1}{(1 + 2\pi/3)\sqrt{r^2 + (z-z_o)^2}} \qquad \text{(A2.10)}$$

A2.2 Construction of Q for a Rectangular Region

Though a "P" and "S" mapping may be used to construct Q as for the x-y plane, the structure of the shift matrix for a rectangular region is simple enough to warrant writing the elements of P and S explicitly. Consider a rectangular region in the r-z plane bounded on one side by the z-axis, as shown in Figure A2.1. The mesh size is M+1 radial by N+2 axial nodes and the contours S1 and S2 are indicated by

o's and x's respectively. Let the points on S1 and S2 be numbered counterclockwise, starting from the top left corner. Then, referring to the three sides of the region separately, the S and P matrices may be partitioned as

$$S = \begin{bmatrix} S^{(1)} & S^{(2)} & S^{(3)} \\ S^{(4)} & S^{(5)} & S^{(6)} \\ S^{(7)} & S^{(8)} & S^{(9)} \end{bmatrix} \qquad P = \begin{bmatrix} P^{(1)} & P^{(2)} & P^{(3)} \\ P^{(4)} & P^{(5)} & P^{(6)} \\ P^{(7)} & P^{(8)} & P^{(9)} \end{bmatrix}$$

If i,j are the indices of the submatrices, there results, for S,

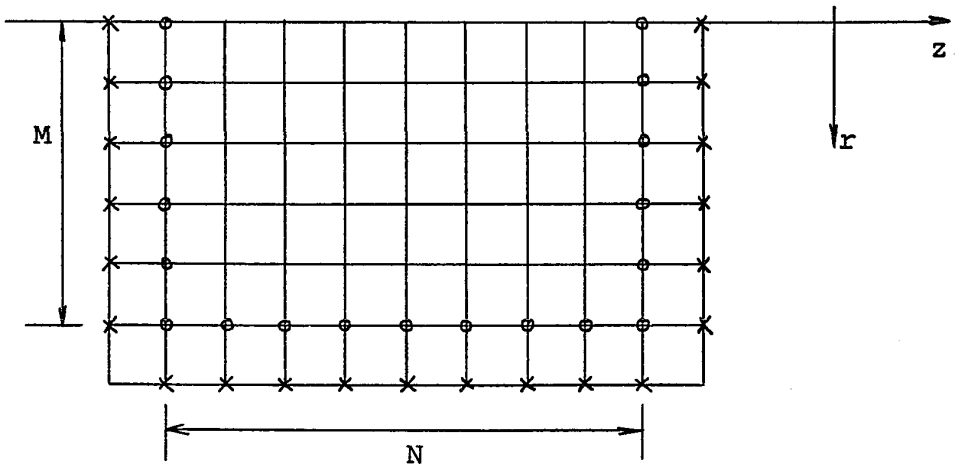

FIGURE A2.1: RECTANGULAR REGION OF INTEREST IN R-Z PLANE

NOTE: $\psi \equiv \psi(z,\tau;\tau_0,0)$

$$S_{ij}^{(1)} = \psi(0,i-1;j-1,0), \qquad 1 \le i \le M,\ 1 \le j \le M$$

$$S_{ij}^{(2)} = \psi(j,i-1;M-1,0), \qquad 1 \le i \le M,\ 1 \le j \le N-2$$

$$S_{ij}^{(3)} = \psi(N-1,i-1;M-j,0), \qquad 1 \le i \le M,\ 1 \le j \le M$$

$$S_{ij}^{(4)} = \psi(i,M-1;j-1,0), \qquad 1 \le i \le N-2,\ 1 \le j \le M$$

$$S_{ij}^{(5)} = \psi(j-i,M-1;M-1,0) \qquad 1 \le i \le N-2,\ 1 \le j \le N-2 \qquad \text{(A2.11)}$$

$$S_{ij}^{(6)} = \psi(N-1-i,M-1;M-j,0) \qquad 1 \le i \le N-2,\ 1 \le j \le M$$

$$S_{ij}^{(7)} = \psi(N-1,M-i;j-1,0) \qquad 1 \le i \le M,\ 1 \le j \le M$$

$$S_{ij}^{(8)} = \psi(N-1-j,M-i;M-1,0) \qquad 1 \le i \le M,\ 1 \le j \le N-2$$

$$S_{ij}^{(9)} = \psi(0,M-i;M-j,0) \qquad 1 \le i \le M,\ 1 \le j \le M$$

and for P,

$$P_{ij}^{(1)} = \psi(1,i-1;j-1,0) \qquad 1 \le i \le M,\ 1 \le j \le M$$

$$P_{ij}^{(2)} = \psi(j+1,i-1;M-1,0) \qquad 1 \le i \le M,\ 1 \le j \le N-2$$

$$P_{ij}^{(3)} = \psi(N,i-1;M-j,0) \qquad 1 \le i \le M,\ 1 \le j \le M$$

$$P_{ij}^{(4)} = \psi(i-1,M;j-1,0) \qquad 1 \le i \le N,\ 1 \le j \le M$$

$$P_{ij}^{(5)} = \psi(i-j-1,M;M-1,0) \qquad 1 \le i \le N,\ 1 \le j \le N-2$$

$$P_{ij}^{(6)} = \psi(N-i,M;M-j,0) \qquad 1 \le i \le N,\ 1 \le j \le M$$

$$P_{ij}^{(7)} = \psi(N,M-i;j-1,0) \qquad 1 \le i \le M,\ 1 \le j \le M \qquad \text{(A2.12)}$$

$$P_{ij}^{(8)} = \psi(N-j,M-i;M-1,0) \qquad 1 \le i \le M,\ 1 \le j \le N-2$$

$$P_{ij}^{(9)} \quad \psi(1,M-i;M-j,0) \qquad 1 \le i \le M,\ 1 \le j \le M$$

The matrices S and P as well as the resulting Q matrix possess a "reverse" symmetry, in that

$$Q_{2M+N+1-i,2M+N-1-j} = Q_{i,j} \qquad \text{(A2.13)}$$

so that, for even N, the matrix Q may be written in the partitioned form

$$Q = \begin{pmatrix} Q_1 \\ Q_1^r \end{pmatrix}$$

Hence only one half of Q need be stored.

A2.3 FORTRAN Program Listings

This section lists the various programs necessary for implementation of the above. As before, the programs are in FORTRAN IV Language, Level G. The matrix inversion routine 'INVERT' has been described in Appendix 1.

```
C
C     SHIFT MATRIX PROGRAMME FOR THE R-Z PLANE.  THE SIZE OF THE REGION
C     IS M2 BY N2 (TOTAL) AND (2*M2&N2-4) SHOULD BE LESS THAN OR EQUAL
C     TO 100. REQUIRES SUBPROGRAMMES 'RING','ELINK' AND 'ARAD'.
C
      DIMENSION S(100,100),P( 51,100),WK(100)
      DIMENSION RAD(40)
      COMMON RAD
      READ(5,100) M2,N2
      M=M2-1
      N=N2-2
      NN=N-2
      NO=N/2
      IF(NO*2.NE.N) NO=NO+1
      KK=M+NO
      LL=2*M+NN
      CALL ARAD(M)
      DO 1 I=1,M
      DO 1 J=1,M
      CALL RING(0,I-1,J-1,X)
      S(I,J)=X
      J3=M+NN+J
      CALL RING(N-1,I-1,M-J,X)
      S(I,J3)=X
       I7=M+NN+I
      CALL RING(N-1,M-I,J-1,X)
      S(I7,J)=X
      CALL RING(0,M-I,M-J,X)
      S(I7,J3)=X
      CALL RING(1,I-1,J-1,X)
      P(I,J)=X
      CALL RING(N,I-1,M-J,X)
    1 P(I,J3)=X
C
      DO 2 I=1,M
      DO 2 J=1,NN
      J2=M+J
      CALL RING(J,I-1,M-1,X)
      S(I,J2)=X
      CALL RING(J+1,I-1,M-1,X)
      P(I,J2)=X
      I8=M+NN+I
      CALL RING(N-1-J,M-I,M-1,X)
    2 S(I8,J2)=X
C
      DO 3 I=1,NN
      DO 3 J=1,M
      I4=M+I
      J6=M+NN+J
      CALL RING(I,M-1,J-1,X)
      S(I4,J)=X
      CALL RING(N-1-I,M-1,M-J,X)
    3 S(I4,J6)=X
C
```

```
      DO 4 I=1,NO
      DO 4 J=1,M
      I4=M+I
      J6=M+NN+J
      CALL RING(I-1,M,J-1,X)
      P(I4,J)=X
      CALL RING(N-I,M,M-J,X)
    4 P(I4,J6)=X
C
      DO 5 I=1,NN
      DO 5 J=1,NN
      I5=M+I
      J5=M+J
      CALL RING(-I+J,M-1,M-1,X)
    5 S(I5,J5)=X
      DO 6 I=1,NO
      DO 6 J=1,NN
      I5=M+I
      J5=M+J
      CALL RING(-I+J+1,M,M-1,X)
    6 P(I5,J5)=X
C
      CALL INVERT(S,100,100,LL,LL,DELTA,EPS)
C
      DO 7 I=1,KK
      DO 8 II=1,LL
    8 WK(II)=0.
      DO 9 J=1,LL
      DO 9 K=1,LL
    9 WK(J)=WK(J)+P(I,K)*S(K,J)
      DO 10 J=1,LL
   10 P(I,J)=WK(J)
    7 CONTINUE
C
      CALL OUTPUT(P,KK,LL)
      WRITE(6,103) DELTA,EPS
      STOP
  100 FORMAT(2I2)
  103 FORMAT(1HO,10X,6HDELTA=,E12.3,6H  EPS=,E12.3)
      END
```

RING

```
      SUBROUTINE RING(M1,N1,NR1,VALU)
      DIMENSION RAD(40)
      COMMON RAD
      M=IABS(M1)
      N=IABS(N1)
      NR=IABS(NR1)
      IF(N.NE.NR) GO TO 1
      IF(M.NE.0) GO TO 1
      VALU=1.
      RETURN
    1 IF(N.NE.0) GO TO 3
      IF(NR.EQ.0) GO TO 3
      VALU=.5*FLOAT(NR)*RAD(NR)/SQRT(FLOAT(M**2+NR**2))
      RETURN
    3 IF(NR.EQ.0) GO TO 4
      AK=2.*SQRT(FLOAT(NR*N))/SQRT(FLOAT(M**2+(N+NR)**2))
      VALU=0.15915492*AK*ELINK(AK)*RAD(NR)*SQRT(FLOAT(NR)/FLOAT(N))
      RETURN
    4 RADSQ=FLOAT(N**2+N**2)
      VALU=1./(3.0943933*SQRT(RADSQ))
      RETURN
      END
```

ARAD

```
      SUBROUTINE ARAD(N)
      DIMENSION RAD(40)
      COMMON RAD
      FACTOR=0.5/3.14159
      DO 1 I=1,N
      IF(I.NE.1) GO TO 2
      VI=0.5
      GO TO 3
    2 AKI=2.*SQRT(FLOAT(I*(I-1)))/SQRT(FLOAT((I+I-1)**2))
      VI=FACTOR*SQRT(FLOAT(I)/FLOAT(I-1))*AKI*ELINK(AKI)
    3 AKE=2.*SQRT(FLOAT(I*(I+1)))/SQRT(FLOAT(I+I+1)**2)
      VE=FACTOR*SQRT(FLOAT(I)/FLOAT(I+1))*AKE*ELINK(AKE)
      AKN=2.*FLOAT(I)/SQRT(1.+FLOAT((I+I)**2))
      VN=FACTOR*AKN*ELINK(AKN)
      RH=1./FLOAT(2*I)
      VO=.25*(VI*(1.-RH)+VE*(1.+RH)+2.*VN+1.)
      RAD(I)=1./VO
    1 CONTINUE
      RETURN
      END
```

ELINK

```
      FUNCTION ELINK(Z)
      P=1.-Z*Z
      IF(P) 1,1,2
    2 ELINK=1.38629436+P*(0.096663443+P*(0.035900924+P*(0.037425637+
     1 0.014511962*P)))-ALOG(P)*(0.5+P*(0.12498594+P*(0.068802486+P*
     2 (0.033283553+0.0044178701*P))))
      RETURN
    1 ELINK=EXP(88.)
      RETURN
      END
```

OUTPUT

```
      SUBROUTINE OUTPUT(P,KK,LL)
      DIMENSION P(51,100),CARD(9)
      WRITE(6,104)
      LP=(LL-1)/9+1
      IND=0
      DO 11 I=1,KK
      DO 12 II=1,LP
      IND=IND+1
      JJ=9*(II-1)
      DO 13 J=1,9
   13 CARD(J)=0.
      DO 14 J=1,9
      JP=J+JJ
      IF(JP.GT.LL) GO TO 15
   14 CARD(J)=P(I,JP)
   15 CONTINUE
      WRITE(6,101)(CARD(J),J=1,9),IND
      WRITE(7,102)(CARD(J),J=1,9),IND
   12 CONTINUE
      WRITE(6,105)
   11 CONTINUE
      RETURN
  105 FORMAT(1H )
  101 FORMAT(1H ,1P9E13.5,I8)
  102 FORMAT(9Z8,I8)
  104 FORMAT(1H1)
      END
```

APPENDIX 3

SHIFT MATRICES FOR COAXIAL LINES AND STRIPS

A3.1 EXISTENCE OF THE CONTINUOUS GREEN'S FUNCTION

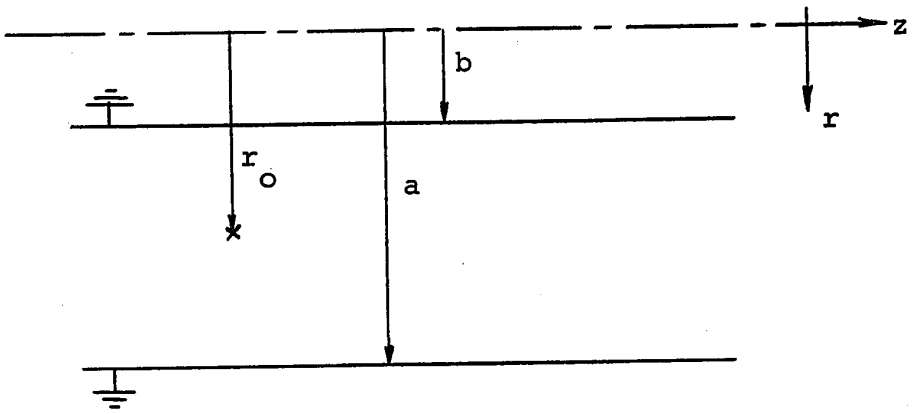

FIGURE A3.1

Consider the uniform infinite coaxial line shown in Figure A3.1. Assuming axial symmetry, i.e., $\frac{\partial \psi}{\partial \theta} = 0$, the Green's function ψ is found by solving

$$\frac{\partial^2 \psi}{\partial r^2} + \frac{1}{r}\frac{\partial \psi}{\partial r} + \frac{\partial^2 \psi}{\partial z^2} = \frac{\delta(r-r_o)}{r}\ \delta(z-z_o) \qquad \text{(A3.1)}$$

where (r_o, z_o) are the coordinates of the singularity. Take a finite Hankel transform [57, p.85] of equation (A3.1),

resulting in

$$-\xi_i^2 \hat{\psi}_H + \frac{\partial^2 \hat{\psi}_H}{\partial z^2} = \int_b^a \frac{r\delta(r-r_o)}{r} \delta(z-z_o)[J_o(r\xi_i)G_o(a\xi_i) - J_o(a\xi_i)G_o(r\xi_i)]\, dr$$

or

$$\frac{\partial^2 \hat{\psi}_H}{\partial z^2} - \xi_i^2 \hat{\psi}_H = W\delta(z-z_o) \tag{A3.2}$$

where

$$W = J_o(r_o\xi_i)G_o(a\xi_i) - J_o(a\xi_i)G_o(r_o\xi_i) \tag{A3.3}$$

and ξ_i are all the positive roots of

$$J_o(\xi_i b)G_o(\xi_i a) - J_o(\xi_i a)G_o(\xi_i b) = 0 \tag{A3.4}$$

J_o is the Bessel function at the first kind, order zero, and G_o is defined in terms of the familiar Hankel function* as

$$G_n(x) = \tfrac{1}{2}\pi i \; H_n^{(1)}(x)$$

Taking a Fourier transform as

$$F(\alpha) = \frac{1}{\sqrt{2\pi}} \int_{-\infty}^{\infty} f(x)^{i\alpha x}\, dx$$

---

* See, for example, M. Abramowitz and I. Stegun, Handbook of Mathematical Functions, New York: Dover, p. 358.

there results

$$-\alpha^2 F - \xi_i^2 F = \frac{W}{\sqrt{2\pi}} \int_{-\infty}^{\infty} \delta(z-z_o)\, e^{i\alpha z}\, dz$$

$$= \frac{W}{\sqrt{2\pi}}\, e^{i\alpha z_o}$$

from which,

$$F = \frac{-W\, e^{i\alpha z_o}}{\sqrt{2\pi}\ (\alpha^2+\xi_i^2)}$$

Take the inverse transform of F as

$$\hat{\psi}_H = \frac{1}{\sqrt{2\pi}} \int_{-\infty}^{\infty} F\ e^{-i\alpha z}\, d\alpha$$

$$\hat{\psi}_H = -\frac{W}{2\pi} \int_{-\infty}^{\infty} \frac{e^{-i\alpha(z-z_o)}}{\alpha^2+\xi_i^2}\, d\alpha$$

$$= -\frac{W}{2\pi} \int_{-\infty}^{\infty} \frac{\cos[\alpha(z-z_o)] - i\, \sin[\alpha(z-z_o)]}{\alpha^2+\xi_i^2}\, d\alpha$$

In the last integral, $\sin[\alpha(z-z_o)]$ is an odd function about z_o, so for a finite value of z_o the contribution due to the sine term vanishes. Hence,

$$\hat{\psi}_H = -\frac{W}{2\pi} \int_{-\infty}^{\infty} \frac{\cos[\alpha(z-z_o)]}{\alpha^2+\xi_i^2}\, d\alpha$$

The last integral may be put in a standard form as

$$\hat{\psi}_H = -\frac{W}{\xi_i \pi} \int_0^\infty \frac{\cos[\xi_i(z-z_o)\cdot \alpha/\xi_i]}{\alpha^2/\xi_i^2 + 1} \, d\alpha/\xi_i$$

which is evaluated from tables* as

$$\hat{\psi}_H = -\frac{W}{2\xi_i} e^{-\xi_i(z-z_o)} \quad , \; z>z_o$$

$$= -\frac{W}{2\xi_i} e^{-\xi_i(z_o-z)} \quad , \; z<z_o$$

Taking the inverse Hankel transform there results

$$\psi = \sum_i \frac{2\xi_i^2 \, J_o^2(\xi_i b)\hat{\psi}_H}{J_o^2(\xi_i a) - J_o^2(\xi_i b)} [J_o(\xi_i r) G_o(\xi_i a) - J_o(\xi_i a) G_o(\xi_i r)]$$

$$= -\sum_i \frac{\xi_i J_o^2(\xi_i b)[J_o(\xi_i r_o) G_o(\xi_i a) - J_o(\xi_i a) G_o(\xi_i r_o)]}{J_o^2(\xi_i a) - J_o^2(\xi_i b)} \cdots$$

$$\cdots [J_o(\xi_i r) G_o(\xi_i a) - J_o(\xi_i a) G_o(\xi_i r)] \exp(-\xi_i |z-z_o|)$$

Convergence of the above series is very poor for the case z=0. Hence, the above development is useful only since it proves

---

* H.B. Dwight, Tables of Integrals and Other Mathematical Data, New York: Macmillan, (#859.3).

uniqueness and existence of the Green's function as $h \to 0$.

A3.2 Iterative Construction of the Shift Matrix

An iterative scheme for calculation of the shift matrix Q has been developed in Chapter 6, § 6.3 as

$$Q^{(k+1)} = [C - Q^{(k)}]^{-1} \tag{6.4}$$

The structure of the matrix C will now be examined. Each row of C represents the negative of the self and radial coefficients of the finite difference formula for the r-z plane. Hence, the diagonal elements of C are equal to 4. If the potentials on the radial planes defined in Figure 6.11 are numbered sequentially outward from the z-axis, the matrix C is tri-diagonal. The upper off-diagonal elements are set to $-(1+\frac{h}{2r})$ while the lower off-diagonal elements are set to $-(1-\frac{h}{2r})$, where r is the radius of the point corresponding to the coefficient in the diagonal. For example, if the radius of the first node on each plane in Figure 6.11 is r_1, that of the second is r_2 and so on, since the inner and outer conductors have been assumed at zero potential, the matrix C is structured as

$$C = \begin{pmatrix} 4, & -(1+\frac{h}{2r_1}), & 0, & 0, & \cdots \\ -(1-\frac{h}{2r_2}), & 4, & -(1+\frac{h}{2r_2}), & 0, & \cdots \\ \vdots & & & & \end{pmatrix}$$

In the case of strips, the off-diagonal coefficients are unity, so that the matrix C is structured as

$$C = \begin{pmatrix} 4 & -1 & 0 & 0 & 0 & \cdots \\ -1 & 4 & -1 & 0 & 0 & \cdots \\ 0 & -1 & 4 & -1 & 0 & \cdots \\ \text{etc.} & & & & & \\ \vdots & & & & & \end{pmatrix}$$

The initial iterate of Q is usually taken as zero or as the identity matrix. The iterations are continued until the difference between two successive iterates of Q is floating point zero or some other small preassigned number. In the case of strips, the Q matrix is symmetric.

A3.3 Verification of Q for Strips

If each mesh line is replaced by a unit resistance, the semi-infinite conducting strip may be considered as a semi-infinite square resistance mesh, bounded by two parallel conducting bars, as shown in Figure A3.2. Let the nodes in the mesh be numbered as shown in the figure. At the nodes or "terminals" along the line n=0, the currents into the mesh may be related to the potentials at the terminals by an admittance matrix as

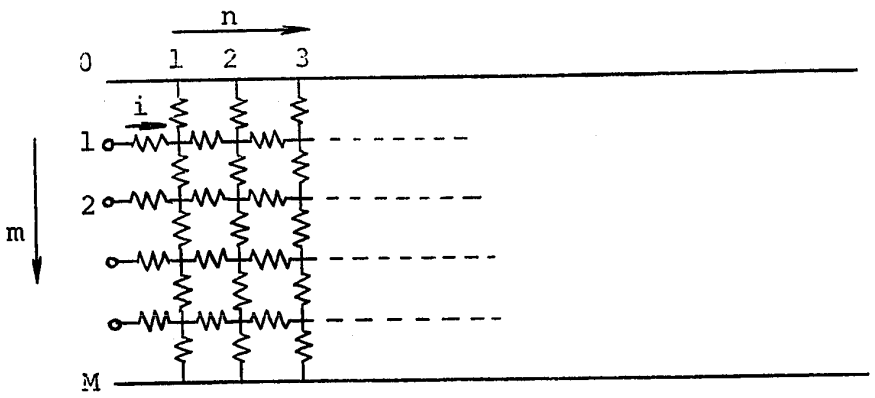

FIGURE A3.2: SEMI-INFINITE STRIP

$$i = GV_1$$

However, the potentials along n=0 and n=1 are related by the shift matrix

$$V_2 = QV_1$$

For unit resistances in the mesh, the current vector i is given by

$$i = V_1 - V_2$$

so that the relationship between G and Q is

$$G = I - Q$$

where I is the identity matrix.

The admittance matrix G for the strip may be found analytically and has been calculated by Sander [58]. Sander's solution is presented briefly below.

The equation relating the potential differences between adjacent nodes is

$$V(m+1,n) + V(m-1,n) + V(m,n+1) + V(m,n-1) = 4V(m,n)$$

This is satisfied by functions of the form $\exp(jm\mu + n\lambda)$ provided that

$$\sinh \lambda/2 = \pm \sin \mu/2$$

The boundary conditions are V=0 at m=0 and m=M. A trial general solution may therefore be constructed, of the form

$$V(m,n) = \sum_{p=1}^{M-1} A_p \exp(-n\lambda_p) \sin m\frac{p\pi}{M}$$

where λ_p is given by

$$\sinh \tfrac{1}{2} \lambda_p = \sin \frac{p\pi}{2M}$$

and p is an integer. The coefficients A_p may be found explicitly from

$$\sum_{m=1}^{M-1} \sin \frac{pm\pi}{M} \sin \frac{qm\pi}{M} = 0, \quad p \neq q$$
$$= \tfrac{1}{2}M, \quad p=q \leq M-1$$

Now since

$$V(m,0) = \sum_{p=1}^{M-1} A_p \sin \frac{mp\pi}{M}$$

then

$$A_q = \frac{2}{M} \sum_{m=1}^{M-1} V(m,0) \sin \frac{qm\pi}{M}$$

To construct the G matrix, V(m,0) is set to unity for m=k and to zero for m≠k. Then,

$$A_q = \frac{2}{M} \sin \frac{qk\pi}{M}$$

and

$$V(m,n) = \frac{2}{M} \sum_{p=1}^{M-1} \exp(-n\lambda_p) \sin \frac{pk\pi}{M} \sin \frac{pm\pi}{M}$$

The G matrix may thus be constructed as

$$G_{jk} = -\frac{2}{M} \sum_{p=1}^{M-1} \exp(-\lambda_p) \sin \frac{pk\pi}{M} \sin \frac{pj\pi}{M}, \quad j \neq k$$

$$G_{kk} = 1 - \frac{2}{M} \sum_{p=1}^{M-1} \exp(-\lambda_p) \sin^2 \frac{pk\pi}{M}, \quad j=k$$

Note that $Q_{jk} = -G_{jk}$, $k \neq j$, and $Q_{kk} = 1-G_{kk}$. The shift matrix for strips as obtained by iteration has been verified with Sander's results and exact agreement has been obtained.

A3.4 FORTRAN Program Listings

The necessary programs for generation of Q matrices for coaxial lines are presented below. As before, the comments in the programs are self-explanatory.

MAIN

```
C     Q MATRIX GENERATION PROGRAMME FOR COAXIAL CABLE PROBLEMS.
C     Q IS FOUND BY ITERATION.  REQUIRES SUBROUTINES 'CMATRX'
C     'ITER' AND 'OUTPUT' AND THE FOLLOWING DATA--
C       A--OUTER RADIUS OF CABLE, ARBITRARY UNITS
C       B--INNER RADIUS OF CABLE, SAME UNITS
C       N--NO. OF RADIAL NODES INSIDE CABLE
C       ERR--REQUIRED ABSOLUTE ACCURACY OF EACH ELEMENT OF Q.
C            MAY BE SPECIFIED AS FLOATING POINT ZERO
C       NITER--MAXIMUM NO. OF ITERATIONS ALLOWED
C
      DIMENSION C(50,50),Q(50,50)
C
C     READ DATA
C
  100 FORMAT(2I5,3F10.0)
   50 READ(5,100) N,NITER,A,B,ERR
      IF(N.EQ.0) STOP
C
C     GENERATE C MATRIX
C
      CALL CMATRX(C,A,B,N)
C
C     GENERATE INITIAL GUESS OF Q
C
      DO 2 I=1,N
      DO 1 J=1,N
    1 Q(I,J)=0.
    2 Q(I,I)=1.
C
C     ITERATION LOOP
C
      DO 3 I=1,NITER
      CALL ITER(C,Q,N,BIGEST,DELTA,EPS)
      IF(BIGEST.LE.ERR) GO TO 4
    3 CONTINUE
C
C     OUTPUT ROUTINE
C
    4 CALL OUTPUT(Q,N,N)
      WRITE(6,101) BIGEST,I,DELTA,EPS
  101 FORMAT(1HO,'BIGEST=',1PE9.2,' KOUNT=',I3,' DELTA=',E9.2,' EPS='
     1E9.2)
      GO TO 50
      END
```

CMATRX

```
      SUBROUTINE CMATRX(C,A,B,N)
C     FINDS RADIAL COEFFICIENT MATRIX C FOR COAXIAL CABLE PROBLEM
C     USING FIVE-POINT FINITE DIFFERENCE OPERATOR.
C       A--OUTER RADIUS OF CABLE
C       B--INNER RADIUS OF CABLE
C       N--NO. OF RADIAL NODES INSIDE CABLE
C     DIAGONAL ELEMENTS OF C ARE SET TO 4.  SUPRA-DIAGONAL
C     ELEMENTS ARE SET TO  -(1+H/2R) AND LOWER DIAGONAL TO
C     -(1-H/2R).  ALL OTHER ELEMENTS ARE ZERO
C
      DIMENSION C(50,50)
      W=A-B
      Z=B*FLOAT(N+1)*2.
      TW=2.*W
      DO 1 I=1,N
      DO 1 J=1,N
    1 C(I,J)=0.
      DO 2 I=1,N
      FACT=W/(FLOAT(I)*TW+Z)
      C(I,I)=4.
      IF(I.EQ.1) GO TO 3
      C(I,I-1)=FACT-1.
    3 IF(I.EQ.N) GO TO 2
      C(I,I+1)=-FACT-1.
    2 CONTINUE
      RETURN
      END
```

ITER

```
      SUBROUTINE ITER(C,Q,N,BIGEST,DELTA,EPS)
C     SUBROUTINE INPUTS MATRICES C AND Q AND RETURNS INVERSE
C     OF  (C-Q) UNDER Q.  'BIGEST' IS THE MAXIMUM ABSOLUTE DIFFERENCE
C     BETWEEN CORRESPONDING ELEMENTS IN INPUT Q AND OUTPUT Q MATRICES.
C     DELTA IS DETERMINANT VALUE AND EPS IS SMALLEST PIVOT OF
C     INVERSION.  REQUIRES MATRIX INVERSION ROUTINE 'INVERT'.
      DIMENSION C(50,50),Q(50,50),S(50,50)
C
C     STORE OLD Q IN S
C
      DO 1 I=1,N
      DO 1 J=1,N
    1 S(I,J)=Q(I,J)
C
C     FORM (C-Q) AND STORE IN Q
C
      DO 2 I=1,N
      DO 2 J=1,N
    2 Q(I,J)=C(I,J)-Q(I,J)
C
C     INVERT (C-Q) AND STORE IN Q
C
      CALL INVERT(Q,50,50,N,N,DELTA,EPS)
C
C     FIND BIGGEST DIFFERENCE
C
      BIGEST=0.
      DO 3 I=1,N
      DO 3 J=1,N
      DIF=ABS(Q(I,J)-S(I,J))
      IF(DIF.GT.BIGEST) BIGEST=DIF
    3 CONTINUE
      RETURN
      END
```

OUTPUT

```
      SUBROUTINE OUTPUT(P,KK,LL)
      DIMENSION P(50,50),CARD(9)
      WRITE(6,104)
      LP=(LL-1)/9+1
      IND=0
      DO 11 I=1,KK
      DO 12 II=1,LP
      IND=IND+1
      JJ=9*(II-1)
      DO 13 J=1,9
   13 CARD(J)=0.
      DO 14 J=1,9
      JP=J+JJ
      IF(JP.GT.LL) GO TO 15
   14 CARD(J)=P(I,JP)
   15 CONTINUE
      WRITE(6,101)(CARD(J),J=1,9),IND
      WRITE(7,102)(CARD(J),J=1,9),IND
   12 CONTINUE
      WRITE(6,105)
   11 CONTINUE
      RETURN
  105 FORMAT(1H )
  101 FORMAT(1H ,1P9E13.5,I8)
  102 FORMAT(9Z8,I8)
  104 FORMAT(1H1)
      END
```

APPENDIX 4

INTERIOR POINT S.O.R. PROGRAMS

A4.1 TWO-DIMENSIONAL (X-Y PLANE) PROGRAMS

The interior routines used in this research for problems in the x-y plane are essentially the same as those used in the previous experimental work in boundary relaxation by using gradients [41]. The necessary housekeeping routines are described in the above reference to facilitate solution of problems with as many as four different media in the interior region of interest. The reader is referred to the above for further details of these interior routines.

A4.2 AXIALLY SYMMETRIC INTERIOR PROGRAMS

As for the problems in the x-y plane, the routines for point S.O.R. solution of the interior region in the r-z plane make use of a field description array to define the appropriate formula to be used at each point of the mesh. The problem geometry is read in from a quasi-graphical data deck in which punches indicate the presence or absence of conductors and/or dielectrics at each node in the mesh. The

problem geometry is encoded as follows:

CODE	MEANING
0	Dielectric interface
1	Region R1 with dielectric constant ε_1 (normally = 1)
2	Region R2 with dielectric constant ε_2
3	Constant potential V1, adjacent to R1 region
4	Constant potential V2, adjacent to R1 region
5	Constant potential V3, adjacent to R1 region
6	Constant potential V1, adjacent to R2 region
7	Constant potential V2, adjacent to R2 region
8	Constant potential V3, adjacent to R2 region

To illustrate how the problem geometry is encoded, consider the problem in Figure A4.1. The figure shows a hollow rectangular conductor with a dielectric rod in the interior. The four sides are held at different fixed potentials as shown. The problem is shown modelled in a mesh of 7 x 8 nodes. Seven data cards are required to describe the problem, one for each horizontal row of nodes:

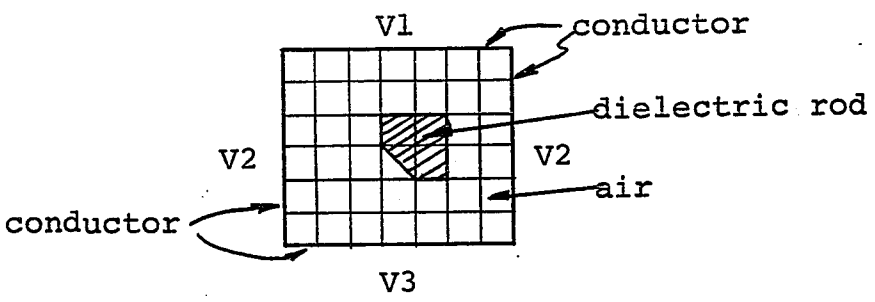

FIGURE A4.1: HYPOTHETICAL PROBLEM

```
Card # 1      3 3 3 3 3 3 3 3
Card # 2      4 1 1 1 1 1 1 4
Card # 3      4 1 1 0 0 0 1 4
Card # 4      4 1 1 0 2 0 1 4
Card # 5      4 1 1 1 0 0 1 4
Card # 6      4 1 1 1 1 1 1 4
Card # 7      5 5 5 5 5 5 5 5
```

The above "field geometry array" is then converted to a field description array by the subroutine FIELD2, one code number for each node in the field. This code number is then used to determine the appropriate formula at each point in the interior S.O.R. cycle. In order to minimize the number of operations, all radial multipliers (or coefficients) are calculated beforehand by subroutine ARAD and stored for subsequent use.

All subroutines are heavily commented, to the point where they are self-descriptive.

A4.3 Boundary Relaxation R-Z Plane Programs

This section gives the FORTRAN program listings of the necessary routines for boundary relaxation in the r-z plane, using the interior routines described in the preceding section. The only listing not heavily commented is that of the main calling program, as this is the one part of the overall program that undergoes most change. The programs, as listed

here, will work without modification on IBM series 360 computers with at least 110 Kbytes of available core.

In addition to the routines, a data deck describing problem parameters is required. The data deck is assembled as follows:

	No. of Cards	Name(s)	Format
1)	1	M1,M2,N1,N2	4I5
2)	deck	P(I,J)	9Z8
3)*	1	NPROB	I5
4)	1	V1,V2,V3,V4,R1,R2, ALPHA,UDIF	8F10.0
5)	deck	field coding (as above)	nI1
6)	1	NCOR,IFORM,IWIDTH, NCONTR,NEXTRA,NPASS	6I5
7)*	1	BETA,BDIF	2F10.0

where the variable names are,

M1,M2 -- Start and end of field in radial direction; M1 is the Z-axis and is specified as 1;

N1,N2 -- start and end of field in axial direction;

P(I,J) -- is the shift matrix (top half) as produced by the programs described in Appendix 2;

NPROB -- is the number of the problem. The execution is terminated when NPROB=0. Sections 3) to 7) in the data deck may be repeated as often as desired and terminated with an NPROB=0 card;

V1,V2,V3 -- are the fixed potentials corresponding to the field codings of 3,4 or 5 respectively;

V4 -- all nodes in the mesh whose potentials are not fixed are initially set equal to V4;

R1,R2 -- dielectric constants of regions R1 and R2. R1 is normally specified as 1.0;

ALPHA -- interior overrelaxation factor;

UDIF -- maximum allowable interior residual;

NCOR -- maximum allowed boundary corrections;

IFORM -- determines the format of printed potential values - see comments in subroutine VALUES;

IWIDTH -- width of equipotential plot in printer spaces;

NCONTR -- no. of potential contours desired;

NEXTRA -- boundary correction number when extrapolation is desired. Extrapolation is performed at each integer multiple of NEXTRA;

NPASS -- maximum allowed <u>interior</u> S.O.R. passes for each boundary correction;

BETA -- boundary correction factor (normally = 1.5);

BDIF -- maximum permissible boundary correction for convergence.

Preceding the program listing is a sample output printout for the conducting sphere problem of Chapter 6, Figure 6.1. In this example, NEXTRA was specified as 6.

PROBLEM NO. 1

BOUNDARY CORRECTION NUMBER	INTERIOR RELAXATION FACTOR	NO. OF INT. RELAXATION PASSES	BOUNDARY CORRECTION FACTOR	LARGEST BOUNDARY DIFFERENCE	BOUNDARY ERROR NORM	TOTAL ERROR NORMSQ
KBAR	ALPHA	ITER-1	BETA	BIGEST	ENORM	ESQ
1	1.3500	25	1.4000	0.349E 00	0.526E 01	0.130E 01
2	1.3500	25	1.4000	0.195E 00	0.392E 01	0.650E 00
3	1.3500	25	1.4000	0.142E 00	0.318E 01	0.424E 00
4	1.3500	25	1.4000	0.114E 00	0.256E 01	0.273E 00
5	1.3500	25	1.4000	0.904E-01	0.204E 01	0.174E 00
6	1.3500	25	1.4000	0.714E-01	0.163E 01	0.110E 00
7	1.3500	25	1.4000	0.107E-01	0.936E-01	0.620E-03
8	1.3500	18	1.4000	0.444E-02	0.484E-01	0.129E-03
9	1.3500	17	1.4000	0.207E-02	0.267E-01	0.364E-04
10	1.3500	16	1.4000	0.109E-02	0.149E-01	0.112E-04
11	1.3500	14	1.4000	0.591E-03	0.849E-02	0.362E-05
12	1.3500	14	1.4000	0.338E-03	0.481E-02	0.117E-05
13	1.3500	15	1.4000	0.225E-03	0.722E-03	0.678E-07
14	1.3500	4	1.4000	0.629E-04	0.336E-03	0.836E-08

UDIF= 0.1000E-04 BDIF= 0.1000E-03

MAIN

```
      DIMENSION IND(40,80),U(40,80),POT(21),RADOT(40),RADIN(40),AK3(40,3
     1),AK7(40,3),AK1(40,2),AK5(40,2)
      DIMENSION VI(100),VEO(102),VEN(102),P( 51,100),VEOO(102)
      COMMON IND,U,POT,RADOT,RADIN,AK3,AK7,AK1,AK5,VI,VEO,VEN,P,VEOO
      READ(5,100) M1,M2,N1,N2
      N=N2-N1-1
      NO=N/2
      IF(NO*2.NE.N) NO=NO+1
      KK=M2-M1+NO
      LL=M2+M2+N2-N1-5
      DO 1 I=1,KK
      READ(5,105)(P(I,J),J=1,LL)
    1 CONTINUE
      WRITE(6,120)(P(1,J),J=1,LL)
  120 FORMAT(1H ,6E20.7)
    5 READ(5,100) NPROB
      IF(NPROB.EQ.0) STOP
      READ(5,101) V1,V2,V3,V4,R1,R2,ALPHA,UDIF
      CALL FIELD2(M2,N2,1)
      CALL RADX(M2,R1,R2)
      READ(5,100) NCOR,IFORM,IWIDTH,NCONTR,NEXTRA,NPASS
      READ(5,101) BETA,BDIF
      CALL SETUP2(M1,M2,N1,N2,V1,V2,V3,V4)
      WRITE(6,110) NPROB
      KBAR=0
    2 CONTINUE
      CALL RELAX2(M1,M2,N1,N2,ALPHA,UDIF,NPASS,ITER,0)
      K2=LL+2
      DO 7 I=1,K2
    7 VEOO(I)=VEO(I)
      CALL VECTOR(M2,N1,N2,BIGEST,ENORM,ESQ)
      KBAR=KBAR+1
      WRITE(6,107) KBAR,ALPHA,ITER,BETA,BIGEST,ENORM,ESQ
      IF(KBAR.GE.NCOR) GO TO 50
      IF(BIGEST.LE.BDIF) GO TO 50
      CALL CHANGE(M2,N1,N2,BETA)
      IF(KBAR.NE.(KBAR/NEXTRA)*NEXTRA) GO TO 4
      CALL EXTRA(M2,N1,N2)
    4 CONTINUE
      GO TO 2
   50 WRITE(6,104) UDIF,BDIF
      U(M2,1)=U(M2-1,1)+U(M2,2)-.5*(U(M2-2,1)+U(M2,3))
      U(M2,N2)=U(M2,N2-1)+U(M2-1,N2)-.5*(U(M2,N2-2)+U(M2-2,N2))
      CALL VALUES(M1,M2,N1,N2,IFORM,IWIDTH,NCONTR,1)
      GO TO 5
  100 FORMAT(16I5)
  101 FORMAT(8F10.0)
  104 FORMAT(1H0,10X,5HUDIF=,E11.4,5X,5HBDIF=,E11.4)
  105 FORMAT(9Z8)
  107 FORMAT(1H ,4X,I3,10X,F6.4,7X,I3,8X,F8.4,5X,3(E11.3,2X))
  110 FORMAT(1H1/35X,11HPROBLEM NO.,I2                                //5X,8HBOU
     1NDARY,5X,8HINTERIOR,5X,10HNO.OF INT.,3X,8HBOUNDARY,5X,7HLARGEST,
     26X,8HBOUNDARY,5X,8HTOTAL    /5X,10HCORRECTION,3X,10HRELAXATION,3X,
     310HRELAXATION,3X,10HCORRECTION,3X, 8HBOUNDARY,5X,5HERROR,8X,5HERRO
```

MAIN

```
4R/5X,6HNUMBER,7X,6HFACTOR,7X,6HPASSES,7X,6HFACTOR,7X,10HDIFFERENCE
5,3X,4HNORM,9X,6HNORMSQ//5X,4HKBAR,9X,5HALPHA,8X,6HITER-1,7X,4HBETA
6,9X,6HBIGEST,7X,5HENORM,8X,3HESQ/)
 END
```

RADX

```
      SUBROUTINE RADX(M,R1,R2)
C
C   THIS SUBROUTINE COMPUTES RADIAL MULTIPLIERS FOR USE WITH 'RELAX2'
C   ROUTINE AND STORES THEM IN COMMON
C      M--NO OF POINTS IN R-DIRECTION
C      R1--DIELECTRIC CONSTANT NO.1 (NORMALLY =1.)
C      R2--DIELECTRIC CONSTANT NO.2
C
      DIMENSION IND(40,80),U(40,80),POT(21),RADOT(40),RADIN(40),AK3(40,3
     1),AK7(40,3),AK1(40,2),AK5(40,2)
      COMMON IND,U,POT,RADOT,RADIN,AK3,AK7,AK1,AK5
      DO 1 I=2,M
      RM=0.5/FLOAT(I-1)
      RMH=0.25/FLOAT(I-1)
      RADOT(I)=1.+RM
      RADIN(I)=1.-RM
      AK3(I,1)=RADOT(I)*(R1+R1)
      AK3(I,2)=RADOT(I)*(R1+R2)
      AK3(I,3)=RADOT(I)*(R2+R2)
      AK7(I,1)=RADIN(I)*(R1+R1)
      AK7(I,2)=RADIN(I)*(R1+R2)
      AK7(I,3)=RADIN(I)*(R2+R2)
      AK1(I,1)=(1.+RMH)*R1
      AK1(I,2)=(1.+RMH)*R2
      AK5(I,1)=(1.-RMH)*R1
    1 AK5(I,2)=(1.-RMH)*R2
      AK3(1,1)=2.*(R1+R2)
      AK3(1,2)=0.5*(1.+R1)
      AK3(1,3)=0.5*(1.+R2)
      AK7(1,1)=2.5*(R1+R2)+1.
      RETURN
      END
```

FIELD2

```
      SUBROUTINE FIELD2(M1,N1,IREAD)
C  THIS SUBROUTINE GENERATES A  FIELD DESCRIPTION MATRIX IND(I,J) FROM A
C  FIELD CODE MATRIX INDIC(I,J), THE SIZE OF BOTH BEING M1 BY N1.
C     M1--NO OF POINTS IN R-DIRECTION,THE ROW M1=1 BEING THE Z-AXIS
C     N1--NO OF POINTS IN Z-DIRECTION
C  CODE MATRIX 'INDIC' IS SUPPLIED ROWWISE AND MUST BE CODED AS FOLLOWS-
C     0-DIELECTRIC INTERFACE
C     1-DIELECTRIC CONSTANT =R1,(NORMALLY=1.)
C     2-DIELECTRIC CONSTANT =R2
C     3-CONSTANT POTENTIAL V1,ADJACENT TO R1 REGION
C     4-CONSTANT POTENTIAL V2,ADJACENT TO R1 REGION
C     5-CONSTANT POTENTIAL V3,ADJACENT TO R1 REGION
C     6-CONSTANT POTENTIAL V1,ADJACENT TO R2 REGION
C     7-CONSTANT POTENTIAL V2,ADJACENT TO R2 REGION
C     8-CONSTANT POTENTIAL V3,ADJACENT TO R2 REGION
C  IN THE CASE THAT A DIELECTRIC INTRFACE MEETS A CONSTANT POTENTIAL
C  SURFACE, THE CODE AT THAT POINT SHOULD BE THE ONE FOR DIELECTRIC R2,
C  I.E. CODE  6,7 OR 8.
C      NO ACUTE ANGLES OF DIELECTRIC SURFACE ARE PERMITTED, CONCAVE OR
C  CONVEX. THE SHARPEST ANGLE PERMITTED IS A RIGHT ANGLE. THE ONLY DIE-
C  LECTRIC INTERFACE ALLOWED ON THE Z-AXIS IS AT RIGHT ANGLES TO THE
C  Z-AXIS.
C     THE CODES 6,7 AND 8 ARE REALLY ONLY NECESSARY WHERE THERE MIGHT BE
C  CONFUSION SUCH AS AROUND AIR-DIELECTRIC-CONSTANT POTENTIAL INTERFACES
C
      DIMENSION IND(40,80),INDIC(40,80),ICODE(9),IER(8)
      COMMON IND,INDIC
      IF(IREAD.EQ.0) GO TO 2
      DO 1 I=1,M1
      READ(5,100)(INDIC(I,J),J=1,N1)
    1 CONTINUE
    2 DO 3 N=1,N1
      IND(1,N)=5
      IF(INDIC(1,N).GE.3) GO TO 200
      IF(INDIC(1,N).NE.0) GO TO 3
      IND(1,N)=6
      IF(INDIC(1,N+1).EQ.2) IND(1,N)=7
      IF(INDIC(1,N+1).GE.6) IND(1,N)=7
      GO TO 3
  200 IND(1,N)=INDIC(1,N)-2
      IF(IND(1,N).GE.4) IND(1,N)=IND(1,N)-3
    3 CONTINUE
      DO 11 M=2,M1
      DO 11 N=1,N1
      IF(INDIC(M,N).NE.0) GO TO 10
      ICODE(1)=INDIC(M,N+1)
      ICODE(2)=INDIC(M+1,N+1)
      ICODE(3)=INDIC(M+1,N)
      ICODE(4)=INDIC(M+1,N-1)
      ICODE(5)=INDIC(M,N-1)
      ICODE(6)=INDIC(M-1,N-1)
      ICODE(7)=INDIC(M-1,N)
      ICODE(8)=INDIC(M-1,N+1)
      ICODE(9)=ICODE(1)
```

FIELD2

```
      DO 4 I=1,9
      IF(ICODE(I).GT.5) ICODE(I)=2
      IF(ICODE(I).GT.2) ICODE(I)=1
    4 CONTINUE
      IND(M,N)=0
      DO 9 I=1,8
      IF(ICODE(I).EQ.1.OR.ICODE(I+1).EQ.1) GO TO 7
      IF(ICODE(I).EQ.2.OR.ICODE(I+1).EQ.2) GO TO 6
      IF((I/2)*2.EQ.I) GO TO 5
      IER(I)=ICODE(I+2)-1
      GO TO 8
    5 IER(I)=ICODE(I-1)-1
      GO TO 8
    6 IER(I)=1
      GO TO 8
    7 IER(I)=0
    8 CONTINUE
      IFACT=2**(I-1)
    9 IND(M,N)=IND(M,N)+IER(I)*IFACT
      IND(M,N)=IND(M,N)+10
      GO TO 11
   10 IND(M,N)=4
      IF(INDIC(M,N).GE.3) IND(M,N)=INDIC(M,N)-2
      IF(INDIC(M,N).GE.6) IND(M,N)=INDIC(M,N)-5
   11 CONTINUE
      RETURN
  100 FORMAT(80I1)
      END
```

RELAX2

```
      SUBROUTINE RELAX2(M1,M2,N1,N2,ALPHA,UDIF,NPASS,ITER,NEU)
C  RELAXATION ROUTINE FOR AXIALLY SYMMETRIC FIELDS. REQUIRES FIELD CODE
C  DESCRIPTION MATRIX AS SUPPLIED BY SUBROUTINE 'FIELD2' AND RADIAL
C  MULTIPLIERS AS SUPPLIED BY XUBROUTINE 'RADX'
C     M1,M2--PORTION OF FIELD IN R-DIRECTION
C     N1,N2--PORTION OF FIELD IN Z-DIRECTION
C     ALPHA--RELAXATION FACTOR
C     UDIF--ROUTINE EXITS WHEN ALL CORRECTIONS TO POTENTIALS ARE
C           BELOW 'UDIF'
C     NPASS--ROUTINE EXITS WHEN NUMBER OF PASSES OVER FIELD EXCEEDS
C            'NPASS'
C     ITER--NO OF ACTUAL RELAXATION PASSES TAKEN. IF ROUTINE EXITED
C           BECAUSE OF CONVERGENCE, THE NUMBER OF PASSES EQUALS
C           'ITER+1'. IF EXIT BECAUSE 'NPASS ' EXCEEDED, NUMBER OF
C           PASSES EQUALS 'ITER'
C     NEU--0-NO NEUMANN BOUNDARIES
C        --1-NEUMANN BOUNDARIES AT J=N1 AND J=N2.  IN THIS CASE N1=2
C            OR GREATER AND N2=79 OR LESS, AND THE FIELD CODING SUPPLIED
C            TO 'FIELD2' WOULD FOR EXAMPLE HAVE THE SAME CODING AT J=1
C            AS AT J=3 WHEN THE NEUMANN BOUNDARY IS AT J=2. IF ONLY ONE
C            NEUMANN BOUNDARY IS DESIRED, THE OTHER MUST BE CODED AS A
C            DIRICHLET BOUNDARY
C
      DIMENSION IND(40,80),U(40,80),POT(21),RADOT(40),RADIN(40),AK3(40,3
     1),AK7(40,3),AK1(40,2),AK5(40,2)
      COMMON IND,U,POT,RADOT,RADIN,AK3,AK7,AK1,AK5
      ALPHA1=ALPHA*0.25
      ALPHA2=ALPHA/6.
      ALPHA3=ALPHA/AK7(1,1)
      ITER=0
    1 CONTINUE
      IF(NEU.EQ.0) GO TO 3
      DO 2 I=M1,M2
      U(I,N1-1)=U(I,N1+1)
      U(I,N2+1)=U(I,N2-1)
    2 CONTINUE
    3 KONVRG=0
      DO 99 I=M1,M2
      DO 99 J=N1,N2
      INDX=IND(I,J)
      IF(INDX.GE.8) GO TO 8
      GO TO (99,99,99,4,5,6,7),INDX
    4 CHANGE=ALPHA1*(U(I+1,J)*RADOT(I)+U(I-1,J)*RADIN(I)+U(I,J-1)+
     1U(I,J+1)-4.*U(I,J))
      GO TO 77
    5 CHANGE=ALPHA2*(4.*U(I+1,J)+U(I,J+1)+U(I,J-1)-6.*U(I,J))
      GO TO 77
    6 CHANGE=ALPHA3*(AK3(1,1)*U(I+1,J)+AK3(1,2)*U(I,J+1)+AK3(1,3)*U(I,J-
     11)-AK7(1,1)*U(I,J))
      GO TO 77
    7 CHANGE=ALPHA3*(AK3(1,1)*U(I+1,J)+AK3(1,3)*U(I,J+1)+AK3(1,2)*U(I,
     1J-1)-AK7(1,1)*U(I,J))
      GO TO 77
    8 NL=INDX-10
```

RELAX2

```
      IEPS8=NO/128
      NO=NO-IEPS8*128
      IEPS7=NO/64
      NO=NO-IEPS7*64
      IEPS6=NO/32
      NO=NO-IEPS6*32
      IEPS5=NO/16
      NO=NO-IEPS5*16
      IEPS4=NO/8
      NO=NO-IEPS4*8
      IEPS3=NO/4
      NO=NO-IEPS3*4
      IEPS2=NO/2
      IEPS1=NO-IEPS2*2
      C1=AK1(I,IEPS1+1)+AK5(I,IEPS8+1)
      IP1=IEPS2+IEPS3+1
      C3=AK3(I,IP1)
      C5=AK1(I,IEPS4+1)+AK5(I,IEPS5+1)
      IP2=IEPS6+IEPS7+1
      C7=AK7(I,IP2)
      CP=C1+C3+C5+C7
      CHANGE=ALPHA/CP*(C3*U(I+1,J)+C7*U(I-1,J)+C1*U(I,J+1)+C5*U(I,J-1)-
     1CP*U(I,J))
   77 IF(ABS(CHANGE).GT.UDIF) KONVRG=1
      U(I,J)=U(I,J)+CHANGE
   99 CONTINUE
      IF(KONVRG.EQ.0) RETURN
      ITER=ITER+1
      IF(ITER.GE.NPASS) RETURN
      GO TO 1
      END
```

SETUP2

```
      SUBROUTINE SETUP2(M1,M2,N1,N2,V1,V2,V3,V4)
C
C  THIS SUBROUTINE SETS THE STARTING POTENTIAL VALUES AND IS TO BE
C  USED WITH SUBROUTINES 'FIELD2 AND 'RELAX2'.
C     M1,M2--PORTION OF FIELD IN R-DIRECTION
C     N1,N2--PORTION OF FIELD IN Z-DIRECTION
C     V1,V2,V3--CONSTANT POTENTIALS AS IN 'FIELD2' COMMENTS
C     V4--ALL OTHER POINTS SET TO THIS POTENTIAL
C
      DIMENSION IND(40,80),U(40,80),POT(21)
      COMMON IND,U,POT
      DO 1 I=M1,M2
      DO 1 J=N1,N2
      U(I,J)=V4
      IF(IND(I,J).EQ.1) U(I,J)=V1
      IF(IND(I,J).EQ.2) U(I,J)=V2
      IF(IND(I,J).EQ.3) U(I,J)=V3
    1 CONTINUE
      RETURN
      END
```

VECTOR

```
      SUBROUTINE VECTOR (M2,N1,N2, BIGEST, ENORM, ESQ)
C
C     SUBROUTINE FORMS REQUIRED POTENTIAL VECTORS,USING MATRIX P, FOR
C     FIELD OF (1,M2) BY (N1, N2) WHERE M = 1 IS THE AXIS AND (2*M2+N2-
C     -N1-5).LE.100.  LARGEST BOUNDARY POTENTIAL DIFFERENCE IS RETURNED
C     UNDER 'BIGEST', ARITHMETIC SUM OF DIFFERENCES UNDER 'ENORM', AND
C     SUM OF SQUARES UNDER 'ESQ'
C
      DIMENSION IND(40,80),U(40,80),POT(21),RADOT(40),RADIN(40),AK3(40,3
     1),AK7(40,3),AK1(40,2),AK5(40,2)
      DIMENSION VI(100),VEO(102),VEN(102),P( 51,100)
      COMMON IND,U,POT,RADOT,RADIN,AK3,AK7,AK1,AK5,VI,VEO,VEN,P
      N=N1+1
      M=M2-1
      NN2=N2-1
      NN=N2-N1-3
      MM=N2-N1-1
      KK=M+M+MM
      LL=KK-2
      NO=MM/2
      IF(NO*2.NE.MM) NO=NO+1
      NP=M2-1+NO
C
C     FIND VI AND VEO
C
      DO1 I=1,M
      VI(I)=U(I,N)
    1 VEO (I)= U(I,N1)
      DO2 I=1,NN
      II=M+I
      JJ=N1+I+1
    2 VI(II)=U(M,JJ)
      DO 3 I=1,MM
      II=M+I
      JJ = N1 + I
    3 VEO (II) = U(M2,JJ)
      DO 4 I=1,M
      II = M+NN+I
      JJ = M2 - I
    4 VI (II) = U(JJ,NN2)
      DO5 I = 1,M
      II = M+MM+I
      JJ = M2 - I
    5 VEO(II) = U(JJ,N2)
C
C     FIND VEN
C
      DO6 I = 1,KK
    6 VEN(I)=0.
      DO 7 I=1,NP
      DO 7 J=1,LL
    7 VEN(I) = VEN(I) + P(I,J) * VI(J)
      NO1=NP+1
      DO 9 I=NO1,KK
```

VECTOR

```
      DO 9 J=1,LL
      I1=KK+1-I
      J1=LL+1-J
    9 VEN(I)=VEN(I)+P(I1,J1)*VI(J)
C
C     FIND BIGGEST DIF. AND NORM
C
      BIGEST = 0.
      ENORM=0.
      ESQ=0.
      DO 8 I=1,KK
      DIF = ABS (VEO (I) - VEN (I))
      IF (DIF.GT. BIGEST)  BIGEST = DIF
      ENORM = ENORM + DIF
    8 ESQ = ESQ + DIF * DIF
      RETURN
      END
```

CHANGE

```
      SUBROUTINE CHANGE(M2,N1,N2,BETA)
      DIMENSION IND(40,80),U(40,80),POT(21),RADOT(40),RADIN(40),AK3(40,3
     1),AK7(40,3),AK1(40,2),AK5(40,2)
      DIMENSION VI(100),VEO(102),VEN(102),P( 51,100)
      COMMON IND,U,POT,RADOT,RADIN,AK3,AK7,AK1,AK5,VI,VEO,VEN,P
      M=M2-1
      MM=N2-N1-1
      KK=M+M+MM
      DO 1 I=1,KK
    1 VEN(I)=VEO(I)+BETA*(VEN(I)-VEO(I))
      DO 2 I=1,M
    2 U(I,N1)=VEN(I)
      DO 3 I=1,MM
      II=M+I
      JJ=N1+I
    3 U(M2,JJ)=VEN(II)
      DO 4 I=1,M
      II=M+MM+I
      JJ=M2-I
    4 U(JJ,N2)=VEN(II)
      RETURN
      END
```

VALUES

```
      SUBROUTINE VALUES(M1,M2,N1,N2,IFORM,IWIDTH,NCONTR,IFLAG)
C  PRINTS FIELD VALUES IN SQUARE GRID ACCORDING TO--
C     IFORM#1, FORMAT F5.2
C     IFORM#2, FORMAT F10.6
C     IFORM#0, NO FIELD VALUES PRINTED
C  IF NUMBER OF FIELD VALUES ACROSS ONE PAGE IS TOO GREAT FOR
C  ONE PAGE, FIELD IS SPLIT UP AND PRINTED ONE PAGE WIDE AT
C  A TIME.
C        ALSO ALLOWS WIDTH SPECIFICATION TO @PLOT@ ROUTINE
C  TO EXCEED 130.  PLOT IS SPLIT UP AND PRODUCED ONE PAGE WIDE AT
C  A TIME.  SPECIFIED BY @IWIDTH@.  ALL OTHER ARGUMENTS SAME AS
C  IN OTHER PROGRAMS.
C
      DIMENSION IND(40,80),U(40,80),POT(21)
      COMMON IND,U,POT
      IF(IWIDTH.EQ.0) GO TO 20
      IF(IWIDTH.GT.130) GO TO 1
      WRITE(6,100)
      CALL PLOT(M1,M2,N1,N2,NCONTR,IWIDTH,IFLAG,1)
      GO TO 20
    1 NA=IWIDTH/(N2-N1)
      IWIDTH=NA*(N2-N1)
      NSPACE=130/NA
      LWIDTH=NSPACE*NA
      NPAGE=IWIDTH/LWIDTH
      LAST=IWIDTH-NPAGE*LWIDTH
      IF(IFLAG.EQ.0) GO TO 97
      BIG=0.
      SML=0.
      DO 95 I=M1,M2
      DO 95 J=N1,N2
      IF(U(I,J).GT.BIG) BIG=U(I,J)
      IF(U(I,J).LT.SML) SML=U(I,J)
   95 CONTINUE
      CONTR=(BIG-SML)/FLOAT(NCONTR-1)
      DO 96  I=1,NCONTR
   96 POT(I)=SML+CONTR*FLOAT(I-1)
      IFLAG=0
   97 CONTINUE
      DO 2 I=1,NPAGE
      NN1=N1+(I-1)*NSPACE
      NN2=NN1+NSPACE
      WRITE(6,100)
    2 CALL PLOT(M1,M2,NN1,NN2,NCONTR,LWIDTH,IFLAG,1)
      IF(LAST.EQ.0) GO TO 20
      WRITE(6,100)
      CALL PLOT(M1,M2,NN2,N2,NCONTR,LAST,0,0)
   20 IF(IFORM.NE.1) GO TO 21
      NA=26
      GO TO 22
   21 IF(IFORM.NE.2) GO TO 23
      NA=13
   22 NPAGE=(N2-N1+1)/NA
      IF(NPAGE.EQ.0) GO TO 5
```

VALUES

```
      LAST=N2-N1+1-NA*NPAGE
      DO 3 I=1,NPAGE
      NN1=N1+NA*(I-1)
      NN2=NN1+NA-1
      WRITE(6,100)
      DO 3 J=M1,M2
      IF(IFORM.EQ.2) GO TO 30
      WRITE(6,101)(U(J,K),K=NN1,NN2)
      GO TO 3
   30 WRITE(6,102)(U(J,K),K=NN1,NN2)
    3 CONTINUE
      GO TO 7
    5 NL=N1
      GO TO 6
    7 IF(LAST.EQ.0) GO TO 23
      NL=NN2+1
    6 WRITE(6,100)
      DO 4 I=M1,M2
      IF(IFORM.EQ.2) GO TO 31
      WRITE(6,101)(U(I,J),J=NL,N2)
      GO TO 4
   31 WRITE(6,102)(U(I,J),J=NL,N2)
    4 CONTINUE
   23 RETURN
  100 FORMAT(1H1)
  101 FORMAT(/1H0,26F5.2)
  102 FORMAT(////1H0,13F10.6)
      END
```

EXTRA

```
      SUBROUTINE EXTRA(M2,N1,N2)
      DIMENSION IND(40,80),U(40,80),POT(21),RADOT(40),RADIN(40),AK3(40,3
     1),AK7(40,3),AK1(40,2),AK5(40,2)
      DIMENSION VI(100),VEO(102),VEN(102),P( 51,100),VEOO(102)
      COMMON IND,U,POT,RADOT,RADIN,AK3,AK7,AK1,AK5,VI,VEO,VEN,P,VEOO
      M=M2-1
      MM=N2-N1-1
      KK=M+M+MM
      DO 1 I=1,M
      C=(VEOO(I)-VEO(I))/(VEO(I)-VEN(I))
    1 U(I,N1)=VEO(I)+(C/(1.-C))*(VEO(I)-VEN(I))
      DO 2 I=1,MM
      II=M+I
      JJ=N1+I
      C=(VEOO(II)-VEO(II))/(VEO(II)-VEN(II))
    2 U(M2,JJ)=VEO(II)+(C/(1.-C))*(VEO(II)-VEN(II))
      DO 3 I=1,M
      II=M+MM+I
      JJ=M2-I
      C=(VEOO(II)-VEO(II))/(VEO(II)-VEN(II))
    3 U(JJ,N2)=VEO(II)+(C/(1.-C))*(VEO(II)-VEN(II))
      RETURN
      END
```

```
C     CONTOUR PLOTTING SUBROUTINE FOR SQUARE GRID OF FUNCTION VALUES,
C     CALLED BY
C    --CALL PLOT(N1,M1,N2,M2,M3,LWIDTH,IFLAG,IPRINT)
C
C     U--ARRAY OF FUNCTION VALUES ASSUMED EQUALLY SPACED.SUPPLIED THRU
C     COMMON
C     POT--ARRAY OF CONTOUR VALUES. CALLING PROGRAMME MUST DIMENSION
C          POT(21)
C     N1,M1--START AND END OF PLOT IN Y DIRECTION
C     N2,M2--START AND END OF PLOT IN X DIRECTION, WHERE (M2-N2) MUST
C            NOT EXCEED 132
C            THE ABOVE FOUR INTEGERS SPECIFY THE PORTION OF THE ARRAY
C            'U' TO BE PLOTTED, AND N1 AND N2 WOULD NORMALLY BE SPECI-
C            FIED AS 1
C     M3--NUMBER OF CONTOURS TO BE PLOTTED
C     LWIDTH--WIDTH OF PLOT IN PRINTER SPACES. THE ACTUAL WIDTH OF THE
C             PLOT WILL BE EQUAL TO N*(M2-N2) WHERE N EQUALS THE INTE-
C             GER PART OF 'LWIDTH/(M2-N2)'. LWIDTH MUST BE SPECIFIED AS
C             EQUAL TO OR GREATER THAN (M2-N2)
C     IFLAG--0, ARRAY 'POT' SUPPLIED BY CALLING PROGRAMME
C          --1, SUBROUTINE FINDS MINIMUM AND MAXIMUM 'U' IN THE INTER-
C            VAL SPECIFIED AND PLOTS M3 CONTOURS OF EQUAL 'U' INCREMENT
C     IPRINT--0,NO CONTOUR VALUES PRINTED
C           --1,CONTOUR VALUES PRINTED IN E11.4 FORMAT
C
C     SUBROUTINE DOES LINEAR INTERPOLATION FIRST IN X-DIRECTION TO
C     'LWIDTH' VALUES.THEN IN Y-DIRECTION FOR THE SAME INCREMENTS
C
C     CALLING PROGRAMME MUST START NEW PRINTER PAGE AND/OR PRINT A
C     HEADING IF DESIRED BEFORE PLOT IS CALLED
C
      SUBROUTINE PLOT(N1,M1,N2,M2,M3,LWIDTH,IFLAG,IPRINT)
C
      DIMENSION A(2,132),B(6,132),POT(21),VAL(132),VOLD(132),LINE(131),
     1CHAR(21)
      DIMENSION IND(40,80),U(40,80)
      COMMON IND,U,POT
      REAL LINE
      DATA BLANK,CHAR/1H ,1H1,1H2,1H3,1H4,1H5,1H6,1H7,1H8,1H9,1H0,1HA,1H
     1B,1HC,1HD,1HE,1HF,1HG,1HH,1HI,1HJ,1HK/
      NA=LWIDTH/(M2-N2)
      IF(NA.GT.0) GO TO 67
      WRITE(6,101) LWIDTH
      RETURN
   67 IF(IFLAG.EQ.0) GO TO 68
      BIG=U(N1,N2)
      SML=U(N1,N2)
      DO 70 I=N1,M1
      DO 70 J=N2,M2
      IF(U(I,J).GT.BIG) BIG=U(I,J)
      IF(U(I,J).LT.SML) SML=U(I,J)
   70 CONTINUE
      CONTR=(BIG-SML)/FLOAT(M3-1)
      DO 71 I=1,M3
```

```
 71 POT(I)=SML+CONTR*FLOAT(I-1)
    POT(1)=POT(1)+.0001*CONTR
 68 MM1=M1-N1+1
    NN=(M2-N2)*NA
    NN1=NN+1
    J2=1
    K=0
    DO 77 I=1,MM1
    DO 78 J=1,NN
    JJ=(J-1)/NA+N2
    FACTOR=FLOAT(J-1-((J-1)/NA)*NA)/FLOAT(NA)
    DO 79 J79=1,2
    I79=I+J79-2+N1
    A(J79,J)=U(I79,JJ)+FACTOR*(U(I79,JJ+1)-U(I79,JJ))
 79 CONTINUE
 78 CONTINUE
    I77=I+N1-1
    A(1,NN1)=U(I77,M2)
    A(2,NN1)=U(I77+1,M2)
    DO 81 J1=1,NA
    FACT=FLOAT(J1-1)/FLOAT(NA)
    DO 82 J82=1,NN1
 82 B(J2,J82)=A(1,J82)+FACT*(A(2,J82)-A(1,J82))
    IF(J2.NE.6) GO TO 83
 95 CONTINUE
    IF(J2.LT.3) GO TO 96
    DO 90 J=1,NN1
    B(2,J)=B(2,J)+.6667*(B(3,J)-B(2,J))
    IF(J2.LT.5) GO TO 90
    B(3,J)=B(4,J)+.3333*(B(5,J)-B(4,J))
    IF(J2.LT.6) GO TO 90
    IF(I.NE.MM1) GO TO 90
    B(4,J)=B(6,J)
 90 CONTINUE
 96 CONTINUE
    ICAL=3
    IF(J2.LT.3) ICAL=1
    IF(J2.LT.5) ICAL=2
    IF(ICAL.NE.3) GO TO 300
    IF(I.EQ.MM1) ICAL=4
300 CONTINUE
    DO 400 J400=1,ICAL
    K=K+1
    DO 401 I401=1,NN1
401 VAL(I401)=B(J400,I401)
    IF(K.EQ.1) GO TO 405
    DO 402 I402=1,131
402 LINE(I402)=BLANK
    DO 403 I403=1,NN
    BIG=AMAX1(VAL(I403),VOLD(I403),VAL(I403+1),VOLD(I403+1))
    SML=AMIN1(VAL(I403),VOLD(I403),VAL(I403+1),VOLD(I403+1))
    DO 403 J=1,M3
403 IF(BIG.GE.POT(J).AND.SML.LT.POT(J)) LINE(I403)=CHAR(J)
    WRITE(6,100)(LINE(J),J=1,131)
```

PLOT

```
405 DO 406 J=1,NN1
406 VOLD(J)=VAL(J)
400 CONTINUE
    IF(I.EQ.MM1) GO TO 99
    DO 91 J=1,NN1
 91 B(1,J)=B(6,J)
    J2=1
 83 J2=J2+1
 81 CONTINUE
    IF(I.NE.MM1) GO TO 77
    DO 92 J=1,NN1
 92 B(J2,J)=A(2,J)
    GO TO 95
 77 CONTINUE
 99 IF(IPRINT.EQ.0) RETURN
    WRITE(6,102)
    WRITE(6,103)(CHAR(J),POT(J),J=1,M3)
    RETURN
100 FORMAT(1H ,131A1)
101 FORMAT(1H ,10X,14HFIELD WIDTH OF,I3,10H TOO SMALL)
102 FORMAT(1H0,10X,8HCONTOURS)
103 FORMAT(7(3X,A1,1H=,E11.4))
    END
```